ESO, the European Southern Observatory, was created in 1962 to . . . establish and operate an astronomical observatory in the southern hemisphere, equipped with powerful instruments, with the aim of furthering and organising collaboration in astronomy . . . It is supported by eight countries: Belgium, Denmark, France, Germany, Italy, the Netherlands, Sweden and Switzerland. It operates the La Silla observatory in the Atacama desert, 600 km north of Santiago de Chile, at 2,400 m altitude, where fourteen optical telescopes with diameters up to 3.6 m and a 15-m submillimetre radio telescope (SEST) are now in operation. The 3.5-m New Technology Telescope (NTT) became operational in 1990, and a giant telescope (VLT = Very Large Telescope), consisting of four 8-m telescopes (equivalent aperture = 16 m) is under construction. It is being erected on Paranal, a 2,600 m high mountain in northern Chile, approximately 130 km south of Antofagasta. Eight hundred scientists make proposals each year for the use of the telescopes at La Silla. The ESO Headquarters are located in Garching, near München, Germany. It is the scientific, technical and administrative centre of ESO where technical development programmes are carried out to provide the La Silla observatory with the most advanced instruments. There are also extensive facilities which enable the scientists to analyse their data. In Europe ESO employs about 200 international Staff members, Fellows and Associates; at La Silla about 50 and, in addition, 150 local Staff members.

The ESO MESSENGER is published four times a year: normally in March, June, September and December. ESO also publishes conference proceedings preprints, technical notes and other material connected to its activities. Press Releases inform the media about particular events. For further information, contact the ESO Information Service at the following address:

EUROPEAN
SOUTHERN OBSERVATORY
Karl-Schwarzschild-Str. 2
D-85748 Garching bei München
Germany
Tel. (089) 320 06-0
Telex 5-28282-0 eo d
Telefax (089) 3202362
ips@eso.org (internet)
ESO::IPS (decnet)

The ESO Messenger:
Editor: Marie-Hélène Demoulin
Technical editor: Kurt Kjär

Printed by
Druckbetriebe Lettner KG
Georgenstr. 84
D-80799 München, Germany

ISSN 0722-6691

CHILE

SCOBBIE, James (GB), Tel. Software Scientist
BREWER, James (GB), Fellow
MARTIN Pierre (CDN), NTT Fellow
BRILLANT, Stephane (F), Student
METANOMSKI, Agnés (F), Student
CORPORON, Patrice (F), Coopérant

DEPARTURES

EUROPE

ROTH-AHRA, Margarete (A), Adm. Employee
FENDT, Michael (D), Engineer (Systems)
MINNITI, Dante (RA), Fellow
NAUMANN, Michael (D), Paid Associate
GOUDFROOIJ, Paul (NL), Fellow
HUIZINGA, Edwin (NL), Fellow
PATIG né Kissler, Markus (D), Student

CHILE

SWINNEN, Eric (B), Sr. Techn. Engineer

Local Staff Chile

ARRIVALS

NAVARRETE, Pablo (RCH), Elect. Technician
AMESTICA, Rodrigo (RCH), Software Engineer

DEPARTURES

FELIS, Mila (RCH), Secretary
LEON, José (RCH), Informatic Engineer
ROSENFELD, Walter (RCH), Electronic

Contents

FIRST ANNOUNCEMENT

Quasar Hosts

A Workshop co-sponsored by ESO and IAC to be held in Tenerife

23–27 September 1996

Recent theoretical and observational developments are leading us to focus our attention on the nature of quasar hosts, their environment, their influence on what we see of an AGN, and the AGN's influence on them.

Topics to be covered include:

- Latest observational results
- The radio-loud radio-quiet dichotomy
- High-redshift quasar hosts
- Properties of high-redshift active galaxies, e.g., the alignment effect
- Local environments of quasars
- Star formation and the ISM of quasar hosts
- Quasar hosts and Unified Schemes
- Quasar hosts and evolution
- The formation of quasar hosts

Please contact:

D.L. Clements (dclement@eso.org)
I. Perez-Fournon (ipf@ll.iac.es)
P. Crane (pcrane@eso.org)

European Southern Observatory
Karl-Schwarzschild-Str. 2
D-85748 Garching bei München, Germany
FAX: +89 320 23 62

Brunella Monsignori Fossi

Brunella Monsignori Fossi died suddenly on January 22, 1996, in her office at the Astrophysical Observatory in Arcetri. Her recent scientific interests were mainly related to the interpretation of the atmosphere of cool stars. The work which she, together with collaborators and students, had done over the years on the spectroscopy of hot plasmas led to results which were widely known, for example the "Arcetri code".

Brunella Monsignori Fossi loved science, and had developed a programme at Arcetri to bring astronomy to the general public. In this field of activity she also assisted ESO on many occasions. She was an absolute master in conducting such activities that touch thousands of people and demonstrate the fascination of astronomy.

She will be greatly missed by everyone who knew her.

New ESO Proceedings Available

The Proceedings of the ESO/ST-ECF Workshop on

Calibrating and Understanding HST and ESO Instruments

(ESO Conference and Workshop Proceedings No. 53)

have been published. The 300-p. volume, edited by P. Benvenuti, is available at a price of DM 60.– (prepayment required).

Payments have to be made to the ESO bank account 2102002 with Commerzbank München, or by cheque, addressed to the attention of

ESO, Financial Services, Karl-Schwarzschild-Str. 2,
D-85748 Garching bei München, Germany

New Scientific Preprints

(November 1995 – February 1996)

1111. D. Clements et al.: A New Large Sample of Ultraluminous IRAS Galaxies. *M.N.R.A.S.*
1112. P.A. Shaver, J.V. Wall and K.I. Kellermann: PKS 1251–407: A Radio-Loud Quasar at z = 4.46. *M.N.R.A.S.*
1113. H.U. Käufl and L. Stanghellini: Detection of Quasi-Stellar 10 µm Emission in the Central Region of the Elliptical Galaxy NGC 3136B. *Astronomy and Astrophysics.*
1114. M. Kissler-Patig, T. Richtler and M. Hilker: The Elliptical Globular Cluster System of NGC 720. *Astronomy and Astrophysics.*
1115. D.L. Clements et al.: Optical Imaging of Ultraluminous IRAS galaxies: How Many are Mergers? *M.N.R.A.S.*
1116. O. von der Lühe, S. Solanki and Th. Reinheimer: Observing Stellar Surface Structure with the ESO-VLT Interferometer. IAU Symp. 176, "Stellar Surface Structure", ed. K.G. Straßmeier, Vienna, 1995.
1117. S. Cristiani: Cosmological Adventures in the Lyman Forest. Lecture presented at the International School of Physics "Enrico Fermi" Course "Dark Matter in the Universe", Varenna, 25 July – 4 August 1995.
1118. G. Meylan: Studies Through Radial Velocity Measurements of the Peculiar Motions of Stars in Galactic Globular Clusters. IAU Symp. 174, "Dynamical Evolution of Star Clusters: Confrontation of Theory and Observations", eds. P. Hut and J. Makino (Dordrecht: Kluwer), in press.
1119. J. T. van Loon et al.: Discovery of the First Extra-Galactic SiO Maser. *Astronomy and Astrophysics.*
1120. P. Goudfrooij and E. Emsellem: Ionized Gas in Early-Type Galaxies: Its Effect on Mg*b* and Other Stellar Line-StrengthIndices. *Astronomy and Astrophysics.*
1121. G.C. Van de Steene et al.: Optical Observations of Planetary Nebula Candidates from the Northern Hemisphere. *Astronomy and Astrophysics.*
1122. G. Mathys et al.: A Kinematical Study of Rapidly Oscillating Ap Stars. *Astronomy and Astrophysics.*
1123. D. Minniti et al.: Globular Cluster Halos Around Dwarf Elliptical Galaxies. *Astronomy and Astrophysics.*
1124. L. Pasquini: Lithium in Old Clusters. To be published in the Proc. of the Ninth Cambridge Workshop on "Cool Stars, Stellar Systems and the Sun", R. Pallavicini and A. Duprée, eds., in press.
1125. P. Andreani et al.: Looking for the S-Z Effect Towards Distant ROSAT Clusters of Galaxies. *Astrophysical Journal.*
1126. A. Caulet and R. Newell: Probing the ISM of the Superbubble LMC2 in the Large Magellanic Cloud: I. Ti II and Ca II Absorption Lines. *Astrophysical Journal.*
1127. Bo Reipurth et al.: HH110: The Grazing Collision of a Herbig-Haro Flow with a Molecular Cloud Core. *Astronomy and Astrophysics*
1128. L.F. Rodríguez and Bo Reipurth: VLA Detection of the Exciting Sources of HH34, HH114 and HH199. *Revista Mexicana de Astronomía y Astrofísica.*
1129. A.F.M. Moorwood et al.: Starburst Superwind and Liner Activity in NGC 4945. *Astronomy and Astrophysics.*
1130. P. Goudfrooij: The Distribution of Dust and Gas in Elliptical Galaxies. Invited talk given at a conference on "New Extragalactic Perspectives in the New South Africa: Changing Perceptions of the Morphology, Dust Content and Dust-Gas Ratios in Galaxies". Held in Johannesburg, South Africa, during January 22–26, 1996. Proc. ed. by D.L. Block (Kluwer, Dordrecht).

STAFF MOVEMENTS

(1 January – 31 March 1996)

International Staff

ARRIVALS

EUROPE

AGEORGES, Nancy (F), Fellow
SAVAGLIO, Sandra (I), Fellow
YAN, Lin (P.R. China), Fellow
DOUBLIER, Vanessa (F), Student
CASSE, Martin (F), Coopérant

ANNOUNCEMENTS

Sharing Time on the ESO 3.6-m and the CTIO 4-m Blanco Telescopes

G. MONNET, ESO

In order to make more efficient use of the astronomical observing potential of our two institutions, as well as to foster closer co-operation, ESO and CTIO are beginning an experiment to exchange 4m-class telescope time.

The exchange will start with the next proposal period (ESO Period 58, CTIO, 2nd semester 1996). The instrument available for use of the European community on the CTIO 4-m telescope is their Infrared Spectrograph (IRS). This very efficient instrument will provide our user community with spectrographic capabilities in the 1 to 5 micron range certainly not available during the upcoming NTT "big-bang". Only when both SOFI at the NTT and ISAAC at the VLT come on board will we be able to offer equal or superior performances in that domain. A brief outline of the performance of the IRS follows. Prospective users are encouraged to refer to the documentation on the CTIO WWW pages for more details (www.ctio.noao.edu/ftp/pub/manuals/irs/irs.html).

Users from the CTIO community have asked for access to ADONIS, TIMMI and EFOSC at the 3.6-m telescope. We have tentatively agreed to "swap" 12 nights per semester, and envision this initial attempt to run for 3 semesters. The exact number of nights will be determined by scientific merit and proposal pressure.

Proposers from the ESO community who wish to observe at CTIO with IRS should submit a proposal to ESO on our normal telescope request form, for the normal ESO proposal deadline of March 31 and September 30, but indicate clearly on the front page that observations at CTIO are requested. Proposals will be rated by the ESO OPC based on scientific merit, and then passed to the CTIO scheduler, and vice versa. Input to the OPC from the appropriate technical reviewers of the instrument host institution will be sought.

Note in the next proposals due March 31,1996 that, because of differences between semesters, the time being sought for the CTIO infrared spectrometer will be August 1, 1996 – January 31, 1997. CTIO use of the ESO 3.6-m instruments will occur in the October 1, 1996 – March 31, 1997 period 58.

On the ESO side, the idea of initiating a telescope time exchange with another southern Observatory came from the ESO User's Committee last May. This was driven by the unfortunate timing of the NTT big-bang, which puts most of our infrared capability out of use, almost exactly when the bulk of ISO data appear. We think that this exchange will enhance European capability to make the best scientific use of these invaluable data, and we hope that oversubscription for "CTIO" time will be large.

IRS: 1 to 5 micron infrared spectrometer. Uses a 256 × 256 SBRC array, with a 40 e^- r.o.n. and about 7e^-/sec. dark current. Full well is 50,000 e^-. Scale on the detector is 0.32 arcsec. per pixel. Maximum slit length is 16 arcsec. The instrument is cooled at 35 K; its configuration (entrance mirror, slit, filter, grating tilt) is fully computer controlled. A TV camera allows to directly view the field being observed (limiting mag. 19 during full Moon). Two gratings (of a total of 5 available) are mounted side by side. 2 px spectral resolution may vary from 400 to 10,000.

ESO Astrophysics Symposia Proceedings

The proceedings of the following ESO Astrophysics Symposia are available from Springer.

- **The Light Element Abundances**
- **Science with the VLT**
- **The Bottom of the Main Sequence and Beyond**
- **QSO Absorption Lines**

ESO has negotiated an attractive price for these proceedings. They may be ordered directly from books stores or through Springer.

FAX: (49 30) 8201 301
e-mail: orders@springer.de
Post: Springer-Verlag, P.O. Box 311340, D-10543 Berlin

ESO Studentship Programme

The European Southern Observatory has positions available for 12 research students. Six of these positions are at the ESO Headquarters in Garching, and the other six are at the Observatory in Santiago and La Silla, Chile. Students normally stay approximately two years, so that each year a total of 6 students (3 at each location) may be accepted. These positions are available to students enrolled in a Ph. D. (or equivalent) programme in the ESO member states and exceptionally at a university outside the ESO member states.

Note that the closing date for applications is
June 15, 1996.

Potential candidates, or their supervisors should obtain the detailed information about the programme by requesting the brochure and application form from the

European Southern Observatory
Studentship Programme
Karl-Schwarzschild-Str. 2
D-85748 Garching bei München, Germany

The brochure describes the prerequisites for participation in the programme, as well as the research interests of staff members who might work with the students and who would act as the local supervisors.

conjunction with VLT projects involve direct imaging or spectroscopic surveys. Some of these needs can be met by existing ESO telescopes with suitably upgraded instrumentation, and a new state-of-the-art infrared imager/spectrograph (SOFI) and upgraded high-resolution optical imager (SUSI-II) have been approved and are under construction for use at the upgraded NTT from late 1997. The longer-term use of the 3.6-m telescope might also be in such (spectroscopic) surveys.

It is, however, also one of the findings of the WG that ESO does not possess a truly competitive wide-field imaging telescope. Plans must be developed to provide such a facility, perhaps in collaboration with other communities with parallel interests. It is also concluded that multifibre spectroscopy is an area in which La Silla simply cannot become competitive before FUEGOS comes on line at the VLT, and the community's needs in this field will have to be satisfied elsewhere.

Long-Term vs. Medium-Term Planning

The WG estimates that in the steady-state era, when the VLT is fully operational, ESO should operate about four telescopes in the 1–4-m class in addition to the VLT, carefully optimised to complement it as well as possible. The remaining, mostly smaller, telescopes need not necessarily be closed outright at that time, but can be turned over for certain periods to institutes or consortia who want to operate them on a self-contained basis to carry out specific projects, as happens on La Silla already today.

Despite the hypnotic effect of the magic number 2000, ESO will not be in the steady state yet by that year. During the transition period, i.e. for almost another decade from now, La Silla will remain the bread and butter of a sizeable, if decreasing fraction of the ESO community. The WG has attempted to lay out a plan for a gradual change in the complement of facilities offered on La Silla during that period, synchronised with the commissioning of new instruments on the VLT and tuned to obtain the most cost-effective operation. Readers are referred to the report itself for the details.

Paranal vs. La Silla

Suggestions have repeatedly been made that in the somewhat longer term it would be preferable to move some La Silla telescopes to Paranal, or replace them by new ones there, and subsequently close La Silla, since operating only one observatory would be substantially cheaper. However, the practical aspects of this suggestion have not been worked out. Accordingly, the report requests that an assessment be made of the number of sites actually available in the Paranal areas for potential new telescopes, and the cost of building them there.

While this work is still going on, it appears that, first, the number of such sites is actually close to one. Second, in an organisation with a transparent cost structure and low fixed overheads, there is no *a priori* reason why operating a given telescope should in fact be cheaper on Paranal than on La Silla. And telescopes are not built or moved without substantial costs. In other words, while a possible future telescope providing new scientific capabilities and based on modern technical and operational experience might be best placed in the Paranal area, the long-term closure of La Silla is by no means a foregone conclusion.

What is the Plan?

First, it is important that discussions of the plan be based on the final version, which incorporates important modifications requested at the joint meeting of the ESO committees on November 2, 1995. The existence of several versions of the plan does carry some risk of confusion, but is the inevitable result of a real interaction with the community and incorporation of the feedback received. The gain is a reasonable degree of certainty that all constructive ideas and legitimate concerns have been given full opportunity to be expressed and taken into account.

Second, the WG report is a scientific and technical review, not an organisational or financial plan, although it cannot of course be removed from these realities. Organisational and financial aspects were not directly included in the WG's charge, and they cannot be considered separately for La Silla, but must involve ESO as a whole. Thus, the plan addresses the perceived future scientific needs for La Silla and the facilities required to fulfil them, and attempts to assign an order of priority. As ESO's structure and financial situation evolve, due to internal reorganisation and changes in the world around us, circumstances will dictate how far down the priority list it will be possible to go.

How to Use It?

It would be naive to pretend that a first round of addressing such a complex subject as the development of La Silla over the next decade can produce a definitive list of detailed answers. A premier research organisation must be able to adapt to changing scientific priorities and opportunities and exploit new technical developments that we cannot now foresee. And the world outside science is not static either.

Accordingly, what actually happens will no doubt differ from the present description in several respects. Some technical aspects are already identified in the plan for further study and clarification (e.g. the optimal long-term use of the 3.6-m and 2.2-m telescopes); others will find better solutions along the way than those now proposed. Clearly, the actions eventually taken should take such developments into account.

Thus, the goal of the present report is basically to initiate a continuing process of forward planning for La Silla, and to provide a general framework for the detailed elaboration of such plans. It is the final recommendation of the report that it be taken up for revision at regular intervals, e.g. in a three-year cycle. A deliberate approach to the future development will, we hope, benefit both the scientific output of La Silla, ESO's financial planning, and the morale of the staff.

E-mail address: ja@bro835.astro.ku.dk
(Johannes Andersen)

original Palomar Sky Survey or Southern Sky survey. A number of the stars have large proper motions so that up-to-date images would be preferred. [I would welcome images from other sources (e.g. EFOSC or EMMI acquisition images) to replace these finding charts.] The standard star data are usually tabulated as narrow band magnitudes, and in converting the monochromatic AB magnitudes to flux the definition:

$$\text{AB mag} = -2.5 \times \log_{10}(F_\nu) - 48.59$$

(e.g. Hamuy et al., 1992) was used.

Each standard star 'page' also carries clickable entries to the ST-ECF anonymous ftp account where the data are held. For each star and data source (some stars are covered by more than one set of measurements), there are ASCII files of the AB magnitude vs. wavelength and flux (ergs cm^{-2} s^{-1} Å^{-1} and ergs cm^{-2} s^{-1} Hz^{-1}) vs. wavelength. Depending on the data reduction system used, AB mag. or flux (F_λ or F_ν) is required. There is a readme file in each directory of the anonymous ftp account describing the contents. In addition there is a MIDAS command file to convert all the ASCII (flux) files in each directory into MIDAS tables. Clicking from the standard star 'page' to the ftp area moves to the appropriate directory, rather than opening a single file. In each directory there are two files for each star (one for magnitudes, one for fluxes) and there may be other files in another ftp directory for the same star. The user must exercise some judgement here – the data retrieved depend somewhat on the application.

4. Prospects

The WWW provides an ideal method of access to such data and the observing astronomer can display the output on the same screen as the data-viewing tool. It should enable observers to select the most suitable spectrophotometric standard appropriate to their particular observation. When service observing (or queue scheduling) is implemented, the spectrophotometric standard may be automatically chosen. However there are a number of considerations to address in choosing the 'best' standard, as I have emphasised. There should also be allowance for user preference, for example when it is found that a particular standard with a particular instrument combination always gives a consistent value for the Balmer decrement.

Even if an astronomical instrument is internally well calibrated, observation of spectrophotometric standards is still required. The atmosphere, even at optical wavelengths, has time-varying emission and transmission properties, necessitating at minimum zero point calibration. The presence of water vapour, cloud and dust can give a wavelength-dependent atmospheric extinction, which can only be corrected by a calibrator above the atmosphere. Thus ground-based pipeline calibration must always make allowance for night-to-night variations in a way not needed by orbiting telescopes. Good sky coverage by high quality spectrophotometric standards will thus remain a necessity.

I would welcome comments on this tool and in particular suggestions for additional standards to include.

Thanks

I should like to thank Fionn Murtagh for his invaluable help in getting this WWW tool set up and to Michael Naumann for detailed comments on an earlier version.

References

Bohlin, R. C., Harris, A. W., Holm, A. V., Gry, C., 1990, *ApJS*, **73**, 413.
Bohlin, R. C., 1995, in *Calibrating Hubble Space Telescope: Post Servicing Mission*, ed. A. Koratkar, C. Leitherer, p. 49.
Bohlin, R. C., Colina, L., Finlay, D. S., 1995, *AJ*, **110**, 1316.
Colina, L., Bohlin, R. C., 1994, *AJ*, **108**, 1931.
Hamuy, M., Walker, A. R., Suntzeff, N. B, Gigoux, P., Heathcote, S. R., Phillips, M. M., 1992, *PASP*, **104**, 533.
Hamuy, M., Walker, A. R., Suntzeff, N. B., Gigoux, P., Heathcote, S. R., Phillips, M. M., 1994, *PASP*, **106**, 566.
Hayes, D. S., Latham, D. W., 1975, *ApJ*, **197**, 593.
Oke, J. B., 1974, *ApJS*, **27**, 21.
Oke, J. B., 1990, *AJ*, **99**, 1621.
Stone, R. P. S., Baldwin, J. S., 1983, *MNRAS*, **204**, 347.
Taylor,, 1984, *ApJS*, **54**, 259.
Turnshek, D. A., Bohlin, R. C., Williamson, R. L., Lupie, O. L., Koornneef, J., Morgan, D. H., 1990, *AJ*, **99**, 1243.
Walsh, J. R., 1993, *St-ECF Newsletter*, **19**, 3.

E-mail: jwalsh@eso.org

Planning for La Silla in the VLT Era: What Came Out?

J. ANDERSEN, Chairman of the Working Group

As readers will be aware, an ESO Working Group has been engaged in charting the future of the La Silla observatory at the time when it will operate jointly with the VLT. The final (6th) version of the report of the WG was presented to Council and the Director General at the Council meeting in Milan in November 1995. Thus, it is now part of ESO's mid- and long-range scientific and technical planning and available as document ESO/STC-174 rev. (22 Nov. 1995) and from the ESO WWW home page.

Earlier articles (*The Messenger* **78**, 3 and **80**, 4) have described the charge and composition of the Working Group and the procedures it adopted to involve the views and ideas of the community in the preparation of its plan. These included a questionnaire survey of the entire community and discussions of drafts of the plan with the ESO committees in several iterations. The input of the OPC on the scientific aspects was especially appreciated.

Colleagues interested in the detailed recommendations of the WG are advised to consult the report itself. Here, I should like to share with readers a few general points, especially such as have emerged in the discussions over the last few months. I should also like, on behalf of the WG, to thank the many colleagues inside and outside ESO who have contributed to making the report as comprehensive and thorough as possible.

The Impact of the VLT

The VLT will not be an exclusive toy, reserved for a small elite: With a number of foci exceeding the total number of telescopes on La Silla and a collecting area some seven times as large, the VLT will make a major impact on virtually all sections of ESO's user community.

Hence, already for scientific reasons *per se*, La Silla and other observatories with 1–4-m class telescopes will not be conducting "business as usual" in the VLT era. While all analyses show that a broad complement of such intermediate-size facilities will continue to be needed, their work will be largely conditioned by the research done at the 8-m giants, and their tasks then will be different from now. It is therefore appropriate for the community to begin preparing its scientific plans for the use of intermediate-size telescopes in the VLT era, and for ESO to begin preparing to provide the facilities that will be needed.

Future Needs for Intermediate-Size Telescopes

Many of the projected highest-priority uses of intermediate-size telescopes in

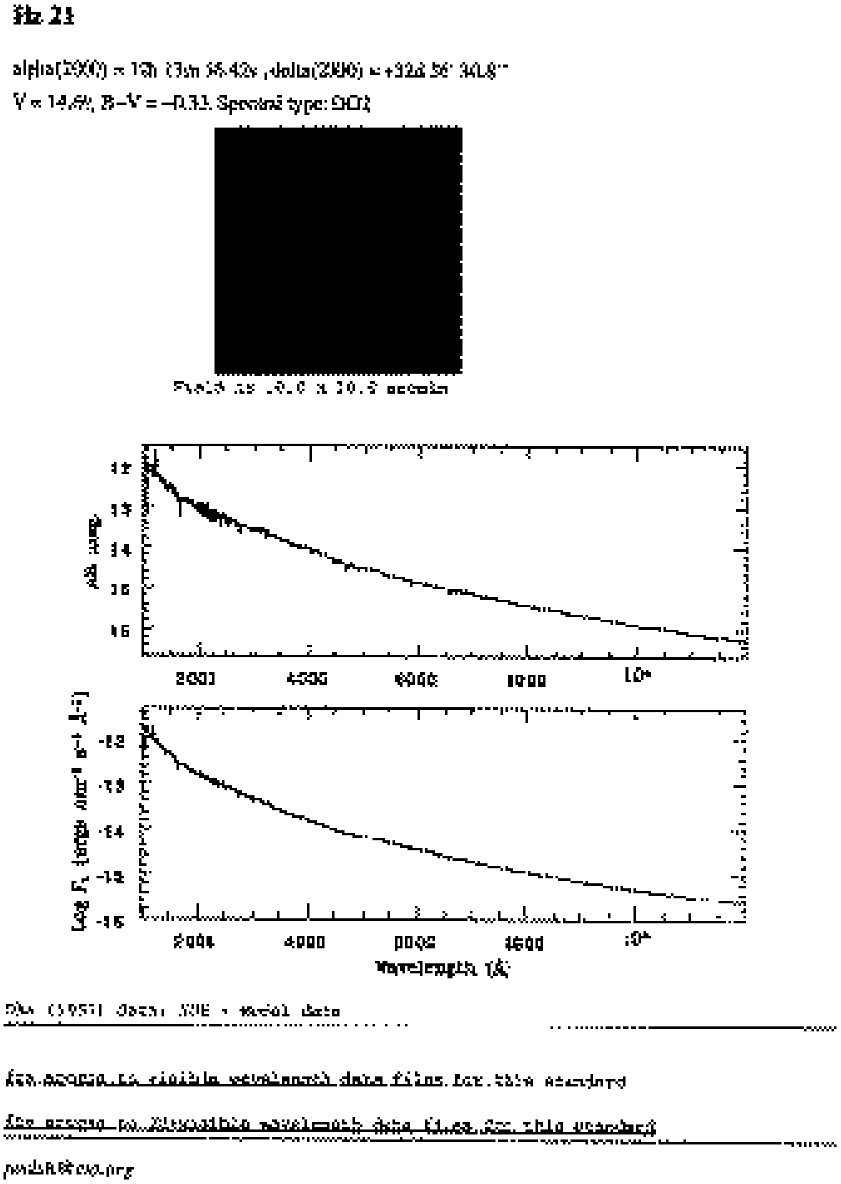

Figure 2: An example 'page' for the standard star Hz 21 taken from the WWW tool.

1990). The V magnitudes synthesised from the Oke data, however, show small offsets from photometric data by 0.03 mag. on average. The Oke (1990) narrow-band magnitudes should therefore be corrected as detailed by Colina & Bohlin (1994).

The Hubble Space Telescope Faint-Object Spectrograph (FOS) has a continuous wavelength coverage from 1140 to 9200 Å at a resolution of ~ 1300, so it is an ideal instrument for spectroscopy of standard stars. Comparison of FOS spectra with model atmospheres however showed some discrepancies in the UV, suggesting that the absolute flux measurements in the UV were not reliable. White-dwarf models have now reached a degree of reliability that they can be used to provide the true flux distributions for standard stars. Bohlin & Colina (1995) (see also Bohlin, 1995) have begun publishing a set of primary white-dwarf spectrophotometric standards which should provide the fundamental basis for calibration. The absolute fluxes are reliable to about 1% and the relative fluxes should be good to about 2%. Eight primary standards are used and FOS observations of another 18 stars provide secondary standards. These stars are of intermediate brightness (V = 9–16 mag.), so are ideal as spectrophotometric standards for large telescopes.

The Oke (1974 and 1990) standards were observed from Palomar and so are restricted to northern declinations and the equatorial region (the most southerly is at $\delta = -21°$). For observation in the south there were standards established by Stone & Baldwin (1983). However, these standards were only tabulated at rather wide wavelength intervals, so were of limited use for work at higher resolution. The CTIO group have re-observed these standards and provide flux measurements at 50 Å intervals from 3300 to 10000 Å for 19 stars. In establishing the absolute magnitudes of these standards they used a set of 11 bright equatorial standards taken from Taylor (1984). Since Vega is the primary standard (Hayes & Latham, 1975) these are secondary standards, and the southern Stone and Baldwin standards therefore tertiary standards. Their spectral type is rather varied with few white dwarfs.

3. A WWW Tool

In 1992 I produced a booklet giving finding charts and magnitude and flux vs. wavelength plots for the Oke (1990) standards and the HST standards (a total of 40 stars). This was distributed to observatories and interested individuals (Walsh, 1993). I have subsequently developed this booklet into a tool on the World Wide Web to allow easy access to information on the standards and their flux distributions. So far the Oke (1990) data, the old HST standards, the primary WD standards (Bohlin, 1995) and the Hamuy et al. (1992, 1994) secondary and tertiary standards have been included (69 stars in total). The aim of the tool is to allow easy access to the standard star data with the observing astronomer in mind. Co-ordinates and finding charts are given and the position of the nearest standard is available on a map. By viewing the flux data for a standard, the astronomer can then quickly decide which is the best standard to use for effective and accurate calibration of the target spectrum. The URL is:

**http: //www.eso.org/
spect-phot-standards/
optuvstandards.html**

The first page of the tool is an introduction which allows brief details of the sources of the data to be viewed. Access to the information on each standard is by two routes: an RA ordered list giving also spectral type and magnitude; a clickable sky map. Figure 1 shows the disposition of all the standards on an RA-Dec plot as used in the WWW tool. There are some regions of the sky which are over-represented by standards and others at high declinations which are under-represented. From either of these entry points, the user arrives at a page for each standard containing the co-ordinates, magnitude and colour, a finding chart and plots of F_λ and AB mag. vs. wavelength. Figure 2 shows a typical such 'page' for the standard star Hz 21. The finding charts for each standard are produced either from publications or from the Digital Sky Survey. The epoch of these images is mostly that of the

A World Wide Web Tool for Spectrophotometric Standard Stars

J. R. WALSH, ST-ECF, ESO

1. Importance of Spectrophotometric Standards

Spectrophotometric standards play a vital role in all aspects of astronomical spectroscopy, independent of the type of objects observed and the spectral resolution. The role of a spectrophotometric standard is to correct for the wavelength-dependent sensitivity of the atmosphere + telescope + spectrograph + detector combination and to provide the absolute zero points of the flux (or magnitude) scale. Without standards, accurate astrophysical diagnostic line ratios cannot be determined, spectral energy distributions cannot be computed and matching of spectra from other wavelength bands (UV, IR, radio) cannot be accomplished, for example. In addition, the provision of spectrophotometric standards enables (photometric) calibration of narrow band imaging data.

To be useful, spectrophotometric standards should satisfy the following criteria:

- be bright (but not too bright that shutter timing or shading at very short exposure times are a source of error)
- be single stars
- have a spectral energy distribution which is 'flat' with wavelength, or at least does not have too many narrow features
- have a sufficient density of flux measurements with wavelength to allow effective calibration of even high-resolution spectra
- be well distributed on the sky so that airmass corrections between the standard and the target are not large.

Of course, no set of stars could be found to satisfy all these criteria. A range of brightness is preferable so that the standards can be used on large and small telescopes and at a range of spectral dispersions. If there are close companions to the stars they should be much fainter and not very much different in colour to minimise calibration uncertainties. There is of course no stellar source with a flat (F_λ or F_ν = constant) spectrum. White dwarfs come closest to being the ideal real standard since they have few lines, and these are usually weak. If the standards have absorption lines they should be broad rather than narrow, otherwise the detected flux at the centre of the lines can critically depend on the spectral resolution. If the standard star fluxes are tabulated at wide wavelength intervals, then spurious features are typically seen at the positions of these absorption lines in the calibrated target spectrum. Providing excellent standard stars with a high density of flux measurements is a long and time-consuming process; there is clearly a compromise between having many standards over the sky and requiring a correction for the different airmass of the target and standard. Currently most standards are within about 30° of any target.

2. Available Spectrophotometric Standards

The best-known set of optical spectrophotometric standards is that of Oke (1974). These are white dwarf standards observed with the Palomar multichannel spectrometer and having a wavelength coverage from about 3300 to 10000 Å. Oke listed fluxes for 38 stars with bandpasses from 20–80 Å in the blue and 40–360 Å in the red. However, these stars were never intended as standards in the accepted sense, but for comparison of the absolute spectral energy distribution of white dwarfs with models. In collaboration with the HST project, which had foreseen the need for UV-optical standards to enable calibration of the Faint-Object Spectrograph and the Goddard High-Resolution Spectrograph, Oke (1990) published uniform data for 25 stars from 3200 to 10200 Å with flux determinations every 1 Å in the blue and 2 Å in the red. These data, taken with the Hale double-beam spectrograph, were combined with IUE and Voyager observations to yield a set of HST spectrophotometric standards (Turnshek et al., 1990; Bohlin et al.,

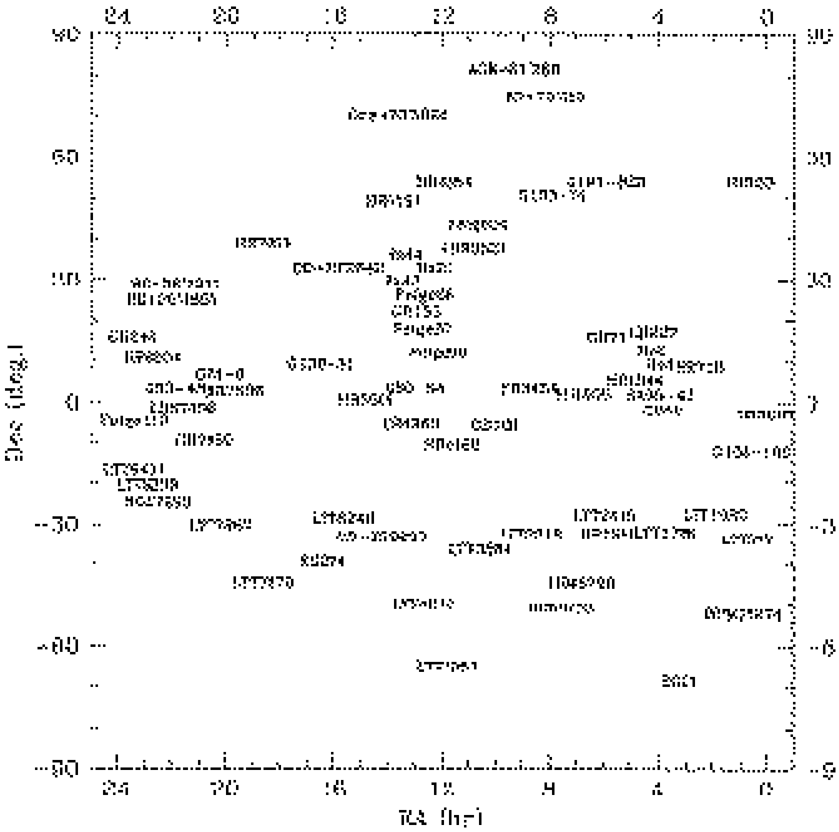

Figure 1: An RA-Dec sky map of the positions of the HST, Oke (1990) and CTIO standard stars. In the WWW tool, clicking at the position of one of the standards brings up a page of details on that particular standard (see Figure 2).

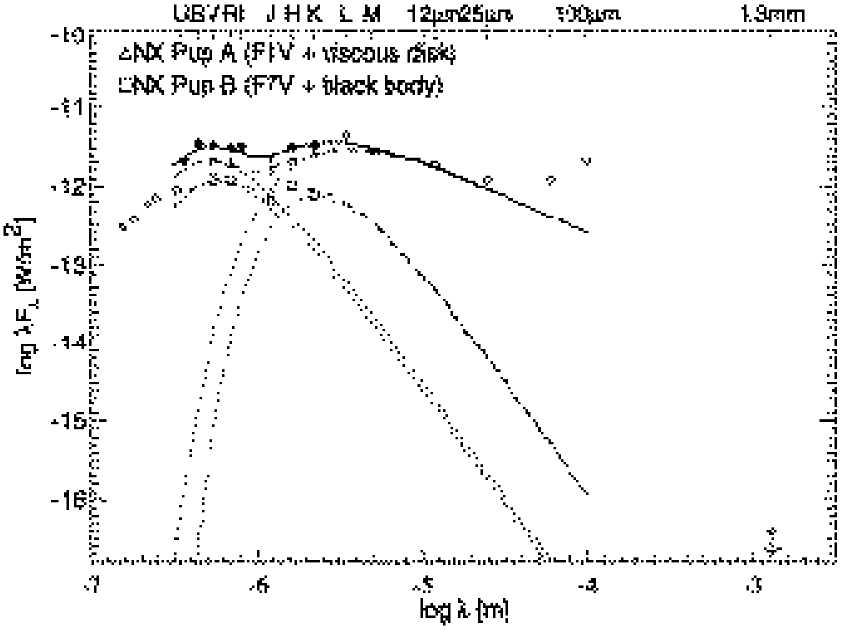

Figure 4: Dereddened (assuming A_v = 0.48^m) spectral energy distribution λF_λ of NX Pup A and B from the UV to the mm range. The filled diamonds, open triangles, and open squares indicate our own simultaneous measurements. The total spectral energy distribution can be decomposed into four parts (dotted lines): the photospheric emission from NX Pup A (F1V) and NX Pup B (F7V), a viscous accretion disk around NX Pup A, and circumstellar matter around NX Pup B which is approximated by a blackbody. The dashed lines mark both the SEDs of the individual stellar photospheres plus the IR excess due to circumstellar matter for NX Pup A and B. The overall SED is indicated by a solid line and gives a reasonable fit to the observed flux distribution (diamonds).

posure can be reduced from 10% to 1% even with shutter maps not obtained in the same night. All short exposure CCD images (observations of CCD standard star fields and of NX Pup) were corrected using the shutter map.

Speckle and adaptive optics observations

The speckle images were reconstructed by the speckle masking method (Schöller et al., 1996). The flux calibration was done by combining the relative photometry of the components derived from the speckle images with the absolute photometry of the (unresolved) components obtained with the Danish 1.54-m telescope.

The adaptive optics images were processed following the procedure described by Tessier et al. (1994). IR standard stars were observed with ADONIS/SHARP to allow for a flux calibration.

Results

Most of the light detected in V and R is emitted by the stellar photospheres of NX Pup A and B. Both components also exhibit a NIR excess. While the SED of NX Pup B peaks at H, the SED of NX Pup A is still rising at K. Hence, the majority of the IR excess arises from component A.

The photometric variability has been studied extensively by Bibo & Thé (1991). We reanalysed the colour magnitude relations derived from the LTPV data and found indications that variable extinction is the main cause for the variability. The blueing in colours when NX Pup is near its minimum brightness can be explained by additional scattered light due to circumstellar material (see Schöller et al., 1996).

If we adopt a MK type of F1 IV–V for NX Pup A, the observed V–R colour (0.30^m) yields a visual extinction $A_v \approx 0.48^m$. By assuming the same extinction for NX Pup B, its V–R colour yields a spectral type F7V. However, the fact that NX Pup B's IR excess is significantly smaller than that of NX Pup A might indicate that, while it suffers the same foreground extinction as NX Pup A, its circumstellar extinction might be considerably less. Studies, e.g. by Krautter (1980), indicate that the amount of foreground extinction in the direction of the Gum nebula might be as small as $A_v \approx 0.15^m$ out till 500 pc from the Sun. If NX Pup B suffered no additional extinction, its V–R colour would yield a spectral type of G4V. Accordingly, we compute $L_{bol} \approx 7.3 - 9.4\ L_\odot$. Mass and age determinations based on theoretical evolutionary tracks computed by D'Antona & Mazzitelli (1994) are summarised in Table 2.

The IR excess of NX Pup A can be approximated by a viscous accretion disk spectrum in which F_λ falls off $\propto \lambda^{-4/3}$ towards longer wavelengths. The non-detection of 1.3 mm dust continuum emission (Henning et al., 1994) suggests that the disk around NX Pup A is cut off at about 20 AU possibly due to the presence of component B which itself has much less circumstellar matter left.

Table 2: Evolutionary status of NX Pup A & B.

NX Pup	A	B
Separation	0."126 ± 0."003	
PA	62.°8 ± 1.°7[a]	
SpT	F0–F2	F7-G4
$L/L_\odot$	16–19	7-9
Mass	$\approx 2\ M_\odot$	1.6–1.9 $M_\odot$
Age	$3–5 \times 10^6$ yr	2—6 x 10^6 yr

In a future observing run we aim at obtaining high spatial resolution observations of NX Pup near its minimum brightness. One would expect that NX Pup A then is completely obscured and would only be visible in the optical though light scattered by circumstellar material, similar to the active Herbig Ae/Be star Z CMa, where the IR companion was detected in the visual e.g. by Barth et al. (1994). Measurements of the polarisation of NX Pup A & B near minimum brightness using speckle polarimetry would be a test for the scattered light hypothesis.

Clearly, for both NX Pup A and B spatially resolved imaging towards longer wavelengths are necessary, which in turn allow for more detailed model calculations and to better constrain the structure and geometry of the circumstellar material around each star. With the equivalent of TIMMI in combination with adaptive optics at one VLT telescope it will become possible to resolve NX Pup also in the L and M, whereas the VLTI will allow high spatial resolution observations of NX Pup at 10 and 20 microns.

Acknowledgements: Many thanks to P.S. Thé and C. Sterken for distributing the LTPV data via CDS.

References

Barth W., Weigelt G., Zinnecker H. 1994, *A&A* **291**, 500.

Bernacca P.L., Lattanzi M.G., Bucciarelli B. et al. 1993 *A&A* **278**, L47.

Bibo E.A., Thé P.S. 1991, A&AS **89**, 319.

Brandner W., Bouvier J., Grebel E.K., et al. 1995 *A&A* **298**, 818.

D'Antona F., Mazzitelli I. 1994, ApJS **90**, 467.

Henning Th., Launhardt R., Steinacker J., Thamm E. 1994, *A&A* **291**, 546.

Krautter, J. 1980, *A&A* **89**, 74.

Schöller M., Brandner W., Lehmann T., Weigelt G., Zinnecker H. 1996 *A&A* submitted.

Sterken C., Manfroid J., Beele, D., et al. 1995 *A&AS* **113**, 31.

Tessier E., Bouvier J., Beuzit J.-L., Brandner W. 1994 *The Messenger* **78**, 35.

Thé P.S., Bibo E. 1990 *The Messenger* **61**, 39.

Weigelt G. 1977, *Optics Commun.* **21**, 55.

E-mail address: Wolfgang Brandner, brandner@astro.uni-wuerzburg.de

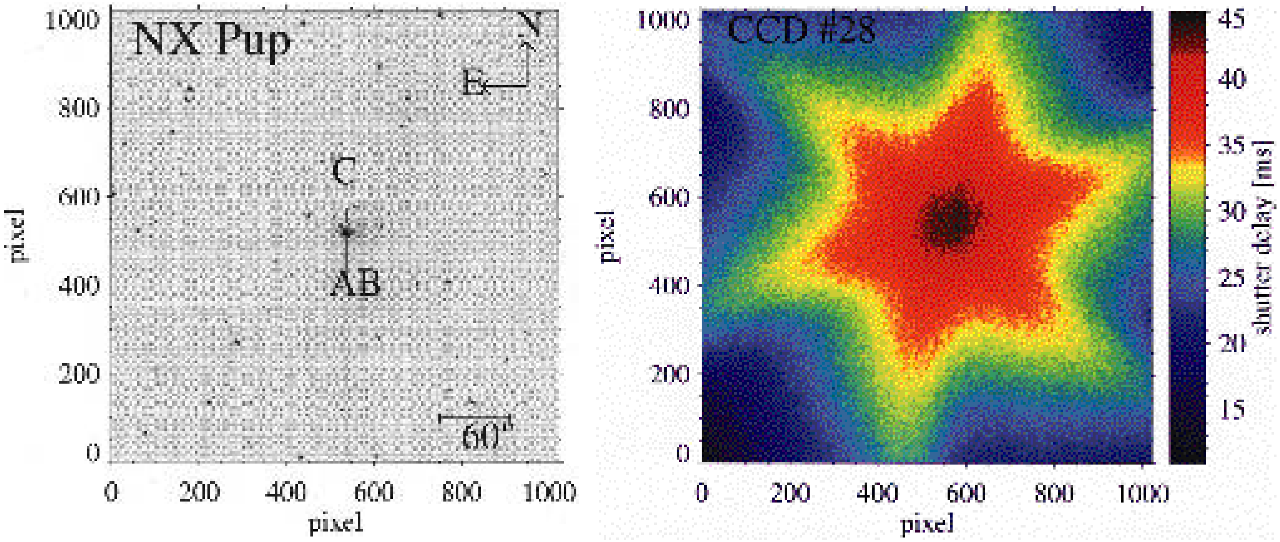

Figure 2: 1.5-s R exposure of the region around NX Pup obtained with the CCD camera at the D1.54-m telescope in 1995 March 11 (left). NX Pup AB (unresolved) and the associated classical T Tauri star NX Pup C are marked. The shutter delay in the central part of the CCD amounts to 45 ms, which in the 1.5-s exposure image induces a photometric error of 3%. The corresponding shutter map is shown on the right.

crease the efficiency of the larger telescopes and to improve the scientific quality of the data).

Data Reduction

Photometric calibration of short-exposure CCD images: shutter maps

All CCD cameras at ESO are equipped with a mechanical shutter. Problems in short exposures (< 10 s) arise from the shutter delay, i.e. the time delay between starting or ending an exposure by sending a signal to the CCD camera and the actual beginning of the shutter movement. Furthermore, mechanical shutters need a certain time to move from the centre of a CCD to its edge and vice versa. The resulting (inhomogeneous) illumination pattern on the CCD leads to gradients across the field and to photometric errors. Mapping the shutter movement yields a typical delay between 50 ms (CCD camera at D1.54-m) and 500 ms (EMMI/Red at the NTT) for the central part of the CCD, which in a 1-s exposure already amounts to a photometric error of 5% to 50%!

This is well known, and the usual advice given to observers to circumvent this problem is not to take exposures shorter than 10 s. However, when observing bright objects (e.g. CCD standard star fields) with a larger telescope, one is forced to defocus the telescope in order to avoid saturation of the brightest stars on the CCD. This in turn induces errors in the photometric transformations for the (usually not defocused) programme stars.

A better approach is to actually map the shutter movement and the resulting illumination pattern on the CCD. The procedure to obtain such a shutter map is straightforward: a series of short-long-short exposures, typically domeflats with exposure times of ≈ 0.5 s (ts) and 3 s (tl) and count rates of a few 1000 ADU (short) to less than 20,000 ADU (long) are repeated eight to ten times. After averaging the two short exposures of each series, the resulting shutter map can be computed by

$$\text{shutter map} = (\text{short} \times \text{tl} - \text{long} \times \text{ts}) \, / \, (\text{long} - \text{short})$$

where "short" and "long" are the raw data (i.e. bias subtracted but not flatfielded) and "ts" and "tl" are the exposure times of the short and the long exposure, respectively.

The resulting shutter map for the CCD camera at the Danish 1.54-m is shown in Figure 2[1]. A comparison of shutter maps obtained several months apart indicate a stability to within 10%. Hence, residual photometric errors for a 1-s scientific ex-

[1] Shutter maps for the CCD cameras at the Dutch 90-cm and the Danish 1.54-m, and EFOSC2 at the ESO/MGP 2.2-m are available via WWW from http://www.astro.uni-wuerzburg.de/~brandner/shuttermaps.html. Shutter maps for EMMI (red & blue) and SUSI will be made available by the NTT team in the near future.

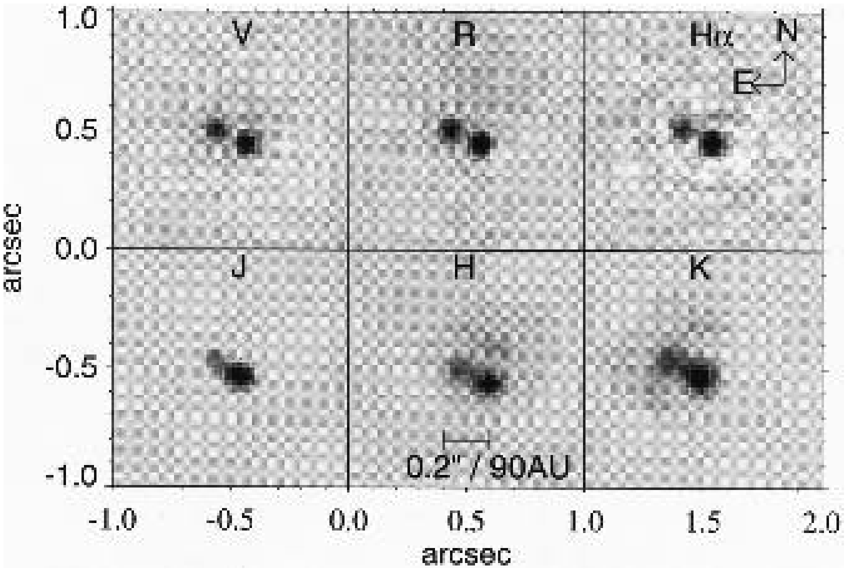

Figure 3: Set of simultaneous high spatial resolution images of NX Pup A and B. The optical data (top) have been obtained with a speckle camera at the ESO/MPI 2.2-m, whereas the near-infrared data have been obtained with ADONIS/SHARP at the ESO 3.6m telescope. The speckle data allow for the determination of the spectral type of the NX Pup B and reveal that the majority of the Hα excess originates in NX Pup A which is also the component with the stronger IR excess.

Simultaneous Optical Speckle and ADONIS Imaging of the 126 mas Herbig Ae/Be Binary Star NX Puppis

W. BRANDNER[1], T. LEHMANN[2], M. SCHÖLLER[3], G. WEIGELT[3], H. ZINNECKER[4]

[1]Astronomisches Institut der Universität Würzburg, Germany
[2]Universitätssternwarte Jena, Germany; [3]MPI für Radioastronomie, Bonn, Germany
[4]Astrophysikalisches Institut Potsdam, Germany

Introduction

We have obtained simultaneous high spatial resolution optical speckle and near-infrared adaptive optics images of the 126 mas Herbig Ae/Be binary star NX Pup and could derive accurate estimates for the evolutionary status of both components. Furthermore, we were able to decompose the overall spectral energy distribution into its constituent parts, namely the contribution of the two stellar photospheres and the infrared excess due to circumstellar material associated with both stars.

The Herbig Ae/Be star NX Pup is located in the Gum nebula at a distance of ≈ 450 pc and belongs to a group of bright PMS stars which have been systematically monitored for more than a decade from La Silla in the course of the Long-Term Photometric Variables project (LTPV, Thé & Bibo, 1990, Sterken et al., 1995 and references therein).

On New Year's Day 1993, NX Pup was resolved as a binary with a separation of 126 mas by the Fine Guidance Sensors (FGS) of the Hubble Space Telescope (HST) in the V band (Bernacca et al., 1993). Exactly one year later (January 1st, 1994) the combined light of the close binary was decomposed from the ground for the first time using ESO's adaptive optics prototype COME-ON+ & SHARP in JHK at the ESO 3.6-m telescope (Brandner et al., 1995, see also Tessier et al., 1994 for details on the image reconstruction).

The combination of the optical HST data, calibrated in flux by interpolating LTPV observations, with the near infrared data obtained with COME-ON+ already allowed for a (crude) determination of the spectral types and luminosities, and hence masses and ages for both components. We could show that both stars are very likely pre-main sequence stars exhibiting an IR excess and that the secondary has a spectral type between mid F and late G. However, by studying more than 350 individual Strömgren photometric measurements which had been accumulated in over 12 years of LTPV monitoring (cf. Fig. 1), we realised that a convergent picture of the evolutionary status of NX Pup A & B could only be obtained by quasi-simultaneous high spatial resolution observations in the optical and near infrared.

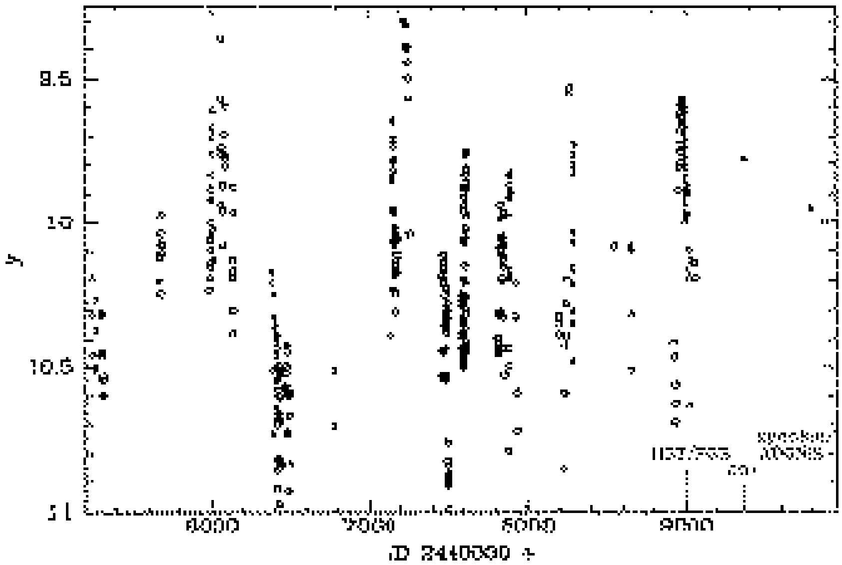

Figure 1: V (y in the Strömgren photometric system) light curve of NX Pup from 1983 to 1995 (compiled from LTPV data, open circles). Note the rapid variations with an amplitude of ≈ 1.7^m. Marked are the dates of the HST/FGS observations, the first NIR adaptive optics observations (CO+), and the current simultaneous data set presented here. At the time of all three high angular resolution observations NX Pup was relatively bright.

Observations

On March 11, 1995, three of La Silla's four largest optical telescopes (D1.54-m, ESO/MPI 2.2-m, ESO 3.6-m) simultaneously observed NX Pup in the optical and in the near infrared utilising two of the most sophisticated high spatial resolution techniques – namely optical speckle in combination with speckle masking reconstruction (Weigelt, 1977) and adaptive optics imaging using ADONIS and the SHARP camera. We obtained simultaneous high spatial resolution images of NX Pup from the V to the K band (cf. Table 1).

The great drawback of all high spatial resolution instruments is their small field of view which makes it very time consuming to obtain absolute photometric calibrations by observing standard stars one by one. Therefore, it proved to be advantageous to have also a "smaller" telescope like the Danish 1.54-m with its "wide field" CCD camera (6′ × 6′ compared to 6″ × 6″ of the speckle camera) available for doing photometric calibrations while at the same time dedicating the larger telescopes to high-resolution imaging alone (a similar approach should be considered for forthcoming high spatial and high spectral resolution observations with the VLT, where flux calibrations could be obtained with an auxiliary telescope thus helping to in-

TABLE 1. Journal of observations (all observations are simultaneous within 3 hrs)

Telescope/instrument	UT (11.3.1995)	Filter (λ_c, FWHM)	Exposure time
D1.54/CCD camera	01:30	B,V,R	5s, 2s, 5s
ESO-MPG 2.2-m/speckle cam.	01:15	V (545 nm, 30 nm)	629×50 ms
ESO-MPG 2.2-m/speckle cam.	00:15, 03:00	R (656 nm, 60 nm)	1927×70 ms
ESO-MPG 2.2-m/speckle cam.	01:00, 02:45	R (656 nm, 30 nm)	2285×70 ms
ESO-MPG 2.2-m/speckle cam.	03:15	Hα (656.3 nm, 4 nm)	1903×70 ms
ESO 3.6-m/ADONIS+SHARP	02:30	H, K	400×0.5 s (each)

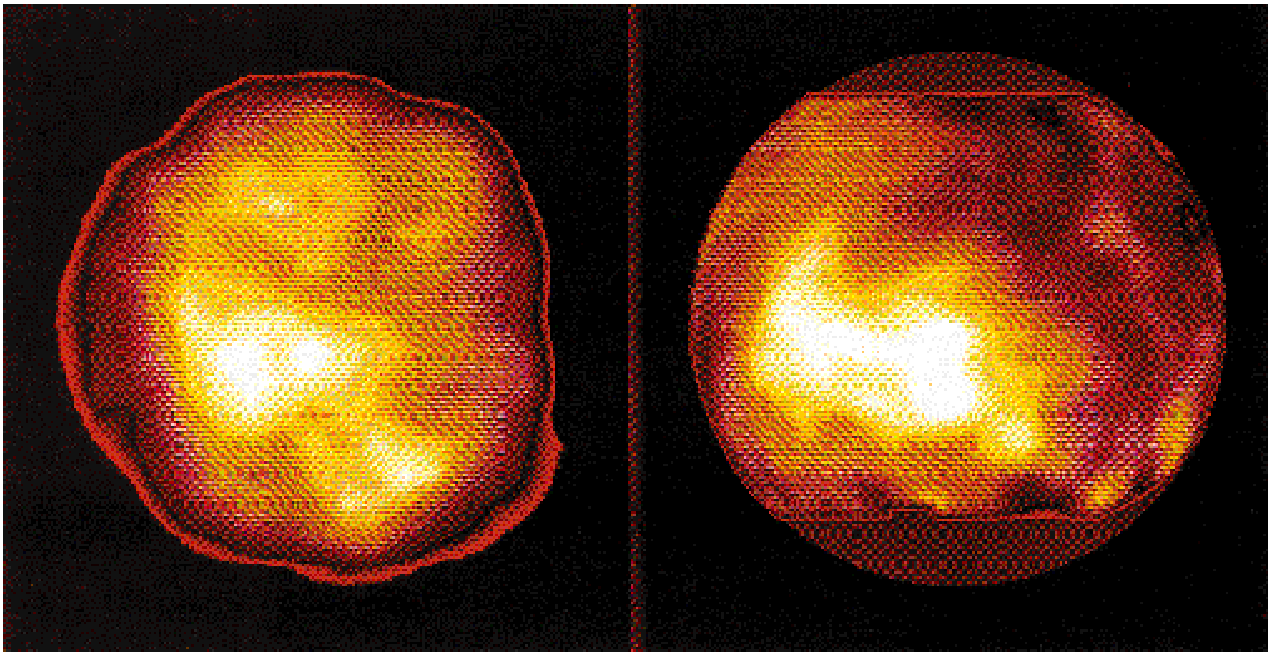

Figure 4: Titan's surface: ADONIS image at 2 micron on the left and Hubble Space Telescope image near 1 micron to the right. The central equatorial bright spot is observed on both, as well as indication of additional features near the limbs. The spatial resolution is similar, the contrast is about 3 times higher in the adaptive optics image.

source in the close vicinity of Titan, in the same filter and with similar exposure time, just after Titan's image recording. A high degree of symmetry could be noticed, showing that the fixed optical aberrations are well corrected by the adaptive optics. The very high signal-to-noise ratio in the PSF allows a very efficient *a posteriori* deconvolution process, using different methods such as Lucy-Richardson, Maximum Entropy and Maximum Likelihood. The final resolution is diffraction-limited (0.13 arcsec) with a sampling of 0.05 arcsec/pixel.

4. Preliminary Analysis and Results

The expected radiance as a function of angle from the centre of the image was modelled using results on the surface albedo and the CH4 absorption coefficients at 2.0 and 2.2 µm from Coustenis et al. (1995, *Icarus* 118, 87–104). The limb effects on each image were then corrected. There is a significant hemispheric asymmetry in the K2 images (more sensitive to the atmospheric contribution than K1), and in particular the southern hemisphere appears brighter than the northern one. After deconvolution, the K2 images show the South limb locally very bright, probably due to a strong aerosol concentration in this area. The K1 images, corresponding to the centre of the 2.0 micron atmospheric window, allow us to sound deeper in the atmosphere and down to the surface and exhibit an additional bright feature near the equator (Fig. 2).

We have deduced the surface contribution in our final images by subtracting K2 images from the K1 ones, as explained in section 3. Our images exhibit a large, well defined equatorial bright spot associated with smaller and fainter features in the southern hemisphere of Titan, all rotating over six consecutive nights at the expected rotation rate of Titan's solid body (Fig. 3).

These findings are in agreement with the Hubble Space Telescope images (Smith et al., 1995, *Icarus*, in press) both on their location and shapes (Fig. 4). As expected from the properties of scattering extinction, the contrast of the surface features is higher in our infrared images (~ 30%) than on HST red images (~ 10%). The spatial resolution (0.13 arcsec) is very similar.

The COME-ON+ Titan images, joined to HST observations, lead to the firm conclusion that the observed features are definitely due to Titan's surface structures. Titan's surface is then inhomogeneous. The model of a global ocean covering Titan must be ruled out. From comparison with 1993 images, under processing, we tentatively infer that large cloud structures are not present in the troposphere.

We have performed a preliminary analysis of 1994 CVF images near 2 micron. At 2.10 µm, in the wing of the H_2O ice band, the absorption by liquid hydrocarbons (C_2H_4, C_2H_6) is expected to be strong. However, the 2.10 µm images are quite similar to K1 images. This does not favour the presence of large (clean) hydrocarbons lakes in the "dark regions".

At 2.00 µm, at the centre of the ices absorption bands (H_20, CO_2, NH_3), a decrease in the contrast between bright and dark regions would be expected if the bright equatorial spot is related to the prominent presence of ices. The 2.00 µm images do not show such a contrast decrease. They are intermediate between K1 images and K2 stratospheric images, suggesting that the surface contribution to the flux is lower than in K1 and that the entire surface of Titan is quite dark in the ices band.

There is no evidence, at the present step of data reduction, for chemical differences between the bright features and their environment.

We have new images recorded using ADONIS in October 1995, near Titan's Western Elongation, that allow us to recover full coverage of the satellite's rotation and should provide more clues for understanding the chemical nature of the bright and dark features. The trailing hemisphere appeared completely dark in the HST images. In our data, however, with a contrast three times higher, we may hope to distinguish new features. The results should provide us with powerful tools for optimising the observing programmes of the instruments of the Cassini-Huygens ESA-NASA mission and in particular of the VIMS instrument on the orbiter and the DISR on the Huygens Probe which both will be able to clearly image Titan's surface.

E-mail address: A. Coustenis
coustenis@megasx.obspm.fr

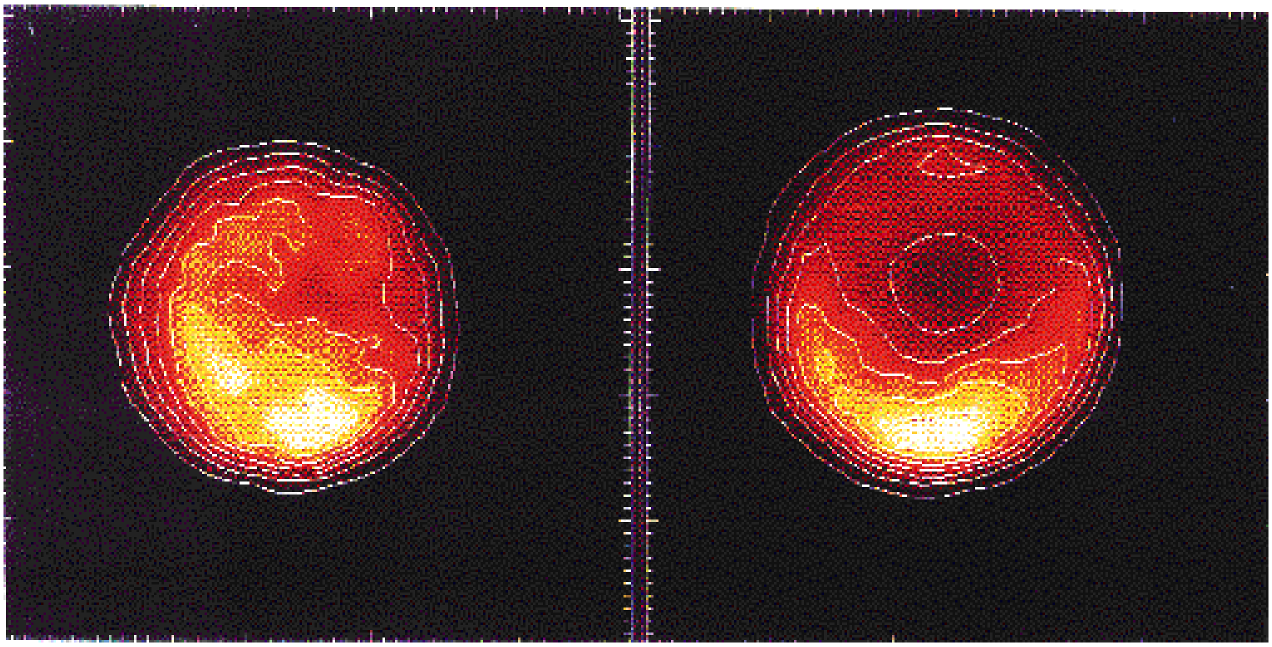

Figure 2: Titan observed in the K1 and K2 narrow-band filters, centred at 2.0 and 2.2 µm, during the night of Sept. 16, 1994. The orbital phase is about 85 degrees LCM (Greatest Eastern Elongation). The images were corrected for flat-field and centre-to-limb effects and deconvoluted by the associated PSF. The images were also oversampled by a factor 3 and then smoothed (with conservation of the recovered spatial resolution – 0.13 arcsec – and have isophot contours). Note the hemispheric asymmetry in the K2 image (more sensitive to the atmospheric contribution than K1), and in particular the bright south limb, probably due to a strong aerosol concentration in this area. The K1 image allows us to sound the deeper atmosphere and the surface. It exhibits an additional bright feature near the equator with respect to K2 images.

surface in the near infrared transparent windows of Titan's atmosphere, in spite of its small angular diameter (0.8 arcsec as seen from Earth) and of degradation effects due to the atmospheric turbulence.

3. Observations and First-Level Data Reduction

Titan was observed in the K1 and K2 narrow-band filters (2.0 and 2.2 µm) during the nights of September 14–18, 1994. The orbital phase is about 85 degrees LCM (Longitude of Central Meridian) on September 16, that is close to Greatest Eastern Elongation.

In K1, one third of the recorded flux is expected to have been reflected by Titan's surface. In K2 the recorded flux is entirely due to backscattering by the stratospheric aerosols. We have deduced the surface contribution in our K1 images by subtracting the stratospheric contribution deduced from the K2 images, according to a weighting factor estimated from the stratospheric transmission in K1 and K2, above the expected level of the aerosols responsible for this stratospheric contribution to the recorded images.

The raw images were corrected for bad pixels and correlated noise, for the sky contribution and for flat-field effects. They are diffraction-limited thanks to the efficiency of the COME-ON+ adaptive optics system. The Point Spread Function is obtained by recording a stellar

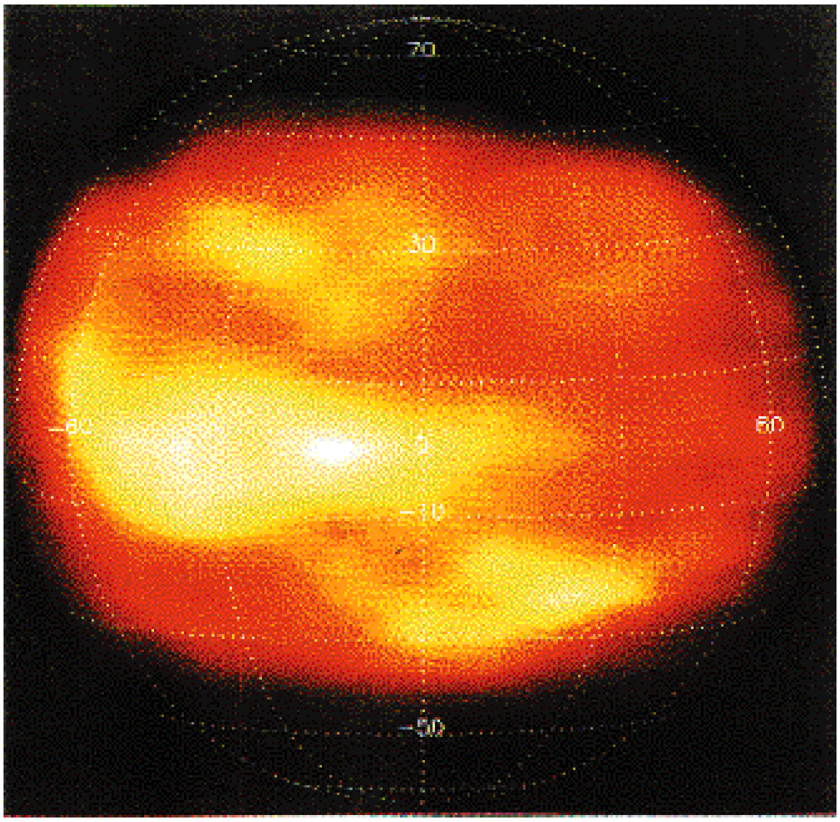

Figure 3: Titan's surface at 2 micron. This image was obtained after subtraction of two thirds of the intensity of the K2 image from the K1 image. This treatment leaves a significant bright equatorial region, centred near 114 degrees LCM and extending over 30 degrees in latitude and 60 degrees in longitude. Other bright spots are visible in the S-W region (near 25° S) and in the northern part (near 30° N).

and to clarify the nature of the absorption feature.

In parallel, the long-term evolution of the optical luminosity of the pulsar has been studied and found to be poorly constrained by the data available so far. Fitting all the available flux measurements as a function of time, we obtain a decrement of 0.008 ± 0.004 mag/yr which is consistent with the expected value of ~ 0.005 mag/yr. However, in view of the error to be attached to the data points, the result is far from conclusive and no claim for a measure of the secular decrease can be put forward at this time. New precise measurements are required to proof the presence of a secular decrease and to quantify its actual value.

Acknowledgements

We are pleased to thank S. Molendi and M.-H. Ulrich who kindly reserved part of their observing run to perform new observations of the Crab.

References

[1] Bessel, M.S.,1990 PA.S.P. **102**, 1181.
[2] Bignami, G.F. et al., 1987 *Ap.J.* **319**, 358.
[3] Caraveo, P.A., Bignami, G.F. and Mereghetti, S., 1994a *Ap.J. Lett.* **422**, L87.
[4] Caraveo, P.A., Mereghetti, S. and Bignami, G.F., 1994b *Ap.J. Lett.* **423**, L125.
[5] Cocke W.J., Disney M.J. e Taylor D.J., 1969, *Nature* **221**, 525.
[6] Kristian, J. et al., 1970, *Ap. J.,* **162**, 475.
[7] Kristian J., 1978, *BAAS,* **10**, 245.
[8] Lasker B.M., 1976 *Ap. J.* **203**, 193.
[9] Melnick J., Dekker H. and D'Odorico S., 1992 *EMMI Operating Manual.*
[10] Middleditch J. and Pennypacker C.,1985 *Nature* **313**,659.
[11] Middleditch J., Pennypacker C. and Burns M.S., 1987 *Ap.J.* **315**, 142.
[12] Oke J.B., 1969, *Ap.J.* **156**, L49.
[13] Pacini F.,1971, *Ap.J.,* **163**, L17.
[14] Pacini F. e Salvati M.,1987, *Ap.J.,* **321**, 447.
[15] Percival J.W. et al., 1993, *Ap. J.,* **407**, 276.
[16] Savage B.D. & Mathis J.S., 1979, *A.R.A.& A.,* **17**, 73.
[17] Stobie, R.S., Sagar, R. and Gilmore, G., 1985 *Astron. Astrophys. Suppl.* **60**, 503.

E-mail address: nasuti@ifctr.mi.cnr.it
(Francesco Nasuti)

2-Micron Images of Titan by Means of Adaptive Optics

M. COMBES, L. VAPILLON, E. GENDRON, A. COUSTENIS and O. LAI

Département de Recherche Spatiale (DESPA), Observatoire de Paris
Unité de Recherche Associée au CNRS (URA 264), Meudon, France

1. Introduction

In this paper we present spatially resolved images of Titan's surface obtained in September 1994, by means of adaptive optics at the ESO 3.6-metre telescope, in narrow-band filters in the near infrared spectral range, defined in such a way that the contribution of the flux reflected by Titan's ground surface is maximised.

Spatially resolved images of Titan would provide significant clues to understand better the controversial nature of Titan's surface. Imagıng Titan is a difficult task due to Titan's small angular diameter as seen from Earth (0.8 arcsec). It must be performed in the near infrared since Titan's surface cannot be observed in the visible range due to a uniform and opaque layer of aerosols in Titan's stratosphere.

During the definition phase of the Cassini-Huygens ESA-NASA mission, T. Encrenaz and M. Combes (DESPA, Paris Observatory) and, independently, M. Tomasko, P. Smith and colleagues (Univ. of Arizona) have shown that there must exist transparency windows in Titan's atmosphere where both the molecular absorption and the scattering extinction are sufficiently faint to allow to probe the Titan's surface. This has been confirmed by several authors who observed photometric or spectroscopic fluctuations of Titan's near infrared flux. The most favourable spectral range is in the near infrared around 2.0, 1.6, 1.28, 1.08 and 0.94 micron.

COME-ON+ is the first adaptive optics system devoted to astronomy. It has been developed for ESO by the Space Research Department (DESPA) of Paris Observatory with the collaboration of French companies (ONERA and LASERDOT).

2. Adaptive Optics

The aim of adaptive optics is to correct in real time the phase perturbations induced by the atmospheric turbulence on the incident wavefront reaching the telescope. These perturbations are measured by a wavefront sensor (Fig. 1) using part of the light of the observed source (if quite stellar-like and sufficiently bright) or of a close star in the isoplanetic field (~30 arcsec). Opposite phase corrections are then applied thanks to a thin deformable mirror in a pupil plan (O. Saint Pé et al., 1993, Icarus 105, 263).

The first spatially resolved image of Titan's disk was obtained, in May 1991, by DESPA (O. Saint-Pé, 1993), demonstrating the feasibility of mapping Titan's

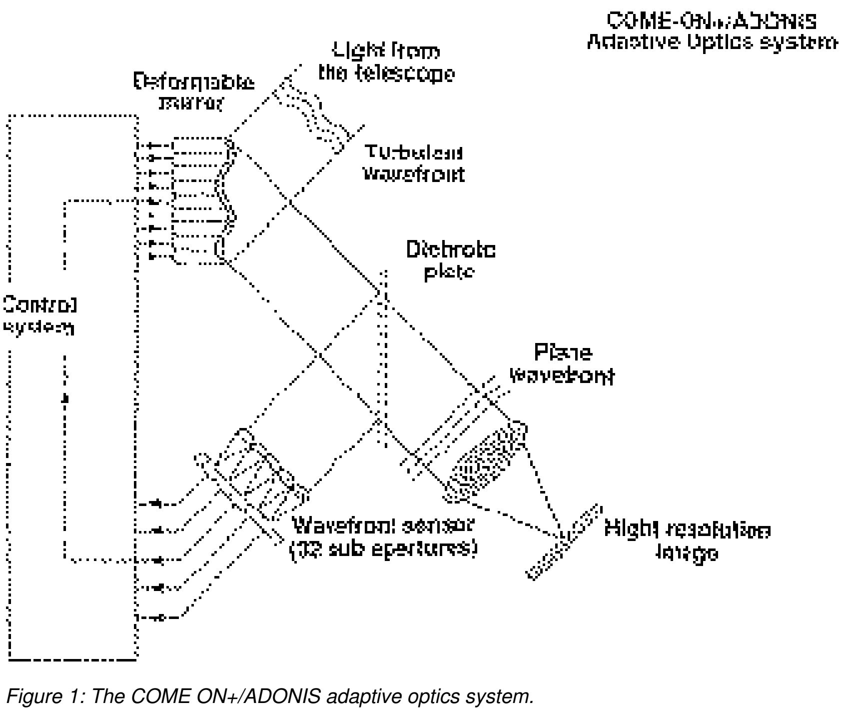

Figure 1: The COME ON+/ADONIS adaptive optics system.

6 arcmin along the remnant. The two-dimensional spectrum was reduced using the spectral analysis packages LONG and ALICE available in MIDAS. After standard reduction (cosmic ray cleaning, bias subtraction and flat-fielding), the wavelength calibration was performed using the spectrum of an He calibration lamp. After sky-subtraction, a one-dimensional averaged spectrum of the pulsar was extracted. The spectrum was then corrected for the atmospheric extinction (z = 1.61), using standard tables for La Silla available in the ESO database, and flux-calibrated using, as a reference, the spectrum of the standard star Feige 24 (Oke, 1974). To obtain a "clean" spectrum of PSR0531+21, the nebular background was also subtracted. The subtraction of emission/absorption features from the nebula was difficult because of the wavelength scatter induced by the spread in radial velocity of the expanding gas. Residual features in the pulsar spectrum, clearly identified as due to excess or defect of subtraction, were removed. The spectrum was finally corrected for the interstellar extinction using an E(B – V) = 0.51 ± 0.04 (Percival et al., 1993) and the extinction curve of Savage & Mathis (1979).

New photometric observations of the Crab Pulsar have been performed on October 1995 by S. Molendi. 7 one-minute V filter exposures have been collected with EFOSC2 at the ESO 2.2-m telescope (Fig. 2). The seeing was around 0.9 arcsec, with an airmass ~ 1.2. Two 3-minute images of the Stobie field F117-18 (Stobie et al., 1987) have been used to compute the zero point magnitude. The aperture photometry, computed on the average frame, yields a magnitude of 16.72 ± 0.05 for the Crab pulsar, where the uncertainty includes both photometry and calibration errors.

3. The Spectrum

The flux distribution *($logF_\nu$ vs. $log\nu$)* of the Crab Pulsar is plotted in Figure 1, to be compared with the one reported by Oke (1969) obtained with much scanter data. The spectral shape is well fitted by a flat power law ($F_\nu \propto \nu^\alpha$) with a best fit spectral index α = –0.10 ± 0.01. For comparison, Oke (1969) gave a spectral index α = –0.2 with no quoted uncertainty, while Percival et al. (1993), fitting the observed fluxes computed at the peak of U, B and V bands, obtained α = –0.07 ± 0.30. The power law spectral index arising from our spectrum is far more precise than anything available so far.

An interesting, unidentified, absorption feature is visible in the otherwise flat continuum of the pulsar close to λ = 5900 Å. Since the feature is barely recognisable also in the raw data, but not in the spectroscopic flats, we are confident that it is real and not due to a variation in the CCD response. However, we can not exclude that the observed feature is due to a data analysis artifact induced by the interpolation of the rather coarse spectral data available for Feige 24 (which has flux value every 80 Å, i.e. 40 times worse than our spectral data).

The origin of this absorption dip is not very clear. Since this has not been observed in the spectrum of the nebula, it can not be due to absorption by the interstellar medium or the nebula itself. An alternative, more likely, explanation suggests that the absorption takes place very close to the pulsar.

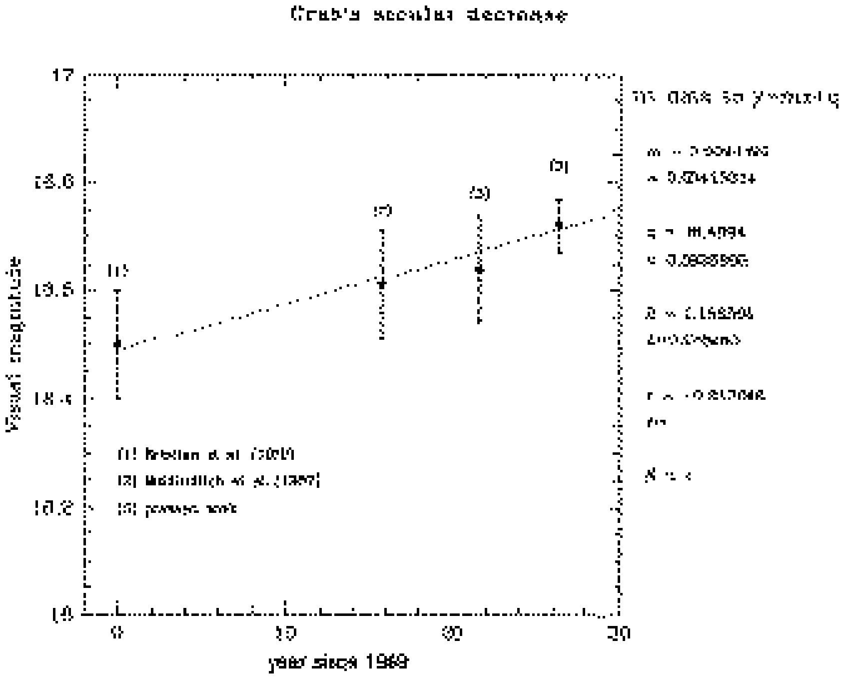

Figure 3: Linear fit of the V magnitudes of the Crab Pulsar vs. time. An apparent correlation is visible, which supports the presence of a decrement in the optical luminosity of the pulsar. The best fitting slope corresponds to a decrement of 0.008 ± 0.004 mag/yr, where the low significance is due to the large errors bars associated with the first three measures.

4. The Secular Decrease

Using the appropriate value for the Crab spin down ($\dot{P}$ ~ 4 10^{-13}s s^{-1}) a secular decrease of ~ 0.005 mag/year is expected. A decrement of ~ 0.5%/yr in the optical flux of the Crab pulsar, based on relative photometry measurements, was indeed announced by Kristian (1978), but without mentioning any magnitude value nor any uncertainty. A measure of Crab's magnitude compatible with the expected decrement was later given by Middleditch, Pennypacker and Burns (1987). In order to have a better grasp of the secular decrease, we compared the published values of the Crab V magnitude with the results of our recent observations. We used our photometric point plus the V magnitude obtained integrating the Crab spectrum over the Johnson's V band, and convolving with a model filter response (Bessel, 1990), yielding a value of 16.64 ± 0.1.

In order to investigate the time dependence of the optical luminosity we plotted our values together with previous measurements from Kristian et al. (1970) and Middleditch et al. (1987). To allow a direct comparison, no interstellar extinction correction has been applied to the visual magnitudes. A linear regression to all the available data was then computed. The points in Figure 3 show a significant correlation (~ 90 %), corresponding to a monotomic increase of the visual magnitude with a rate of 0.008 ± 0.004 mag/year i.e. a value certainly in agreement with the theoretical one (~ 0.005 mag/ year), although of limited significance. Actually, the big error bars attached to the first three measures make it difficult to assess the reality of the effect as well as its real magnitude.

5. Conclusions

The first high-quality optical spectrum of the Crab Pulsar has allowed the accurate measurement of the pulsar spectral shape in the visible domain.

While a flat power law (α = 0.1 ± 0.01) describes well the optical spectrum, a dip is found at λ = 5900 Å. Although of unknown origin, it is probably to be associated with the pulsar (or its immediate surroundings) since no evidence for a similar dip is found in the adjacent nebular spectra. More observations are obviously needed to confirm the existence

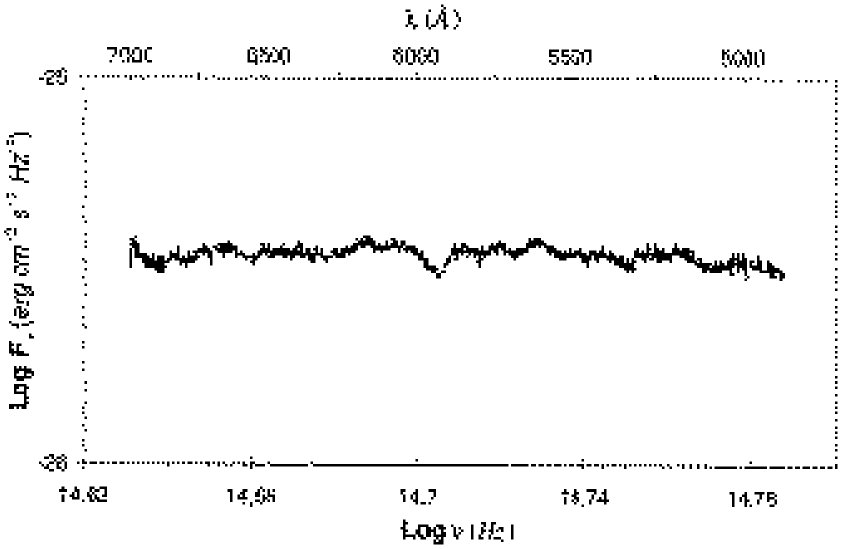

Figure 1: Spectrum of the Crab Pulsar in the wavelength range 4900– 7000 Å as measured with EMMI after a 40-min exposure. The spectrum has been sky subtracted and corrected for interstellar absorption. The flux distribution is modelled by a power law with a best fitting spectral index α = –0.10 ± 0.01. A broad (Δλ ~ 100 Å) absorption feature centred on λ = 5900 Å is visible.

For almost 10 years, the Crab was the only INS seen at optical wavelength. The Vela pulsar was observed in 1976 (Lasker, 1976) and PSR0540-69 in 1985 (Middleditch and Pennypacker, 1985). Thus, it appears natural that the Crab was used as a test case for the understanding of the optical, nonthermal emission from pulsars. The original model of Pacini (1971) explains the optical emission of young pulsars as synchrotron or curvature radiation produced by energetic particles moving in the pulsar magnetosphere, close to the light cylinder. As a result, a simple dependence is found between the optical emission and the pulsar's key parameters. In particular, the bolometric luminosity should scale with B^4P^{-10} where B is the pulsar's magnetic field and P is the period. Using the Crab as a reference, this law was used by Pacini (1971) to predict the optical luminosity of the Vela pulsar. Indeed, a few years later, the Vela pulsar optical counterpart was detected at the expected magnitude (Lasker, 1976).

The above model also implies a regular decrement of the optical luminosity due to the pulsar's slow down ($L \propto P$). When Kristian (1978) claimed the evidence for the Crab secular decrease, the Pacini's law was considered proved.

Doubts were raised with the discovery of optical pulsations from PSR0540-69 (Middleditch & Pennypacker, 1985), but its apparent overluminosity could be explained revisiting the model for the effects of the pulsar's duty cycle (Pacini & Salvati, 1987). More recently, optical counterparts have been found for Geminga (Bignami et al., 1987) and proposed for PSR0656+14 (Caraveo et al., 1994a) and PSR1509-58 (Caraveo et al., 1994b).

However, the Crab remains by far the brightest of the optically emitting INSs, hundreds of times brighter than PSR054069 (V = 22.4), Vela (V = 23.6) and PSR1509-58 (V = 22) and thousands of times brighter than Geminga (V = 25.5) and PSR0656+14 (V = 25). Therefore, it is the only INS within reach of optical spectroscopy. Nevertheless, our knowledge of the optical spectrum of the Crab Pulsar rests mainly on the pioneering observations of Oke (1969), and on multicolour photometry (Kristian et al., 1970; Middleditch et al., 1987; Percival et al., 1993). Thus, it seemed appropriate to bring the knowledge of the Crab optical emission up to modern astronomy standards.

2. The Observations

A 40-minute spectrum of the Crab Pulsar was taken on January 1991 with the NTT. The telescope was equipped with the ESO Multi Mode Instrument (EMMI) (Melnick, Dekker and D'Odorico, 1991) mounting a "Red" THX 10242 CCD detector. The instrument was operated in the Red Medium Dispersion Mode (REMD), with a projected pixel size of 0.44 arcsec. A medium dispersion grating blazed at 6200 Å was used, providing a spectral resolution of 2.1 Å/pixel in the wavelength range 4900–7000 Å. According to the seeing conditions (~ 1.2 arcsec) the Pulsar was centred in a 1.5 arcsec slit, with the long axis oriented East-West and extending

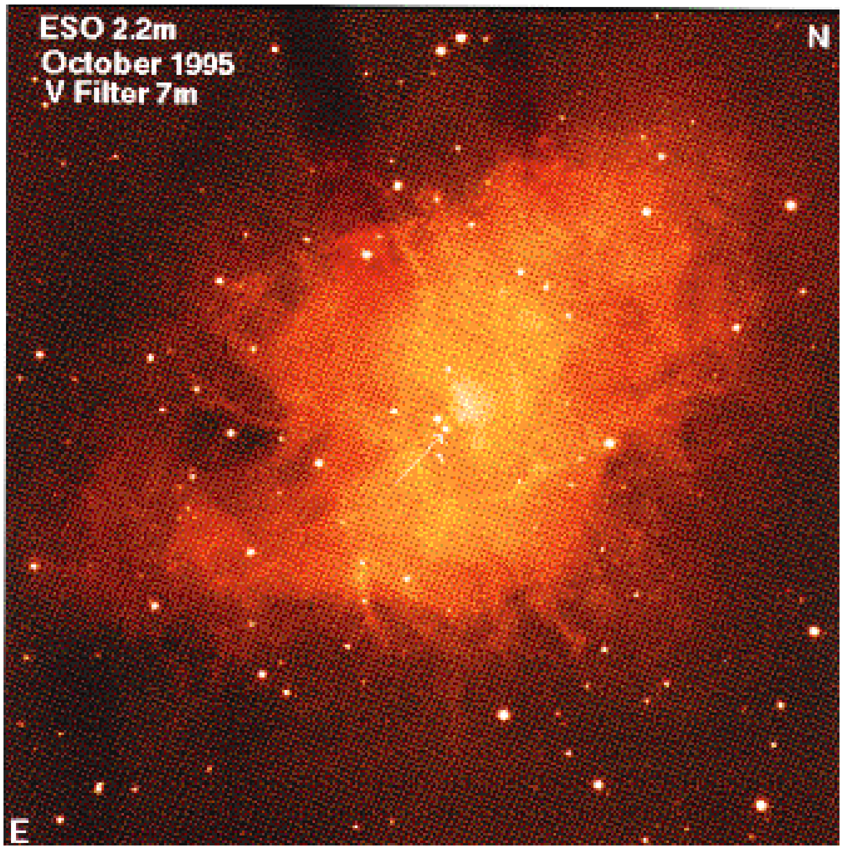

Figure 2: V filter image of the Crab Nebula taken on October 1995 with EFOSC at the ESO 2.2-m. The Crab Pulsar is indicated by the arrow (Courtesy S. Molendi and M.-H. Ulrich).

the abundance of HCO^+ decreases by a factor of ~ 20 (Iglesias & Silk, 1978). The derived [HCO^+]/[CO] ratios in the lobes of Sandqvist 136 then give further support to the notion that the abundances in the lobes are a product of shock chemistry.

In addition to the wing emission detected toward the lobes of Sandqvist 136 in the lines of SiO and CH_3OH, we note the presence of emission at velocities comparable to the systemic velocity of the globule. In particular for silicon monoxide, emission in the velocity range of the ambient cloud is observed only at the position of the lobes. This can be appreciated in Figure 6 which shows velocity-position diagrams of the emission in the SiO lines along the symmetry axis of the outflow. The strength of the emission in the red lobe is roughly constant with velocity, with peaks at –4.1 and –0.8 km s^{-1}, while in the blue lobe the emission peaks at a velocity of –5.0 km s^{-1}, close to the ambient cloud velocity. This result suggests that the enhancement of SiO and CH_3OH molecules might be due to two different processes: heating of grains within the ambient core medium by the UV radiation produced in the shocks, which can evaporate volatile grain mantles and trigger gas-phase reactions, and direct shock processing of dust located within the shocked region. The low velocity emission would then arise from pre-shock gas heated by the radiation from the hot post-shock gas, while the high velocity emission arises from the cold post shock gas.

Conclusions and Outlook

Multiline molecular observations toward the Sandqvist 136 dark globule have revealed a spectacular enhancement in the abundance of silicon monoxide and methanol molecules at the lobes of the associated bipolar outflow. The spatial distribution and broad line profiles of the SiO and CH_3OH emission indicates a common mechanisms for the excitation of these lines: shocks. We conclude that the shocks created by the interaction between flows and the surrounding medium play a major role in the production of these molecules. In particular the strong emission observed in the methanol lines suggest that these lines can be used as powerful signposts of the chemical impact of bipolar outflows on the surrounding ambient medium. It appears that the Sandqvist 136 shock produces the evaporation of icy grain mantles resulting in the injection into the gas phase of large amount of ice mantle constituents, such as methanol. Further, the shock seems to be sufficiently powerful that refractory dust grains are partially destroyed, liberating into the gas phase a significant amount of Si atoms that are later converted to SiO by ion-molecule reactions and/or shock chemistry. Finally, we find that the SiO and CH3OH emission detected toward the lobes not only traces shocked outflowing gas but also ambient medium gas that has been heated by the UV radiation from the hot post shock regions.

It has been suggested that the strength of the emission in diverse trace molecules might be considered an indicator of the evolutionary stage of bipolar outflows (Bachiller & Gómez-González, 1992). It would appear that the profuse emission observed in the lines of methanol and silicon monoxide from the Sandqvist 136 outflow implies that we are witnessing an early stage of the outflow phase in which molecules in icy mantles and atoms in dust grains are efficiently liberated back into the gas phase. How much of the enhancement factor depends on wind velocity and/or on evolutionary age has not, however, yet been established. The determination of the abundance of more complex organic molecules in the lobes, such as CH_3OCH_3, $HCOOCH_3$, and CH_3CN, which can potentially serve as clocks of the evolutionary state of the outflows (van Dishoeck & Blake, 1995), should be obtained to provide answer to these questions.

References

André, P. 1995, *Astr. & Spa. Sci.* **224**, 29.
André, P., Martín-Pintado, J., Despois, D., & Montmerle, T. 1990, *A&A* **236**, 180.
Bachiller, R., Cernicharo, J., Martín-Pintado, J., Tafalla, M., & Lazareff, B. 1990, *A&A* **231**, 174.
Bachiller, R., Fuente, A., & Tafalla, M., 1995, *ApJ* **445**, L51.
Bachiller, R., & Gómez-González, J. 1992, *A&AR* **3**, 257.
Bachiller, R., Liechti, S., Walmsley, C.M., & Colomer, F. 1995, A&A **295**, L51.
Bachiller, R., Martín-Pintado, J., & Fuente, A. 1991, *A&A* **243**, L21.
Bally, J., & Lada, C.J. 1983, *ApJ* **265**, 824.
Bally, J., Lada, E., & Lane, A.D. 1993, *ApJ* **418**, 322.
Bourke, T.L., Garay, G., Lehtinen, K.K., Köhnenkamp, I., Launhardt, R., Nyman, L.-A., May, J., Robinson, G., & Hyland, A.R. 1996, *ApJ* submitted.
Bourke, T.L., Hyland, A.R., Robinson, G., James, S.D., & Wright, C.M. 1995, *MNRAS* **276**, 1067.
Charnley, S.B., Tielens, A.G.G.M., & Millar, T.J. 1992, *ApJ* **399**, L71.
Fukui, Y., Iwata, T., Mizuno, A., Bally, J., & Lane, A.P. 1993, in *Protostars and Planets III*, eds. E.H. Levy & J. Lunine (Tucson: Univ. Arizona Press), 603.
Lada, C.J. 1985, *ARA&A* **23**, 267.
Lada, C.J., & Fich, M. 1996, *ApJ* in press.
Hartquist, T.W., Oppenheimer, M., & Dalgarno, A. 1980, *ApJ* **236**, 182.
Iglesias, E.R. & Silk, J. 1978, *ApJ* **226**, 851.
Martín-Pintado, J., Bachiller, R., & Fuente, A. 1992, *A&A* **254**, 315.
Mikami, H., Umemoto, T., Yamamoto, S., & Saito, S. 1992, *ApJ* **392**, L87.
Millar, T.J., Herbst, E., & Charnley, S.B. 1991, *ApJ* **369**, 147.
Mitchell, G.F. 1987, in Astrochemistry, IAU Symposium No. 120, 275.
Mundt, R. 1988, in *Formation and Evolution of Low Mass Stars*, eds. A.K. Dupree and M.T.V.T. Lago, 257.
Neufeld, D.A., & Dalgarno, A. 1989 *ApJ* **340**, 869.
Raga, A., & Cabrit, S. 1993, *A&A* **278**, 267.
Reipurth, B. 1991, in *The Physics of Star Formation and Early Stellar Evolution*, eds. C.J. Lada and N.D. Kylafis, 497.
Rodríguez, L.F., Ho, P.T.P., & Moran, J.M. 1980 *ApJ* **240**, L149.
Sandqvist, A. 1977, *A&A* **57**, 467.
Snell, R.L., Loren, R.B., & Plambeck, R.L. 1980, *ApJ* **239**, L17 .
Turner, J.L., & Dalgarno, A. 1977, *ApJ* **213**, 386.
van Dishoeck, E.F. & Blake, G.A. 1995, *Astr. & Spa. Sci.* **224**, 237.
van Dishoeck, E.F., Blake, G.A., Draine, B.T., & Lunine, J.I. 1993, in *Protostars and Planets III*, eds. E.H. Levy & J.I. Lunine (Tucson: Univ. Arizona Press), 163.
Zhang, Q., Ho, P.T.P., Wright, M.C.H., & Wilner, D.J. 1995, *ApJ* **451**, L71.

E-mail address:
guido@calan.das.uchile.cl (Guido Garay)

On the Optical Emission of the Crab Pulsar

E.P. NASUTI[1, 3], R. MIGNANI[1], P.A. CARAVEO[1] and G.F. BIGNAMI[1, 2]

[1]Istituto di Fisica Cosmica del CNR, Milan, Italy; [2]Dipartimento di Ingegneria Industriale, Università di Cassino, Italy; [3]Università degli Studi di Milano, Italy

1. Introduction

The Crab Pulsar (PSR0531 +21) was the first Isolated Neutron Star (INS) detected at optical wavelengths. It is identified with a star (V ~ 16.5) near the centre of the Crab Nebula, the remnant of the supernova explosion observed in the summer of 1054. The identification has been confirmed by the discovery of pulsed optical emission at the radio period (Cocke et al., 1969).

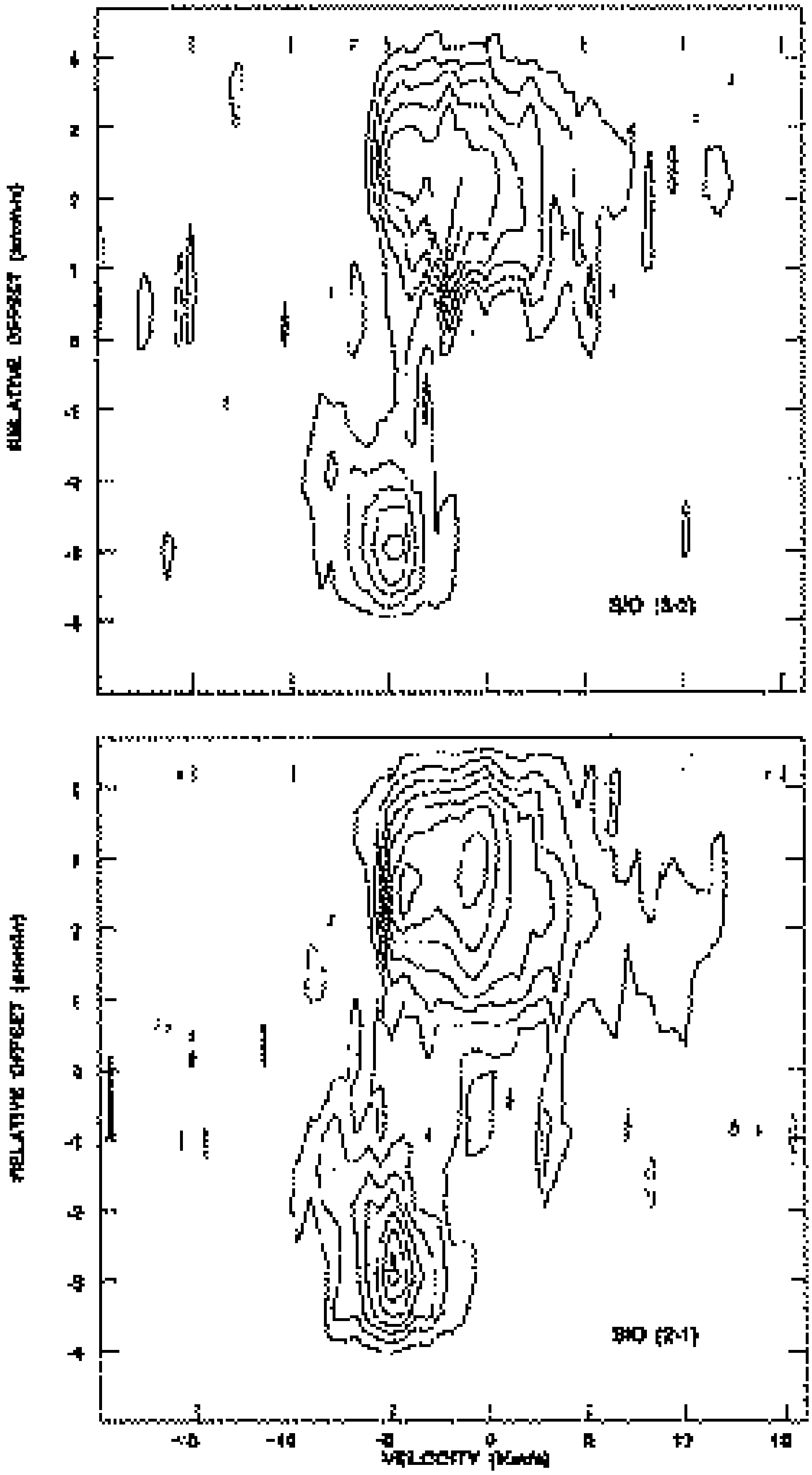

Figure 6. Position-velocity diagram of the SiO emission along the symmetry axis of the outflow. Top: SiO(3 →2). Contour levels are { –1, 1, 2, 3, 4, 5 and 6} × 0.030 K. Bottom: SiO(2 →1). Contour levels are { –1, 1, 2, 3, 4, 5, 6 and 7} × 0.0275 K.

toward the Sandqvist 136 outflow are produced in the gas-phase shock chemistry or released directly from the dust grains by shock evaporation remains to be investigated.

The high abundance of SiO molecules is most likely due to the injection into the gas phase, by shocks, of Si from a population of refractory grains which are composed of silicates and graphites. Once silicon is injected into the gas phase, chemical models based on ion-molecule reactions predict a large abundance of SiO molecules (Turner & Dalgarno, 1977; Hartquist, Oppenheimer & Dalgarno, 1980). Models of the chemistry in regions behind fast dissociative shocks predict a substantial enhancement in the abundance of SiO molecules (Neufeld & Dalgarno, 1989). In particular, for shocks with velocities of 60–80 km s^{-1} propagating in a gas with pre-shock density of 10^4 cm^{-3} (about the density of the Sandqvist 136 globule of 5×10^3 cm^{-3}; Bourke et al., 1996) the predicted column densities of SiO molecules are ~ 2 – 4 $\times 10^{12}$ cm^{-2}, similar to those derived in the lobes of the Sandqvist flow. A possible drawback with dissociative shock models is that the predicted temperatures of the post-shock gas are high (~ 200 K), while the derived rotational temperatures are an order of magnitude smaller. Since the post-shock temperature in C shocks are much lower than in J shocks of the same speeds, the former type of shocks would appear as most promising to explain the observed characteristics of the Sandqvist flow. In particular the synthesis of molecules from atoms and ions can be highly efficient behind non-dissociative C-type shocks. The detection of profuse SiO emission from other highly collimated bipolar outflows have been reported by Bachiller, Martín-Pintado & Fuente (1991), Mikami et al. (1992), Martín-Pintado et al., (1995), and Zhang et al. (1995).

The large [CH_3OH]/[CO] abundance ratio of the outflowing gas in the Sandqvist lobes, greater than in quiescent dark clouds by factors of ~ 200, can not be explained by gas phase chemistry alone (Millar, Herbst & Charnley, 1991). Similar enhancements in the abundance of methanol in other young bipolar outflows have been reported by Bachiller et al. (1995). The large increase in the CH_3OH abundance is most likely the result of desorption from dust grains due to shocks (Charnley, Tielens & Millar, 1992). Refractory grains are likely to be surrounded by icy grain mantles, whose compositions depend on the physical conditions of the ambient medium. Molecules such as H_2O and CH_3OH are expected to dominate in atomic hydrogen-rich ambient medium such as that of molecular clouds. Shocks can raise the temperature of the gas evaporating the icy organic mantles of the grains and returning these material to the gas phase.

We also find that the [HCO^+]/[CO] abundance ratio of the outflowing gas in Sandqvist 136 is smaller than in quiescent dark clouds by a factor of ~ 5. Theoretical models of gas phase chemistry behind shocks predict that the abundance of molecules such as HCO^+, CN, and H_2CO should decrease with respect to the pre-shock abundances (Iglesias & Silk, 1978; Mitchell, 1987). For instance, theoretical calculations of a 10 km s^{-1} shock propagating into a cloud with a pre-shock density of 10^4 cm^{-3}, show that

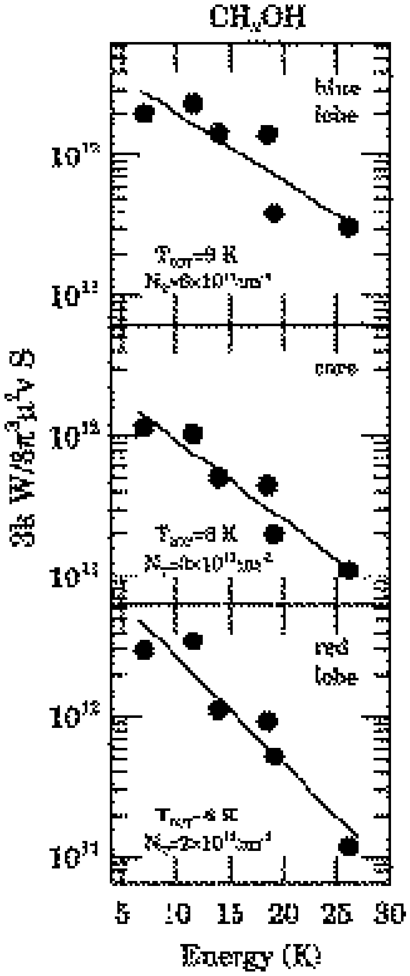

Figure 5. Rotation diagrams for the methanol transitions observed toward the red lobe, central core, and blue lobe of Sandqvist 136. The lines correspond to least squares linear fits to the observed data. The derived values of the rotational temperature and total column density are given in the lower left corner.

in the blue and red wings of the SiO(3→2), $CH_3OH(3_0 \rightarrow 2_0)A^+$, CS(3→2), and $HCO^+(1 \rightarrow 0)$ lines are shown in Figure 4. These maps show that the spatial distribution of the wing emission from the Sandqvist 136 bipolar outflow is similar in all the observed molecular species. The emission peaks of the blue and red lobes are offset by ~ 4′ or 0.2 pc from each other with a position angle of ~ –12°.

Since at least two rotational lines of the CS, SiO, and CH_3OH molecules were observed simultaneously, we performed rotational diagram analysis in order to derive their rotational temperature, T_{rot}, and total column density, N_T. In this method these parameters are derived from a fit to the relationship between the quantity $3\,k \int T_{mb}dv/8\pi^3\mu^2\nu S$ and the energy of the upper level of the transition. Here μ, ν, and S are the transition dipole moment, frequency, and line strength of the transition, respectively, and $\int T_{mb}dv$ is the velocity integrated main beam brightness, obtained directly from the observations. In Table 1 we give the derived rotational temperatures and column densities of CS, CH_3OH and SiO in selected positions of the red and blue lobes of the outflow. For the blue lobe we integrated the emission in the LSR velocity range from –9.3 to –5.3 km s^{-1}, while for the red lobe we integrated the emission in the LSR velocity range from –3.7 to 0.3 km s^{-1}. As a mode of illustration we show in Figure 5 a sample of the data used for the derivation of the parameters associated with the CH_3OH molecule. Plotted are data obtained at three positions within the Sandqvist globule: blue lobe, red lobe, and central core position. The rotational temperature and total methanol column density derived from a linear least squares fit to these data are shown in the lower left corner. The derived rotational temperatures of the outflowing gas at the lobes and of the quiescent gas at the core position are all similar, with an average value of 8 K and a dispersion of 2 K. Further, there is no significant differences among the rotational temperatures derived using different molecular species. These temperatures are somewhat lower than the kinetic temperature derived for the quiescent dark cloud of 13 K (Bourke *et al.,* 1995). Whether the rotational temperatures provide a good estimate of the kinetic temperature of the outflowing gas is not clear. Bachiller *et al.* (l995) suggest that the methanol populations are likely to be extremely sub-thermal and therefore that the rotational temperatures are considerably smaller than the kinetic temperatures.

The abundance of species X relative to CO, [X]/[CO], of the outflowing gas in the lobes of Sandqvist 136 are given in Table 2. They were directly derived as the ratio of the molecular column density of species X, obtained from the rotational analysis (see Table 1), and the column density of CO molecules in the corresponding velocity range. The latter was computed from the ratio of the observed emission in the ^{12}CO and ^{13}CO lines assuming a $^{12}CO/^{13}CO$ ratio of 89 and an excitation temperature of 8 K (see Bourke *et al*., 1996 for a description of the method). Since for the Sandqvist 136 cloud the ambient gas and shocked gas are well distinguishable, both spatially and kinematically, the derived abundances of the outflowing gas are not affected by the emission of the quiescent gas.

Discussion

The data presented in the previous section clearly illustrate that the chemistry of the molecular gas near the core of the globule has been substantially modified as a result of the interaction between the shocks and the ambient medium. Particularly notable are the strong emission in the lines of methanol and silicon monoxide at the position of the lobes, showing that these species are dramatically affected by the shocks. To quantitatively assess the chemical changes of the ambient medium due to the outflow phenomena requires to know the chemical abundances of the quiescent ambient gas. These have not yet been determined for the Sandqvist 136 globule. We note that the spectra observed toward the central position of the core region reflect the conditions of the dense molecular gas that surrounds the recently formed star, with a possible contribution from a circumstellar disk, and thus they do not probe the chemical state of the large scale ambient medium. We will assume that the abundances of the Sandqvist 136 quiescent ambient cloud are similar to those of cold dark clouds which show no evidence of star formation, such as the TMC-1 ridge and the L134N cloud (see van Dishoeck *et al.,* 1993, and references therein). The [X]/[CO] abundance ratios in the TMC-1 dark cloud are given in column 4 of Table 2. A comparison of columns 2, 3 and 4 of Table 2, shows that the $[CH_3OH]/[CO]$ and [SiO]/[CO] abundance ratio in the lobes of the Sandqvist 136 outflow have been enhanced with respect to that of the quiescent ambient gas in dark globules by factors of ~200 and ~1000, respectively.

The spatial distribution of the emission in the SiO and CH_3OH lines and their spectacular enhancement with respect to that of the ambient medium shows that shocks play an essential role in the production of these molecules. The formation route of these species by the action of shocks is twofold: via gas phase and via grain surface processes. Shocks can raise the gas to high temperatures and drive many chemical reactions which are inefficient at ambient cloud temperatures. Shocks can also partially destroy dust grains leading to the injection of several absorbed atoms and molecules from the grain surface into the gas phase. Whether the high abundance of silicon monoxide and methanol molecules seen

TABLE 2. Molecular Abundances Relative to CO.

Molecule	Sandqvist 136		TMC-1
	blue lobe	red lobe	
CH_3OH	4×10^{-3}	8×10^{-3}	2.5×10^{-5}
SiO	1×10^{-5}	3×10^{-5}	$< 2.5 \times 10^{-8}$
CS	1×10^{-4}	2×10^{-4}	1.3×10^{-4}
HCO^+	2×10^{-5}	2×10^{-5}	1.0×10^{-4}

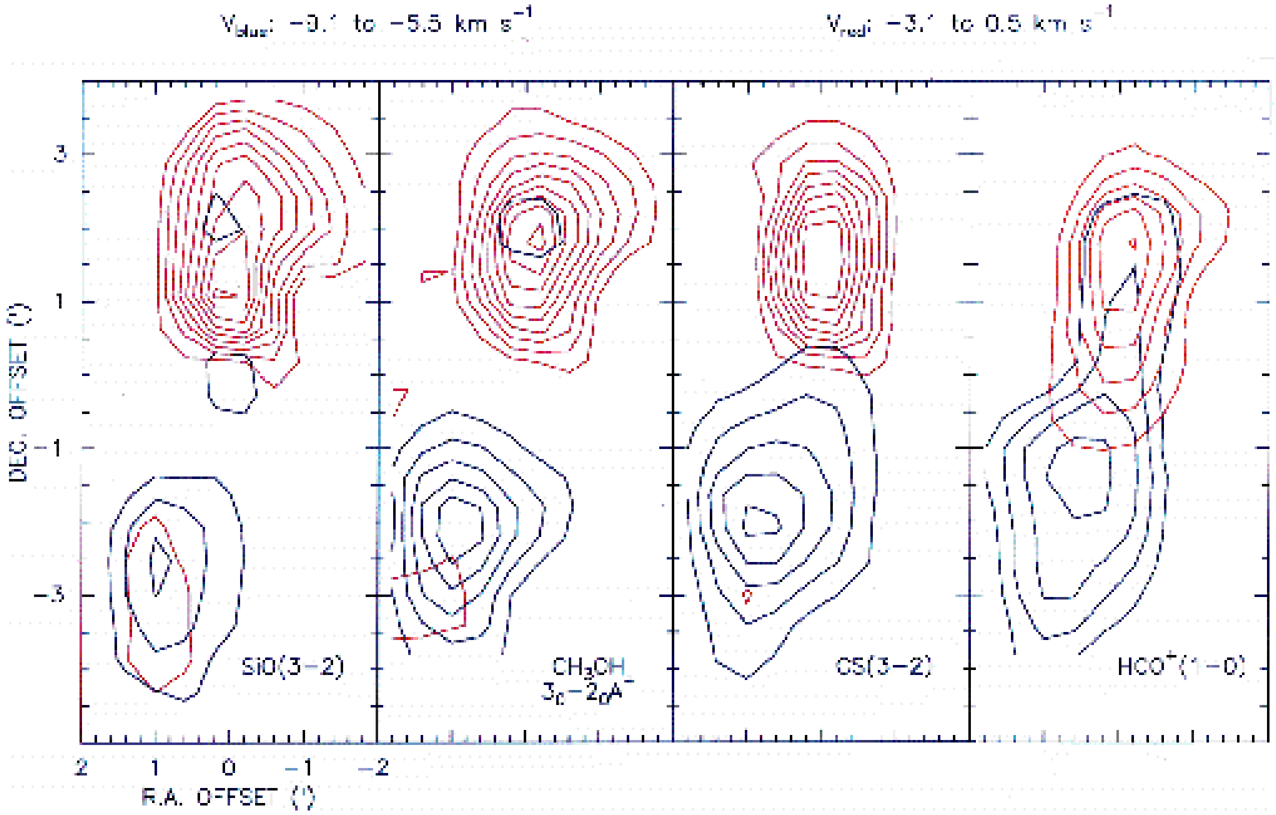

Figure 4. Contour maps of velocity integrated line wing emission from the Sandqvist 136 bipolar outflow. Blue contours correspond to the emission integrated in the velocity range from –9.1 to –5.5 km s^{-1} (blueshifted wing) and red contours to the integrated emission in the velocity range from –3.1 to 0.5 km s^{-1} (redshifted wing). The lowest contour and contour interval are, respectively, 0.1 and 0.1 K km s^{-1} for the SiO(J = 3→2) line (left), 0.3 and 0.3 K km s^{-1} for the $CH_3OH(3_0 \rightarrow 2_0)A^+$ line (middle-left), 0.2 and 0.15 K km s^{-1} for the CS(J=3→ 2) line (middle-right), and 0.4 and 0.3 K km s^{-1} for the HCO^+(J=1 → 0) line (right).

tively. Within the available bandwidths, three rotational transitions of CH_3OH could be observed at 2 mm ($3_0 \rightarrow 2_0A^+$, $3_{-1} \rightarrow 2_{-1}E$, and $3_0 \rightarrow 2_0E$ lines) and three at 3 mm ($2_0 \rightarrow 1_0E$, $2_0 \rightarrow 1_0A^+$, and $2_{-1} \rightarrow 1_{-1}E$ lines). The antenna half-power beam width and main beam efficiency were, respectively, 34″ and 0.66 at the highest observed frequency of 147 GHz and 57″ and 0.75 at the lowest observed frequency of 87 GHz. In each transition, we mapped the molecular emission within a region of ~ 5′× 10′, with 60″ spacings. All the observations were performed in the position switch mode. The integration times on source were typically 3 minutes per position.

Results

The spectra in the J = 2 → 1 lines of CS and SiO and in the $J_k = 2_k \rightarrow 1_k$ and $J_k = 3_k \rightarrow 2_k$ lines of CH_3OH observed across the 5′× 10′ region mapped with SEST are shown in Figure 2. Two emission components, originating from physically and chemically different environments, can be distinguished from this figure. A narrow line emission, at a velocity of –4.5 km s^{-1}, arising from the ambient cloud material at the core of the Sandqvist 136 globule (see upper left panel), and a broad line emission which arises from the bipolar outflowing gas. Particularly striking are the cases of methanol and silicon monoxide molecules, in which the emission from the broad component is much stronger than in the narrow component. The broad emission is detected at redshifted velocities with respect to the systemic ambient cloud velocity toward the northwest region of the map (the red lobe) and at blueshifted velocities toward the southeast region (the blue lobe).

Figure 3 shows the spectra of the spatially integrated line emission, in all the observed transitions, from both the blue and red lobes as well as from the central core position. Emission in the lines of SiO is found to arise only from the lobes, no emission being detected at the core of the globule. The CH_3OH profiles show strong emission from the broad component and weak emission from the narrow ambient cloud, while the CS and HCO^+ profiles show a mixture of strong emission from the quiescent ambient cloud and relatively weaker wing emission at the position of the lobes. The vertical bars shown in the spectra of methanol indicate the expected positions of the three rotational transitions, within the observed velocity ranges, for a rest velocity of –4.5 km s^{-1}. Wing emission is detected in all the observed molecules: CS, SiO, HCO^+ and CH_3OH. Maps of the velocity integrated emission

TABLE 1. Derived Parameters of Sandqvist 136 Outflowing Gas

Offset pos.		Wing	CH_3OH		SiO		CS		HCO^+
Δα (′)	Δδ (′)		T_R (K)	N_T (cm^{-2})	T_R (K)	N_T (cm^{-2})	T_R (K)	N_T (cm^{-2})	N_T (cm^{-2})
1	–3	Blue	6	2.4×10^{14}	9	7.6×10^{11}	6	6.7×10^{12}	9.2×10^{11}
1	–2	Blue	9	1.7×10^{14}	9	6.2×10^{11}	8	5.7×10^{12}	1.0×10^{12}
0	2	Red	6	6.2×10^{14}	8	2.2×10^{12}	7	1.3×10^{13}	2.0×10^{12}
–1	2	Red	6	4.3×10^{14}	6	1.8×10^{12}	6	1.2×10^{13}	8.8×10^{11}

mated bipolar morphologies (André et *al.,* 1990; Bachiller et *al.,* 1990; Bachiller, Fuente & Tafalla, 1995; Lada & Fich, 1996). The class of highly collimated outflows are thought to be driven by jets that accelerate the ambient gas through the propagation of shocks (e.g. Raga & Cabrit, 1993).

The interaction of high-velocity jets from young stars with the surrounding ambient gas generates strong shock waves which are expected to produce a significant transformation of the physical properties of the molecular surroundings as well as of its chemical composition. Although there has been a substantial amount of work on the physical characteristics of outflows, very little is known about their chemical composition. Basic questions such as: How is the chemistry of the swept-up ambient molecular material affected by the winds from young stellar objects? or Do molecular abundances serve as sensitive probes of the evolutionary stage of bipolar outflows? (cf. van Dishoeck & Blake, 1995) have not yet been answered. Shocks in dense molecular clouds are expected to radiate in several molecular lines in the millimetre and submillimeter wavelength ranges and hence are open to investigation by spectroscopic observations at these wavelengths. Since different molecules and their isotopes respond differently to physical conditions (such as temperature and density) their observations provide unique tools to probe the outflows. Mapping outflows in different molecular species is thus essential to the study of the physical and chemical structure of the shocks.

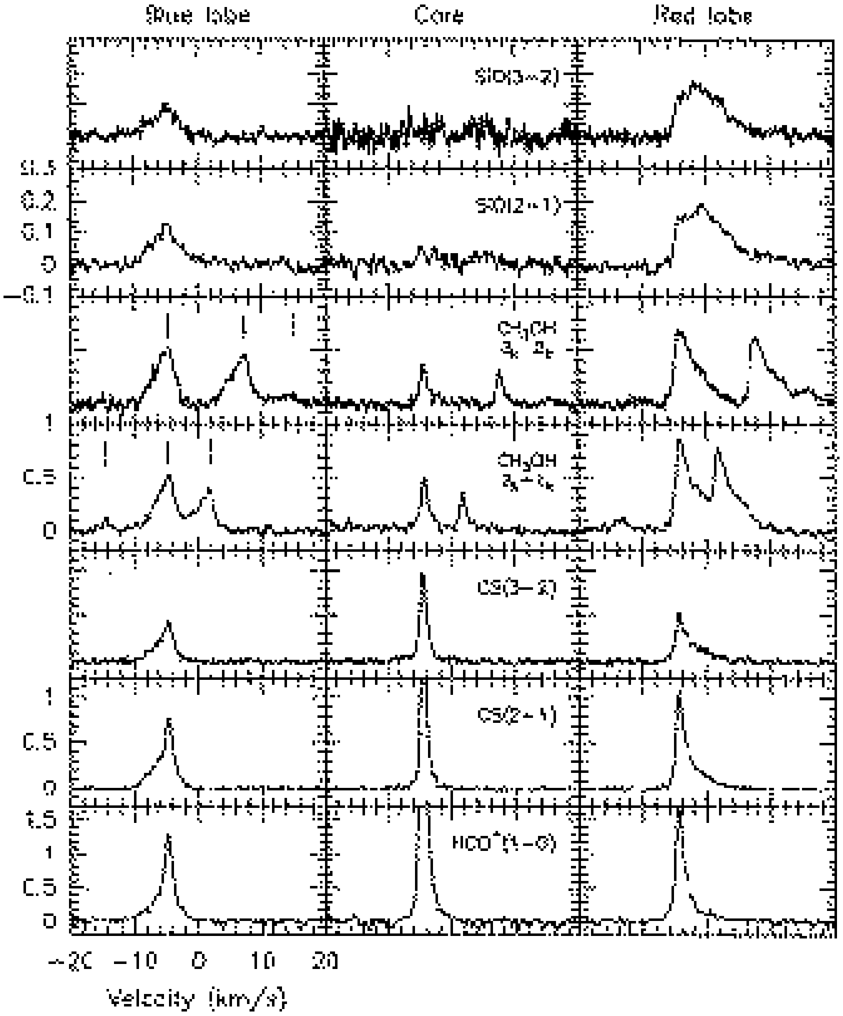

Figure 3. Spectra of the spatially integrated line emission from the blue and red lobes of the Sandqvist 136 outflow and from the central position (Middle column).

Most of the studies of molecular outflows from young stellar objects have focused, to a large extent, on observations of the CO($1\rightarrow0$) line (Bally & Lada, 1983; Lada, 1985). Emission in this transition is easy to detect, both due to the relatively large abundance of CO and easy excitation at the densities and kinetic temperatures of molecular flows. Very few multiline mapping of molecular outflows have been performed so far. Part of the reason, other than the usual constraint on observing time, is that observations in the range of wavelengths that permit us to probe abundances in outflows have been made available only recently. In particular the Swedish-ESO Submillimetre Telescope (SEST) has recently undergone important upgrade in the receiver front end, opening the 2-mm wavelength range for observations and substantially improving the performance in the 3-mm wavelength range. In these ranges, emission from a plethora of molecular lines is expected to be detectable, which can be used to trace the motions and physical conditions of the gas at the earliest stages of star formation. Accordingly, the SEST has opened the avenue for a detailed investigation of the chemical composition of southern skies outflows, which would undoubtedly provide much-needed information about their physical and chemical evolution.

Sandqvist 136 (Sandqvist, 1977) is a small dark cloud or Bok globule, located at a distance of ~175 pc from the Sun, which harbours a highly collimated bipolar outflow near its centre (Bourke et *al*., 1996; see Figure 1) The CO outflow is found to be well described as a biconical flow, with a semi-opening angle of 15° and inclined from the line of sight by an angle of ~ 84°, in which the gas moves outwards with a constant radial velocity (with respect to the cone apex) of ~ 28 km s^{-1} . The outflow appears to be driven by a very young stellar object, with a luminosity of ~ 7 $L_{\odot}$, possibly still undergoing accretion of matter. Its characteristics at infrared and millimetre wavelengths are similar to those of Class 0 objects (André, 1995). Since the lobes of this outflow extend by ~ 4′ in the plane of the sky it is an ideal source for a detailed study, using single-dish instruments, of the physical and chemical characteristics across highly collimated, low velocity shocks. In this article we report extensive molecular SEST observations of this outflow in rotational transitions of silicon monoxide (SiO), methanol (CH_3OH), carbon monosulfide (CS), and formyl ion (HCO^+).

Observations

The observations of the Sandqvist 136 outflow, stimulated by the recent availability at the 15-m SEST radio telescope of sensitive SiS receivers operating in the 2- and 3-mm bands, were performed during September 1995. We used the 2- and 3-mm receivers to simultaneously observe the $J = 3 \rightarrow 2$ and $J = 2 \rightarrow 1$ transitions of CS, the $J = 3 \rightarrow 2$ and $J = 2 \rightarrow 1$ transitions of SiO, and some of the $J_k = 3_k \rightarrow 2_k$ and $J_k = 2_k \rightarrow 1_k$ transitions of CH_3OH. Single-sideband receiver temperatures were typically 120 K for both receivers. As backend we used high-resolution acousto-optical spectrometers providing a channel separation of 43 KHz and a total bandwidth of 43 MHz. This resulted in spectral resolutions of 0.13 and 0.09 km s^{-1} and total velocity coverages of 133 and 89 km s^{-1} at the 96.7 and 145.1 GHz frequencies of the CH_3OH lines, respec-

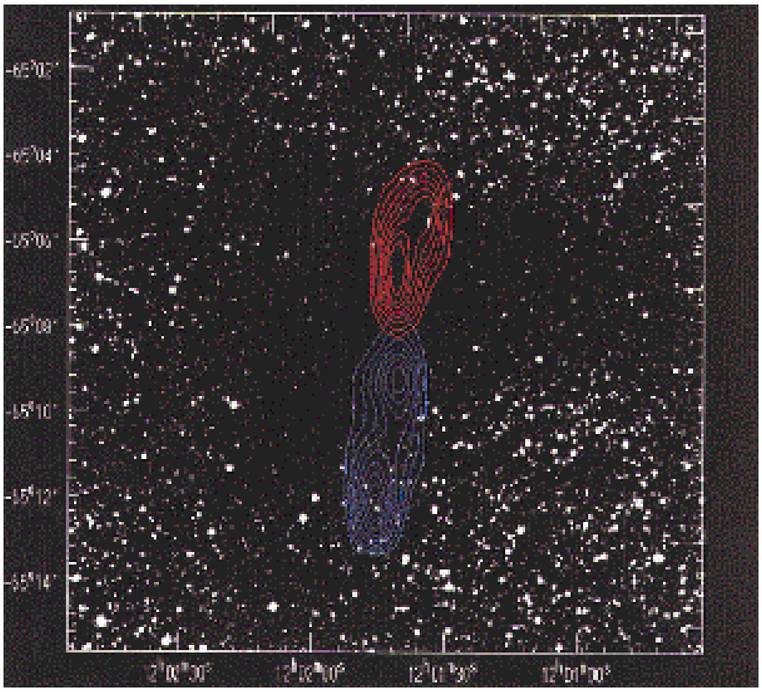

Figure 1: Contour map of velocity integrated CO(1→0) line wing emission from the Sandqvist 136 bipolar outflow, superimposed on a V-band image of the globule taken from the Digitised Sky Survey. Co-ordinate labels are J2000. Blue contours correspond to the emission integrated in the velocity range from –13.5 to –8.5 km s^{-1} (blueshifted wing) and red contours to the integrated emission in the velocity range from –0.5 to 4.5 km s^{-1} (redshifted wing). The lowest contour and contour interval are, respectively, 1.8 and 0.8 K km s^{-1} for the redshifted emission and 1.0 and 0.5 K km s^{-1} for the blueshifted emission.

bient gas in its vicinity, giving rise to the molecular outflows. Bipolar flows are frequently found associated with other tracers of the dynamical interaction between the high-velocity wind and ambient gas, such as Herbig-Haro objects (Reipurth, 1991), shock-excited infrared H_2 emission (Bally, Lada & Lane, 1993), and optical jets (Mundt, 1988). Reviews of the characteristics of bipolar molecular outflows have recently been presented by Bachiller & Gómez-González (1992) and Fukui et *al.* (1993). The majority of the outflows show a moderate degree of collimation, while few have highly colli-

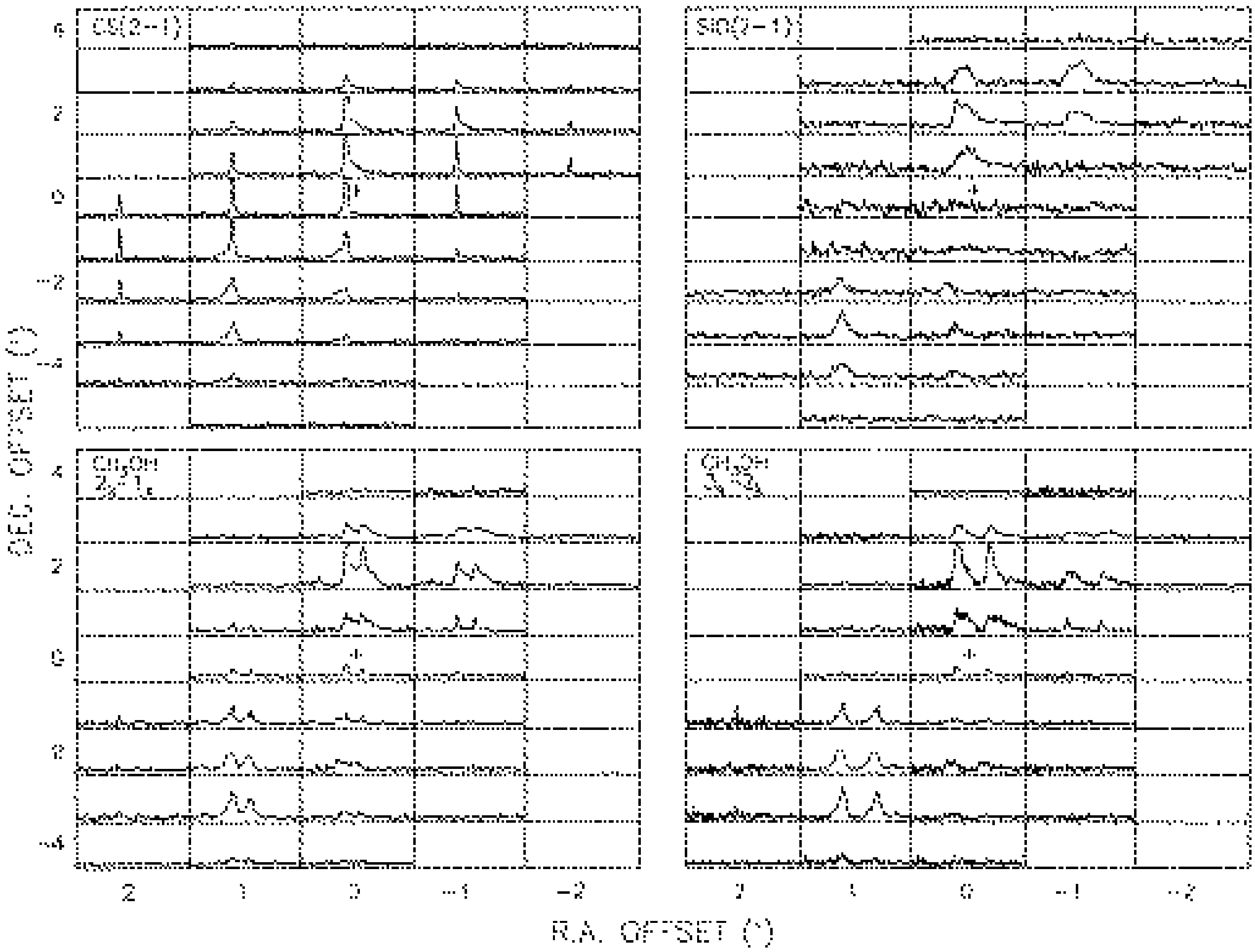

Figure 2. Observed spectra across the 5′× 10′ central region of the Sandqvist 136 globule. The grid spacing is 1′. Offsets are from the reference position at α = 11^{h}59^{m}1.2^s and δ = –64°52′0″. In each box the velocity scale ranges from –20 to 20 km s^{-1} . Upper left: CS(2→1) emission. Antenna temperature scale: –0.1 to 1.5 K. Upper right: SiO(2 →1) emission. Antenna temperature scale: –0.1 to 0.4 K. Bottom left: $CH_3OH(2_k \to 1_k)$ emission. Antenna temperature scale: –0.2 to 1.8 K. Bottom right: $CH_3OH(3_k \to 2_k)$ emission. Antenna temperature scale: –0.2 to 1.8 K. The cross indicates the position of the IRAS source 11590-6452.

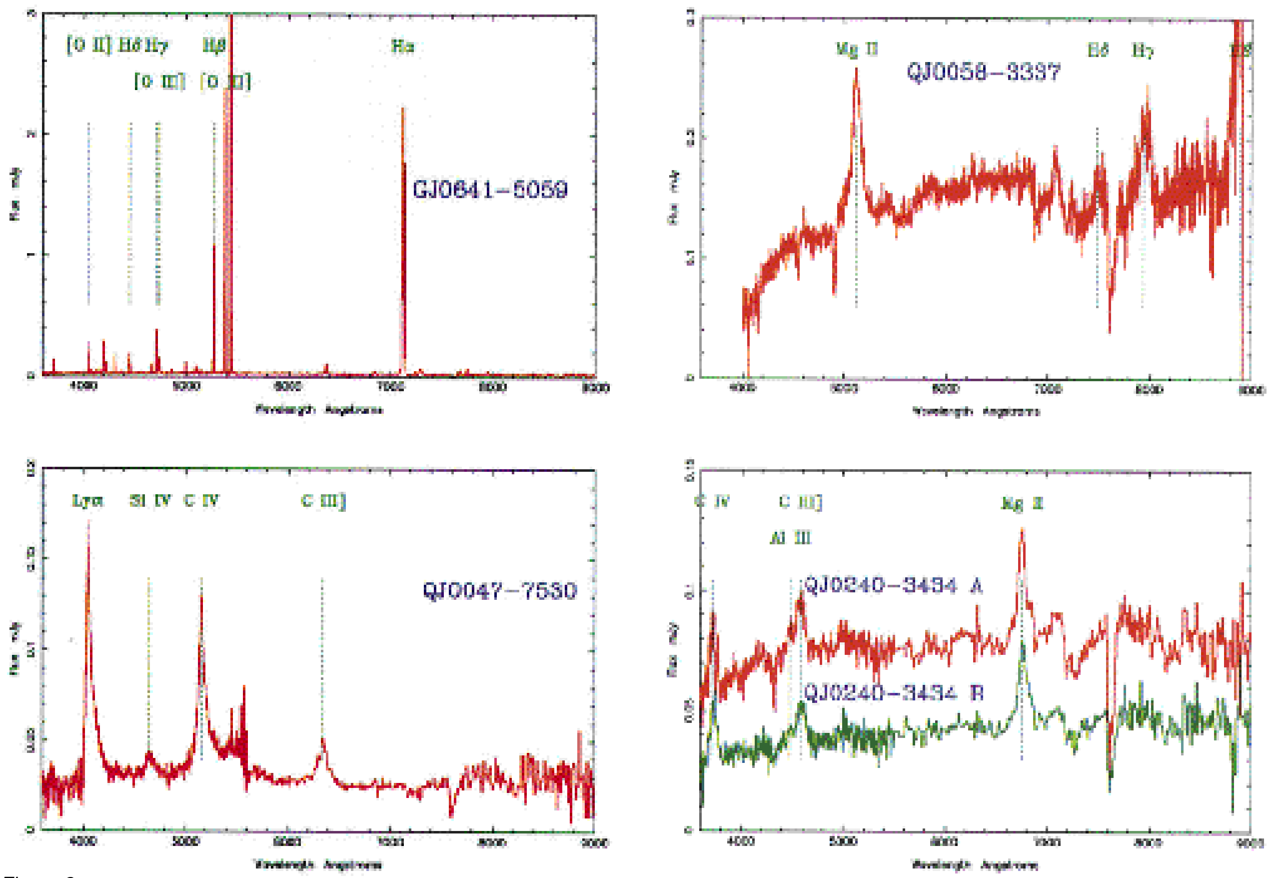

Figure 2.

redshift cluster), it clearly merits to be further studied, and monitoring is being attempted on the AAT.

GJ0641-5059: As its designation suggests, this emission-line galaxy was observed to be resolved and is not a QSO. However, it is still a remarkable object indeed. Its spectrum shows strong H Balmer lines, along with strong [O III], [Ne III], He I and [O II] – so much so that the continuum is almost invisible in the figure. All the lines are unresolved at 200 km/s. An examination of the line ratios shows the system to be a H II galaxy (rather than an AGN – Veilleux & Osterbrock, 1987). However, its extraordinarily high [O III]A5007/Hβ ratio, places it among the most highly excited of such systems known.

Conclusion

We have found that standard QSO survey techniques can be efficiently applied to search for QSOs in arbitrary locations – i.e. behind nearby galaxies. Once such inertial reference objects have been identified, astrometric programmes targeted at these galaxies can be commenced with the NTT. In fact, the NTT will be extremely well placed to commence these programmes later this year, when service mode operations begin after its re-commissioning, since service mode observing offers the best chance of obtaining images in the excellent seeing conditions essential for these high-precision astrometric observations.

References

Lynden-Bell, D. & Lynden-Bell, R.M., 1995, *MNRAS*, **275**, 429.
Majewski, S.R., 1994, *ApJ*, **431**, L17.
Tinney, C.G., 1993, *The Messenger*, **74**, 16.
Tinney, C.G., 1995, *MNRAS*, **277**, 609.
Tinney, C.G., Da Costa, G. & Zinnecker, H., 1996, *MNRAS*, *submitted.*
Veilleux, S. & Osterbrock, D.E., 1987, *ApJS*, **63**, 295.

E-mail address: Chris Tinney, cgt@aaoepp.aao.gov.au

A Multiline Molecular Study of the Highly Collimated Bipolar Outflow Sandqvist 136

G. GARAY [1], I. KÖHNENKAMP [1] and L.F. RODRIGUEZ [2]

1 Departamento de Astronomía, Universidad de Chile, Chile
2 Instituto de Astronomía, Universidad Nacional Autónoma de México, México

Introduction

Following the discovery of bipolar molecular outflows in the earliest 80's (Snell, Loren & Plambeck, 1980; Rodríguez, Ho & Moran, 1980), a wealth of observations have shown that this phenomenon is commonly detected in star-forming regions. During their earliest phase of evolution stellar objects are thought to generate a fast, well collimated bipolar wind that sweeps up the am-

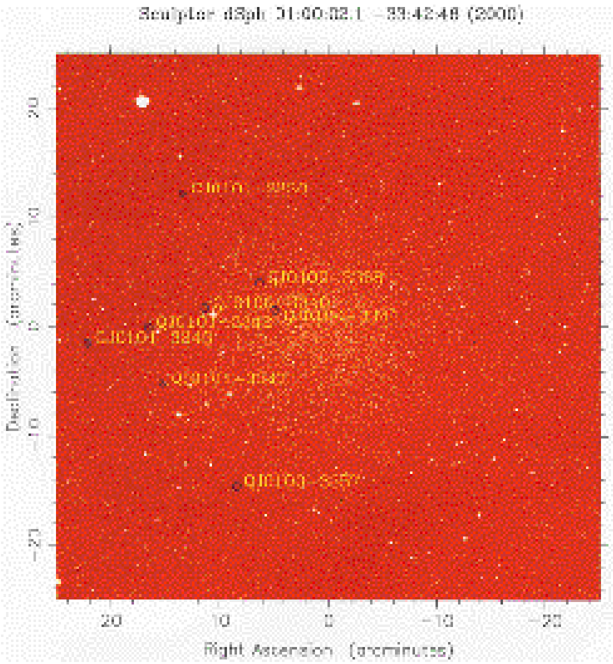

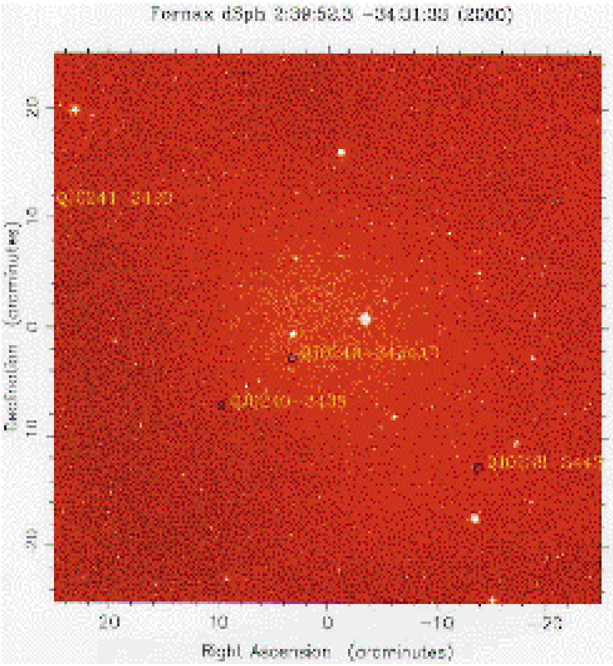

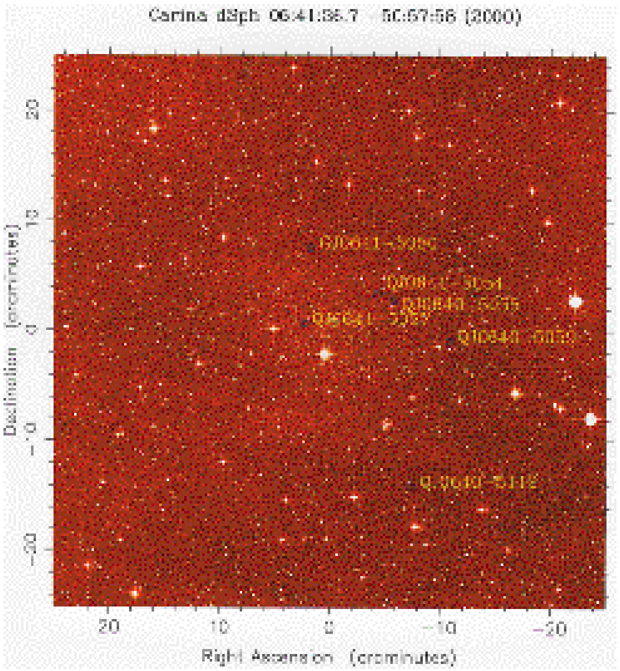

Figure 1.

tion of the Milky Way, and not least the total mass of the Milky Way (see, for example, Majewski (1994), Lynden-Bell & Lynden-Bell (1995) and reference therein).

The one thing stopping us, however, is that to measure such small proper motions, a distant and unresolved reference frame against which to measure motions is needed – i.e. reference QSOs. At the magnitudes at which this astrometry will be carried out (20–21.5 mag) the number density of QSOs is more than adequate to provide ≳ 5 QSOs behind the Dwarf Spheroidal (dSph) galaxies, and ≳ 20 – 100 behind the Magellanic Clouds. Unfortunately, QSO surveys tend (not unreasonably) to avoid such large sources of foreground contamination, meaning that almost no QSOs useful as astrometric references are already known. In 1994 we therefore began a programme of identifying QSOs useful as reference objects on the telescopes of La Silla.

Because our aim is to identify as many QSOs as possible, using as little telescope time as possible, we have used as many data as are available to us to construct lists of QSO candidates. This has included using UBVRI plate data from the 48″ UKST and CCD UBVRI data from the NTT, 3.6-m, MPIA 2.2-m and Danish 1.5-m to search for UV-excess candidates (the CCD data were required to calibrate the plate data, however, it was also searched for UV-excess candidates missed in the shallower plate data sets); using CCD UB data (from the same telescopes as above) to identify the optical counterparts to X-ray sources from ROSAT pointed observations; and, using CCD UB imaging to identify the optical counterparts to radio sources. QSO candidates identified using all these techniques were then spectroscopically observed using EFOSC1 (3.6-m), EFOSC2 (2.2-m), EMMI (NTT), and the RGO+FORS spectrographs on the Anglo-Australian Telescope (AAT). Our search strategy was made considerably more powerful by the flexibility of the EFOSC1/2 and EMMI instruments, which allowed a given night to be used for both imaging and spectroscopy, as dictated by changing weather conditions, and the available spectroscopic candidate lists.

The complete details of this programme will be published elsewhere (Tinney, Da Costa & Zinnecker, 1996), however, Figure 1 nicely summarises the main results to date, for the three primary targets of the Sculptor, Fornax and Carina dSph galaxies. In each case, 3–4 QSOs have been identified sufficiently close to the galaxy centre to have a network of reference stars suitable for astrometry.

Some Serendipitous Results

Figure 2 shows a sample of the spectra for the QSOs identified. Among the more interesting are QJ0240-3434AB and GJ0641-5059.

QJ0240-3434AB (The Fornax QSO Pair): Certainly the most dramatic result of the programme of spectroscopic follow-up was the discovery that the optical counterpart to one of the ROSAT sources behind the Fornax dSph is actually a pair of QSOs at $z = 1.4$ separated by 6.1″ (Tinney, 1995). The exact nature of this system is still unclear. With a separation of 6.1″, this system, if it is interpreted as a gravitational lens, has one of the largest separations known. Moreover, unlike the proto-typical lens 0957+561 (which has a similar separation), no lensing galaxy or cluster is obvious. Whether this system is a 'dark' lens, or a distinct QSO pair (possibly pointing to a high

Evrard et al. (1994) using hierarchical clustering scenarios indicate that rotating disks with radii of several tens of kiloparsecs should be common around forming galaxies at high redshift.

6. The VLT and the Next Decade

Because of their unique diagnostic abilities, high-redshift radio galaxies are among the most important targets both for the HST and the next generation of large optical-IR telescopes, including the VLT. The VLT should allow the enigmatic outer fainter regions of the galaxies to be mapped and the spatial extensions in some of the weaker emission lines to be measured, thereby providing new diagnostics on the state of the gas.

Here we have concentrated on discussing the gaseous properties of high-redshift galaxies. Studies of stars, dust and synchrotron emission are of course also essential if the history of the galaxy formation is to be pieced together. High spatial resolution images and spectra will measure spectral energy distributions and polarisations for the nuclear regions and continuum clumps, while the kinematics and morphological distribution of the gaseous clumps should provide clues to whether and how the observable gas is being converted into stars.

Not only are distant radio galaxies interesting in their own right as laboratories for studying galaxy formation, but their environments are particularly intriguing regions of the Universe to examine in detail. Such topics are outside the scope of the present article. However, we remark that since low-redshift radio-loud objects tend to be in rich clusters of galaxies, the surroundings of high-redshift radio-loud objects are among the most fruitful places to seek the most distant clusters.

We expect that such studies will provide important new insights into the evolution of galaxies and clusters and that the VLT will play a major role in this exciting work.

Acknowledgements

We would like to thank our collaborators, Malcolm Bremer, Chris Carilli and Dick Hunstead for numerous discussions.

References

Begelman M. C., Cioffi D. F., 1989, *ApJ*, **345**, L21.
Chambers K. C., Miley G. K., van Breugel W., 1987, *Nat*, **329**, 604.
de Young D. S., 1989, *ApJ*, **342**, L59.
Evrard A. E., Summers F. J., Davis M., 1994, ApJ, **422**, 11.
Fabian A. C., 1989, *MNRAS*, **238**, 41P.
Longair M. S., Best P. N., Röttgering H. J. A., 1995, *MNRAS*, **275**, L47.
McCarthy P., van Breugel W., Spinrad H., Djorgovski S., 1987, *ApJ*, **321**, L29.
McCarthy P. J., 1993, *ARA&A*, **31**, 639.
Miley G., Chambers K., Hunstead R., Macchetto F., Roland J., Röttgering H.,Schilizzi R., 1989, *The Messenger*, **56**, 16.
Miley G., Röttgering H., Chambers K., Hunstead R., Macchetto F., Roland J., Schillizi R. van Ojik R., 1992, *The Messenger*, **68**, 12.
Rees M. J., 1989, MNRAS, **239**, 1P.
Röttgering H., Hunstead R., Miley G. K., van Ojik R., Wieringa M. H., 1995, *MNRAS*, **277**, 389.
Tadhunter C. N., Fosbury R. A. E., Binette L., Danziger I. J., Robinson A., 1987, *Nature*, **325**, 504.
van Breugel W., 1996, in Parma C., ed., IAU Symposium No. 175: Extragalactic Radio Sources, Kluwer, in press.
van Breugel W., Miley G. K., McCarthy P., Spinrad H., Macchetto F., 1996, preprint.
van Ojik R., 1995, Ph.D. thesis, University of Leiden.
van Ojik R., Röttgering H., Carilli C., Miley G., Bremer M., 1995a, A radio galaxy at $z = 3.6$ in a giant rotating Lyman α halo, *A&A*: in press.
van Ojik R., Röttgering H. J. A., Miley G. K., Hunstead R., 1995b, The Gaseous Environment of Radio Galaxies in the Early Universe: Kinematics of the Lyman α Emission and Spatially Resolved H I Absorption, *A&A*: submitted.

E-mail address: Huub Röttgering, rottgeri@reusel.strw.LeidenUniv.nl

Proper Motions of Galaxies – the Reference Frame

C. TINNEY[1], G. DA COSTA[2] and H. ZINNECKER[3]

[1]Anglo-Australian Observatory, [2]Mount Stromlo and Siding Spring Observatories, [3]Astrophysikalisches Institut Potsdam

Introduction

CCD astrometry offers the possibility of measuring proper motions for the nearest galaxies, either from the ground or using HST, in only 5–10 years. An inertial reference frame, however, is needed against which to measure these motions. We have therefore been using the La Silla telescopes to seek QSOs behind several of the nearest satellite galaxies of the Milky Way, using a variety of techniques.

The Prospects for Proper Motions

In a previous Report, Tinney (1993) discussed some of the features which make CCDs almost ideal detectors for small-angle, relative astrometry at extremely high precisions (i.e., 110 mas). In particular, it was suggested that an astrometric programme targeted at the nearest galaxies could be fruitful.

Since then, observations at two epochs (May and June 1994) of a field in the globular cluster NGC 6752 have been successfully carried out in excellent seeing (better than 0.5″) using SUSI on the NTT. These observations were centred on the known QSO Q1908-6002, and aimed to both test the astrometric limits to which SUSI could be pushed, and to measure the proper motion of NGC 6752 over a baseline of 18 months. Eighty-two reference stars were selected, based on their colour-magnitude diagram membership of the cluster, and used to define a linear transformation (with an allowed rotation) from a single frame in the first epoch to each of rest the frames. The typical one-sigma residuals in α and δ about these transformations were only 3.5 and 4.2 mas (respectively). This means that the position of a single object (i.e. the reference QSO) could be determined in α and δ at a single epoch to within 1.8–2.1 mas. This essentially confirms the expectation that the NTT/SUSI combination will be ideal for high-precision astrometry, and means that with observations carried out every other year over a six-year period, proper motions can be measured to ±0.2 mas/year*.

The Search for Reference Objects

It is therefore clear that, technically, there is no reason why proper motion programmes for the nearest satellite galaxies of the Milky Way (which are expected to have proper motions of 0.5–2 mas/year) can't be begun now. And scientifically, the rewards from such a programme would obviously be of incredible value to our understanding of the dynamics of the Local Group, the forma-

*Unfortunately, no subsequent observations of this field have yet been obtained in sufficiently good seeing to actually produce a proper-motion estimate for NGC 6752.

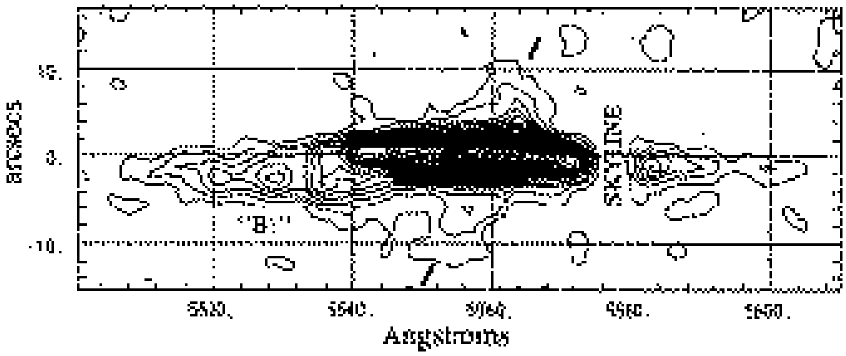

Figure 4: A two-dimensional representation of the 2.8 Å resolution spectrum of Lyα of 1243+036 (z = 3.6) taken through a slit oriented along the main axis of the radio emission.

explained as separate kinematic components of the emission, but that they are definitely due to absorption by neutral hydrogen in the line of sight. An example is provided by the Key-Programme radio galaxy 0943—242 at z = 2.9 (Röttgering et al., 1995). A spectrum of the Lyα profile (Fig. 5) reveals a complex emission line profile which is dominated by a narrow trough centred 250 km s^{-1} blueward of the emission peak and which appears as a "bite" out of the spectrum. The obvious interpretation is that it is due to H I absorption. The necessary column density is 1×10^{19} cm^{-2}. Because the absorption is so deep, it must cover the entire Lyα emission region, which has a spatial scale of 1.7″. The linear size of the absorber is thus at least 13 kpc. This was the first direct measurement of the spatial scale of an absorber with a column density of ~ 10^{19} cm^{-2} .

We have now analysed deep high-resolution spectra for a sample of 18 distant radio galaxies (van Ojik, 1995; van Ojik et al., 1995b). Most of the spectra were taken using the EMMI-spectrograph on the NTT with integration times of a few hours. H I absorption features appear widespread in the Lyα profiles. 11 radio galaxies of the sample of 18 have strong (> 10^{18} cm^{-2}) H I absorption.

Since in most cases the Lyα emission is absorbed over the entire spatial extent (up to 50 kpc), the absorbers must have a covering fraction close to unity. Given the column densities and spatial scales of the absorbing clouds, the typical H I mass of these clouds is ~ 10^8 $M_\odot$.

The Lyα absorption provides a new diagnostic tool for studying and spatially resolving neutral gas at high redshifts. Because the spatial extension of the absorbing region can be studied, the Lyα absorption can provide information about the properties of the neutral gas (e.g. dynamics and morphologies) which cannot be studied using quasar absorption lines.

4. Interaction with the Radio Sources: Nature of the Gas

There are several pieces of indirect evidence from the Lyα emission data that high redshift synchrotron jets have a strong influence on the gas through which they propagate. The gas associated with larger radio sources (> 50 kpc) tends to have (i) larger Lyα sizes, (ii) smaller velocity dispersions and (iii) less likely to undergo Lyα absorption than the gas associated with smaller radio sources. There are also correlations between the distortions in the two-dimensional Lyα spectra and the complexity of the radio structure which implies a link between the radio structure and the gas kinematics.

In addition to these statistical arguments, the data on 1243+036 presented above provides a compelling direct example that the jet-gas interaction can be vigorous enough to bend the jet.

The general properties of both the Lyα absorption and emission data can be explained qualitatively as being produced by different regions within a single large gaseous structure. Three different scenarios can be invoked to explain the observed correlations between the radio and gas properties. They are based on differences in (i) orientation of the system with respect to the line of sight, (ii) evolutionary stage and (iii) properties of the environment, with the smaller radio sources being situated in denser environments than the larger radio sources.

Considering the filling factors and physical parameters derived from our Lyα observations, we estimate that a gas halo has a characteristic mass of ~ 10^9 $M_\odot$, and is typically composed of ~ 10^{12} clouds, each having a size of about 40 light-days, i.e. comparable with that of the solar system. It is tempting to speculate that these clouds are intimately associated with the early formation stages of individual stars and that they delineate a fundamental phase in galaxy evolution.

5. The Formation of Galaxies

An ultimate aim of studying high-redshift galaxies is to constrain models of galaxy formation. Recent observational evidence suggests that distant radio galaxies may well be proto-cD galaxies. Deep continuum images with the HST show that a radio galaxy at z = 3.8 (4C41.17) is composed of many (> 20) distinct sub-kiloparsec clumps distributed within a 100 kpc Lyα halo. These clumps may be undergoing vigorous star formation (van Breugel, 1996; van Breugel et al., 1996).

We have suggested that the ordered motion in the giant gas halos surrounding 1243+036 (Figs. 2, 3 and 4) may well be due to rotation of a protogalactic gas disk at z = 3.6 out of which the galaxy associated with 1243+036 is forming. A gravitational origin of the rotation of such a large disk implies a mass of ~ $10^{12} \sin^{-2}(i)$ $M_\odot$, where i is the inclination angle of the disk with respect to the plane of the sky. Such a picture would be consistent with some current galaxy formation models. For example, numerical simulations by e.g.

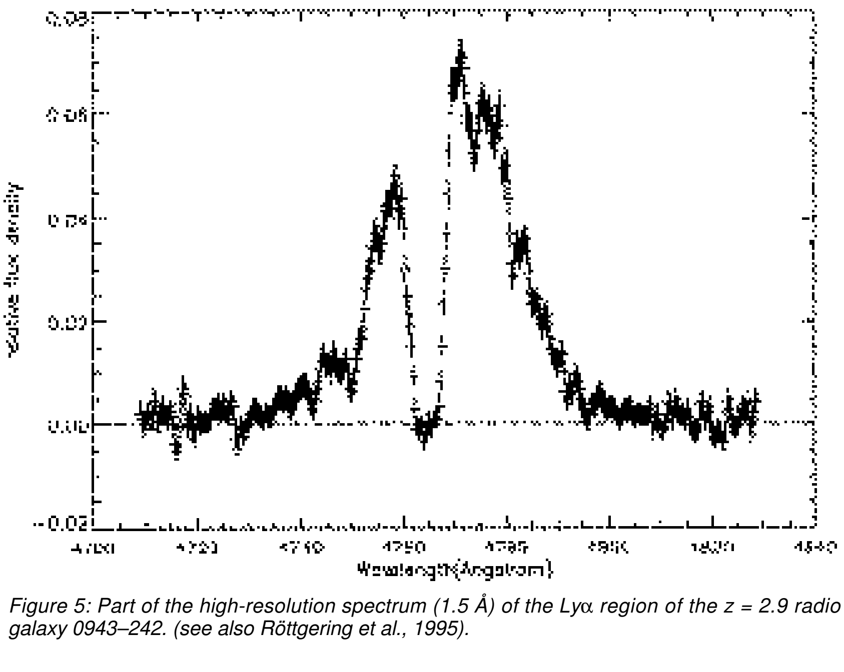

Figure 5: Part of the high-resolution spectrum (1.5 Å) of the Lyα region of the z = 2.9 radio galaxy 0943–242. (see also Röttgering et al., 1995).

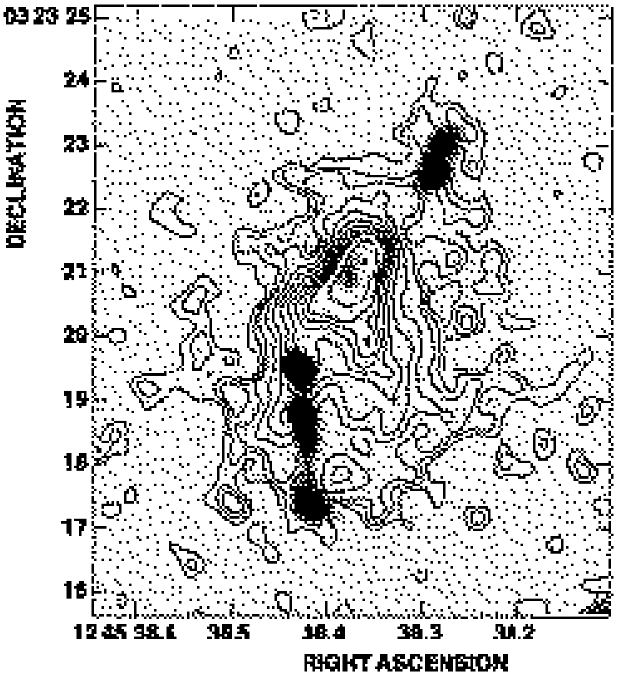

Figure 2: A contour plot of the Lyα halo of the radio galaxy 1243+036 at z = 3.6, with a grey-scale plot of the 8.3-GHz VLA map superimposed.

Programme (Miley et al., 1989; 1992). Here we shall concentrate on one of the most interesting scientific aspects of the project, namely the nature of the gas associated with many of the distant radio galaxies.

2. Lyα Emission: Clues to Galaxy Formation

One of the most remarkable features of distant radio galaxies is that they usually possess giant luminous halos of ionised gas, which can extend to > 150 kpc, with velocity dispersions of typically ~ 1000 km s^{-1}. On the arcsecond scale these halos are highly clumped. In Figure 1 we show NTT and 3.6-m spectra of $z > 2$ galaxies that were discovered during the ESO Key programme. Integration times are typically 1–2 hours. The dominant emission line in these spectra is Lyα λ1216. The Lyα emission can be as luminous as 10^{44} erg s^{-1}. Other lines that are often present, but with fainter intensities (< 10% of Lyα) are C IV, He II, C III].

One of the most spectacular high-redshift gas halos so far known is that associated with one of our Key Programme galaxies, 1243+036 at $z = 3.6$. Deep narrow-band imaging and high-resolution spectroscopy show an extended Lyα halo with complex kinematics (van Ojik, 1995; van Ojik et al., 1995a).

The Lyα halo of 1243+036 has a luminosity ~ 10$^{44.5}$ ergs s^{-1} and extends over ~ 20″ (135 kpc). The Lyα image (Figures 2 and 3) shows that the emission-line gas is aligned with the main axis of the radio source and has structure down to the scale of the resolution. High-resolution spectra show that the Lyα emitting gas has a complex kinematic structure (Fig. 4). The gas contained within the radio structure has a relatively high velocity width (~ 1500 km s^{-1} FWHM). The component of the Lyα emission that coincides with the bend in the radio structure is blueshifted with respect to the peak of the emission by 1100 km s^{-1}. There is low surface brightness Lyα emission aligned with, but extending 40 kpc beyond both sides of the radio source. This halo has a narrow velocity width (~ 250 km s^{-1} FWHM) and a velocity gradient of 450 km s^{-1} over the extent of the emission. The presence of the quiescent Lyα component aligned with the AGN axis, but outside the radio source, is strong evidence that photoionisation by anisotropically emitted radiation from the active nucleus is occurring. Because the halo extends beyond the radio structure with less violent and more ordered kinematics than inside the radio structure, we conclude that the outer halo and its kinematics must predate the radio source. The ordered motion may be large-scale rotation caused by the accretion of gas from the environment of the radio galaxy or by a merger. Although alternatively the halo may be caused by a massive outflow, we argue that bulk inflow of the emission line gas is inconsistent with the most likely orientation of the radio source.

The large velocity-width of the Lyα gas contained within the radio source compared to that of the outer halo suggest a direct interaction of the radio source with the gas. The spatial correlation of enhanced, blueshifted Lyα emission and the sharp bend of the radio structure suggest that the emission-line gas could have deflected the radio jet. The impact of the jet could have accelerated the gas at this position and may have locally enhanced the Lyα emission.

3. Lyα Absorption: A New Diagnostic of High-Redshift Neutral Gas

Another unexpected discovery which came as a direct result of studying the properties of the Key Programme radio galaxies is that deep narrow troughs often “disfigure” the Lyα profiles. High-resolution spectra show that in some cases these features are too sharp to be

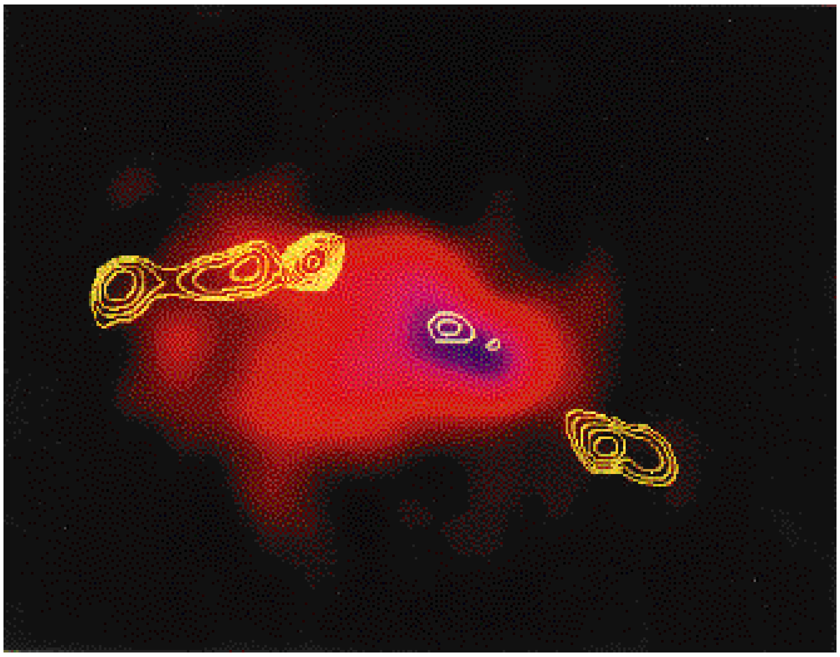

Figure 3: A colour representation of the Lyα halo of the radio galaxy 1243+036 at z = 3.6, with a contour plot of the 8.3-GHz VLA map superimposed.

REPORTS FROM OBSERVERS

Giant Gas Halos in Radio Galaxies: A Unique Probe of the Early Universe

H. RÖTTGERING, G. MILEY and R. VAN OJIK, Leiden Observatory, The Netherlands

1. Introduction

Radio galaxies are important laboratories for studying the early Universe, because they generally emit three components (IR-optical-UV continuum, emission lines and radio continuum) that are all highly luminous. Unlike quasars, the various emission components of radio galaxies are spatially extended and well resolved from the ground. Not only can different diagnostics be derived for each of these components, but studies of the relationships between them can place unique constraints on the emission mechanisms, the contribution of stellar and non-stellar sources, the dynamical state of the thermal plasma, the physical state of the galaxian environment and the star-formation history. These properties are relevant to the formation and evolution of galaxies, active nuclei and radio sources.

During the last decade the number of known radio galaxies with measured redshifts well over 2 has grown dramatically. There are now more than 70 radio galaxies with $z > 2$. This redshift corresponds to look-back times of ~ 90%, close to the epoch at which the galaxies must have formed. It also corresponds to the peak of the "AGN era", when the space-density of luminous quasars and radio galaxies was several hundred times larger than the present value.

Several years ago it came as a big shock when it was discovered that, unlike the case for nearby radio galaxies, the radio emission of $z > 0.6$ radio galaxies is roughly aligned with the optical/IR continuum (Chambers, Miley and van Breugel, 1987; McCarthy et al., 1987). Several models have been proposed or considered to account for this alignment effect (e.g. see McCarthy, 1993). The two most promising models are scattering of light from a hidden quasar by electrons or dust (Tadhunter et al., 1989; Fabian, 1989) and star formation stimulated by the radio jet as it propagates outward from the nucleus (Chambers, Miley and van Breugel, 1987; McCarthy et al., 1987; De Young, 1989; Rees, 1989; Begelman and Cioffi, 1989). Other scenarios involve (i) inverse Compton scattering of CMB photons, (ii) enhancement of radio luminosity by interaction of the jet with an anisotropic parent galaxy, (iii) alignment of the angular momentum of the nuclear black hole with an anisotropic protogalactic distribution and (iv) nebular continuum emission associated with strong emission line regions. Although polarisation results suggest that dust scattering is occurring, as yet no single model for the radio/optical alignment is satisfactory (see Longair, Best and Röttgering, 1995) .

Almost half the known high-redshift galaxies were found in the context of an ESO Key Programme in which we were involved. The results formed the basis of the Ph.D theses of Huub Röttgering and Rob van Ojik and have been presented in several articles. Two previous Messenger articles described our techniques for finding high-redshift objects and the preliminary results of the Key

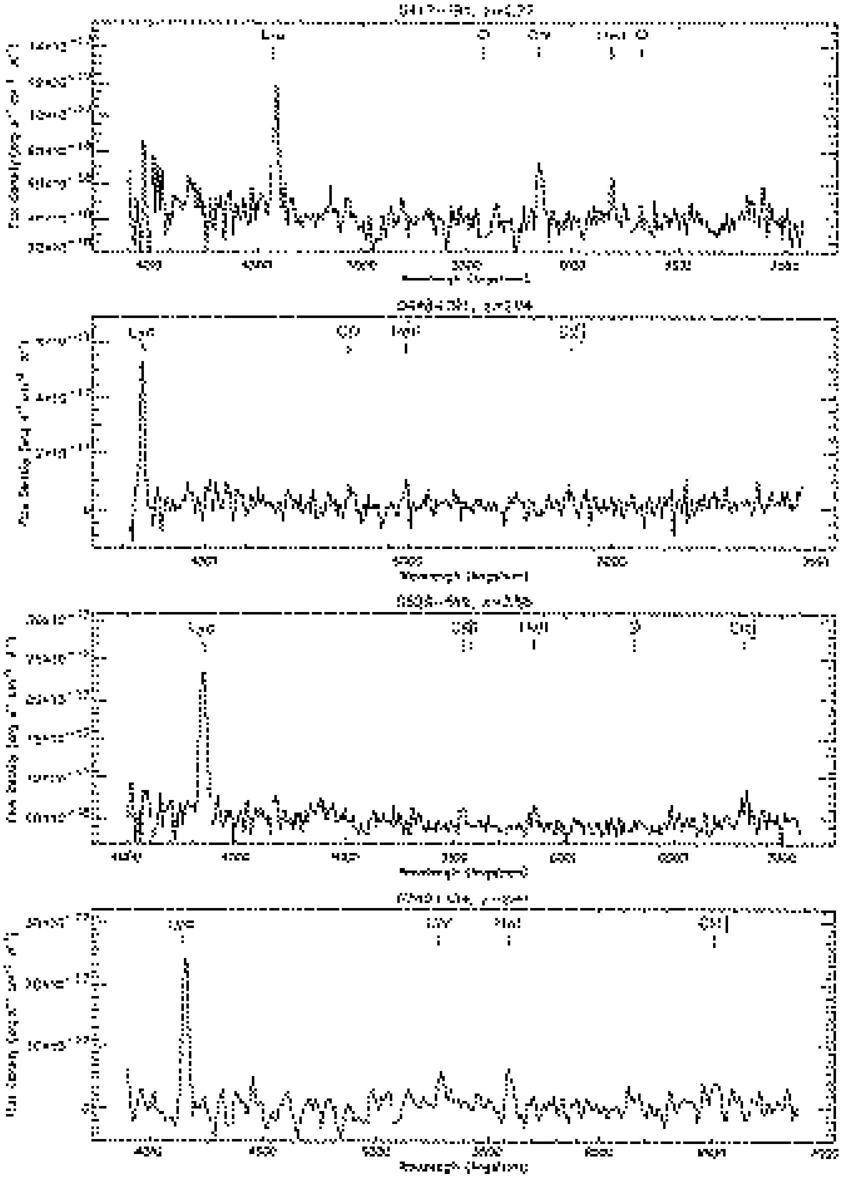

Figure 1: NTT and 3.6-m spectra of 4 z > 2 radio galaxies found during the ESO Key Programme.

observations – the large-size particles of the dust coma. Millimetre spectroscopic observations would be important to determine the molecular composition of the nucleus ices sublimating into the coma, to study the kinematics of the cometary atmosphere and to investigate its physical conditions, as well as searching for new molecular species. The combination of high angular resolution and high sensitivity provided by the LSA would permit the study of the structure and evolution of the gas and dust jets of comets, in relation to the outgassing processes of the cometary nuclei.

J. Lequeux concluded the scientific presentations by considering the synergy between the LSA and the VLT. He pointed out that these two instruments will be highly complementary, as they will both have high sensitivity and angular resolution. Furthermore, he said that the main scientific drivers for both the LSA and the VLT are cosmology and star formation, so that the science programmes will also be complementary – these are also the domains where the synergy will be at its best. For example, in the case of high-redshift galaxies, the millimetre observations will be biased in favour of dust-rich galaxies, whereas the optical is biased against such objects.

There followed a series of presentations about the LSA Study Project, focussing on various technical aspects. R. Booth provided an overview, stressing that, with the Plateau de Bure interferometer and the 10-m HH, 15-m SEST and JCMT, 20-m Onsala, and 30-m IRAM dishes, Europe is already strongly developed in millimetre astronomy, and the LSA is a logical next step.

The obvious location for the LSA is the Atacama desert in Chile, both for the unparalleled atmospheric conditions and for complementarity with the VLT. L. Bååth described the search presently being undertaken for a site sufficiently large for the LSA and at an appropriate altitude and within reasonable distance of infrastructure. One site has already been identified which is worthy of more detailed study. R. Hills discussed the problem of atmospheric phase fluctuations due to water vapour, for which corrections are required in order to obtain angular resolution significantly below 1 arcsec. There are a number of possible correction techniques (also discussed in poster papers by M. Bremer and P. Hall); the most promising is based on measurements of the atmospheric emission in the beam of each antenna.

Possible array concepts and configurations were outlined by S. Guilloteau. The large collecting area of the array, together with the need for a manageable number of dishes, implies large sizes for the individual antennas. They should be moveable, to provide high sensitivity at short baselines. Some initial configuration ideas were outlined, including a hierarchical (fractal) scheme. A. Baudry also made the case for subarrays capable of quick phase calibration, and commented on the use of the extended IRAM array as a testbed. Overall technical requirements (wavelength coverage, angular and spectroscopic resolution, polarization requirements, etc.) were still to be fully defined based on scientific objectives. D. Plathner described possible novel telescope designs that would meet the required specifications at low cost.

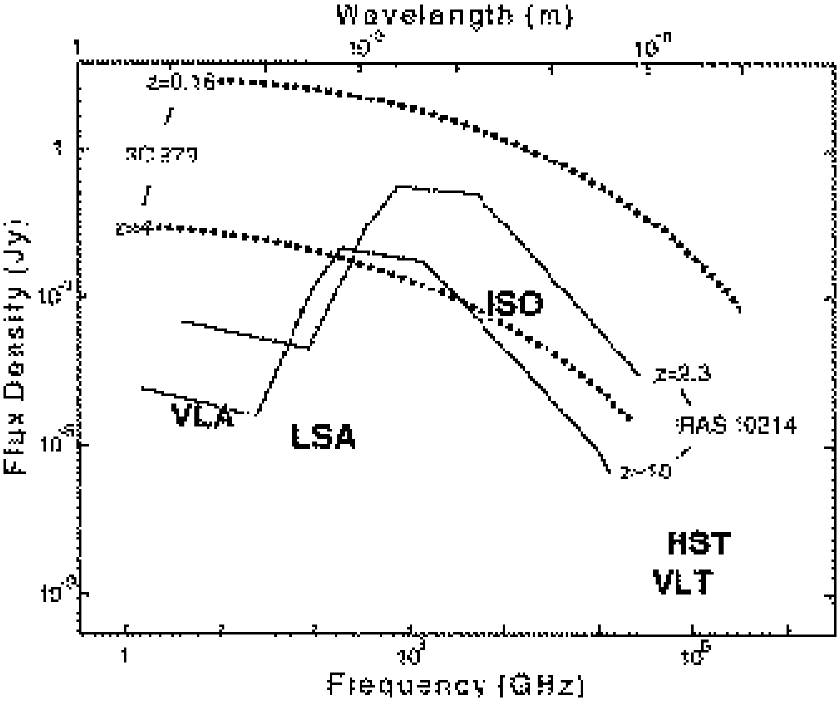

Sensitivity of the Large Southern Array for typical continuum observations, compared with that of some other large telescopes (approximate wavelength and sensitivity are indicated by the location of the telescope name in this plot). The broadband spectra of 3C273 (at z = 0.16 and redshifted to z = 4) and IRAS 10214+4724 (at z = 2.3 and redshifted to z = 10) are also shown for comparison.

J. Lamb commented that the provision of the large number of mixers required for the LSA would be a significant challenge. Millimetre receivers are already close to fundamental sensitivity limits, and the main advances to be made are in reliability and simplicity. Forecasting from the present he would predict SIS receivers with solid-state local oscillators, perhaps with HEMT receivers for frequencies < 150 GHz. Cryogenics would be a major issue. The correlator would also be a technical challenge, but, as A. van Ardenne showed, current developments in microelectronics are promising and the tenfold increase in correlator power is possible.

L. Woltjer concluded the workshop by again placing the LSA in context: it will be a counterpart of both the HST and the VLT, and will also serve the adjacent communities such as those of ISO, FIRST, and SOPHIA. In terms of the evolution in sensitivity and resolving power, the LSA is a logical and necessary development in millimetre astronomy, similar to that now being made in optical astronomy. He mentioned the advantages of ESO being involved in some way in this endeavour. There are many issues to be decided in the technical optimization of the LSA, and that is the purpose of the present Study Project. Funding possibilities should also be explored now, if the LSA is to be built sometime in the next decade.

The complete proceedings of this workshop will be published in the ESO Astrophysics Symposia series.

E-mail address: pshaver@eso.org

The Director General of ESO, Riccardo Giacconi, giving his opening remarks at the workshop.

of young stellar objects – infrared and maser emission – can be followed up at high angular resolution by the large array. The earliest phases require high angular resolution in order to locate the thermal dust emission, the high density molecular clumps, and the small-scale molecular outflows. The study of the evolution from disk to planet formation will require line and continuum observations with an angular resolution of 0.1″ and high sensitivity. One would like to study the morphology and kinematics of disks, the presence of rings, the distribution of molecules and dust. Molecular outflows are important both as an essential ingredient of star formation and for an understanding of the physics of astrophysical jets in general. K. Menten and C. Thum discussed molecular and recombination line masers from stellar envelopes. In addition to the study of the envelopes themselves, these masers can be used for a variety of purposes, ranging from distance measurement to “maser guide stars” that can assist in imaging faint emission around the stars.

The LSA will produce a quantum jump in the multi-wavelength continuum study of stars, as summarized by R. Pallavicini – thousands of stars of many types over practically the entire HR diagram will be detectable. This work will have an impact on studies of the winds of early stars, the photospheres and chromospheres of giants and supergiants, thermal emission from other evolved stars, the disks of pre-main sequence stars, the non-thermal emission from active stars, etc. By observing at mm wavelengths, one can go deeper into a stellar atmosphere, and explore a higher energy (> 1 MeV) electron population in flares. Measurement of the optically-thick free-free emission from the photospheres of normal stars will permit the determination of stellar radii for those stars with well-determined parallaxes. C. Fransson pointed out that the LSA will also be important for supernova research, as radio supernovae are first seen at high frequencies, and the LSA will be able to detect them out to 30 Mpc. VLBI studies of supernovae can be used for distance determinations. The angular resolution of the LSA will be important in the study of supernova remnants and their proper motions. In the case of SN 1987A, the fact that the LSA and HST will have similar angular resolution will be important; the prediction that the supernova shock wave will hit the [OIII] ring in the year 2005±3 may provide impetus for an early construction of the LSA!

Molecular line observations of circumstellar shells around evolved stars provide a unique probe of time-dependent chemistry, and M. Guélin indicated that the LSA will be capable of resolving these shells at distances of 6–10 kpc, the distance of the Galactic molecular ring. Planetary nebulae were described as “dust factories” by P. Cox, and LSA studies will provide important information about the process of interstellar enrichment. Many species of molecules have already been detected in 44 planetary nebulae, and the LSA will greatly advance such studies.

The study of solar-system objects would greatly benefit from combined observations using the LSA in conjunction with spacecraft. The LSA will contribute much to planetary science – our own solar system and possibly evidence about extrasolar planets. A. Marten described the progress that has been made from close encounters with planets by some two dozen spacecraft, and said that millimetre observations with the LSA would contribute to a wide variety of topics – composition, isotope studies, thermal structure, dynamics (winds), meteorology. LSA continuum observations of asteroids would complement radiometric observations at other wavelengths, contributing to the determinations of their size and albedo, as outlined by J. Crovisier*. In addition, it would provide the unique possibility to sample their subsurface temperature and study their thermal properties. LSA continuum observations of comets would explore dust sizes not accessible to optical or radio

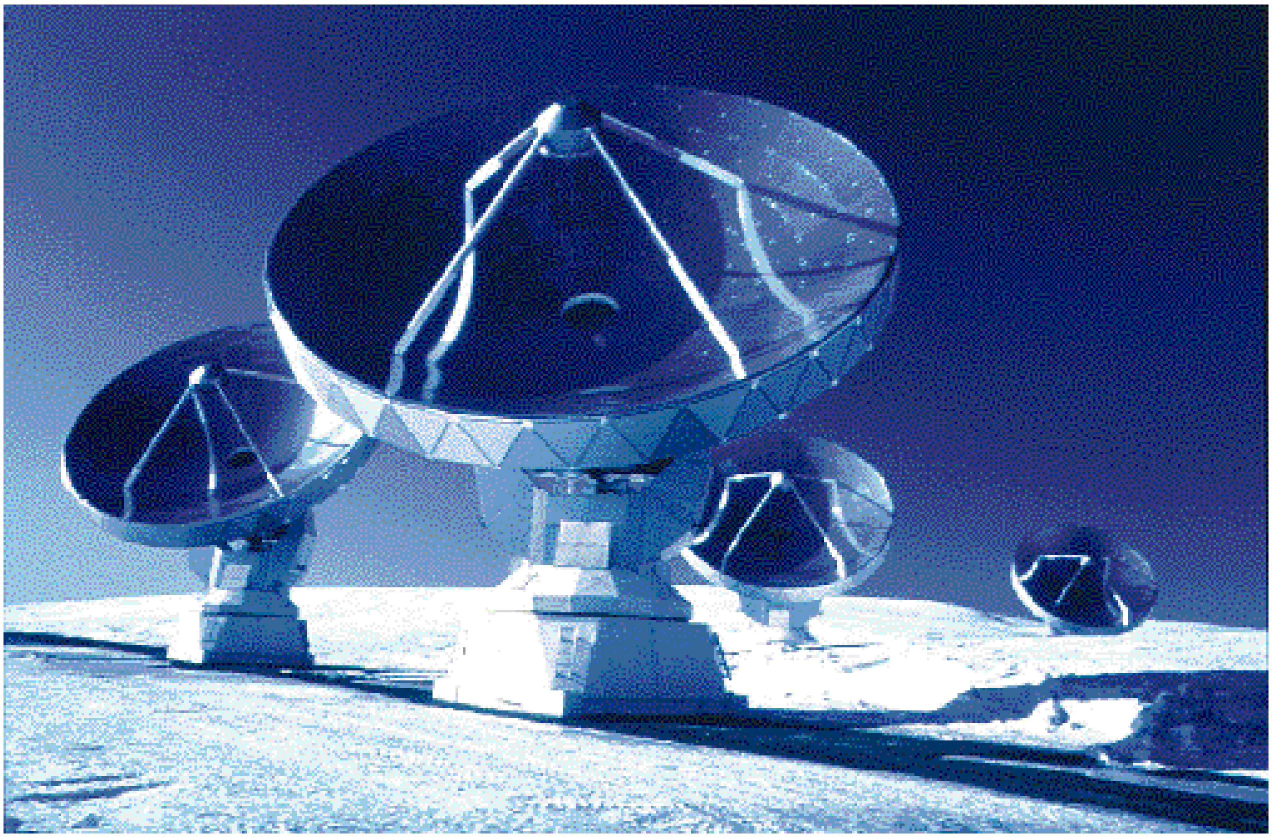

Current state-of-the-art in millimetre arrays: the four 15-m antennas of the IRAM interferometer on Plateau de Bure, France. Photo: A. Rambaud, IRAM.

baselines of hundreds and thousands of kilometres respectively. A variety of new observations would become possible, ranging from the immediate environs of supermassive black holes in galactic nuclei and extragalactic mega-masers, to milliarcsec imaging of Galactic objects with relatively low brightness temperatures (particularly stars and stellar winds) – a new field of scientific research. S. Wagner discussed variability as a diagnostic of AGN, and pointed out that the high sensitivity of the LSA will allow monitoring of a large fraction of the flat-spectrum radio-loud quasars in the Universe. R. Chini discussed mm continuum observations of AGN and galaxies, showing how a combination of infrared and millimetre observations can distinguish between types, even if optically obscured. High resolution millimetre continuum maps of galaxies can provide a powerful tool for studying star formation.

Several presentations by F. Combes, C. Henkel & T. Wiklind, D. Downes, F. Viallefond, R. Genzel and L. Tacconi concerned molecular line studies of galaxies. The LSA will be able to resolve individual clouds in other galaxies and achieve the same angular resolution for galaxies at z ~ 1 as can be achieved now in local galaxies, which will provide direct information on galaxy evolution. The main dynamical features – spiral arms, secondary bars and rings – will be resolved with enough sensitivity to constrain theoretical scenarios. The mass spectrum of molecular clouds in nearby galaxies will be determined, as will insights into large-scale star formation processes and the H_2/CO ratio. Special studies, such as mapping of gravitational arcs in molecular lines, will be possible. The LSA will address questions such as the origin and kinematics of the molecular gas in early-type galaxies. It will make possible detailed studies of the central regions of galaxies – molecular tori and rings, and nuclear star formation. The large collecting area and high sensitivity of the LSA will be required to spatially resolve the tori in AGN (NGC 1068 could be observed with 3 pc resolution), and to kinematically detect the central engines. The Magellanic Clouds provide a laboratory for interstellar medium and stellar studies, and F. Israel summarised the wide range of objects that will be detectable with the LSA.

In our own Galaxy, many classes of objects could be studied in unprecedented detail. P. Mezger pointed out that, if SgrA* at the Galactic centre is an underfed black hole, and if such objects occur in most galaxies, then as the closest example it will be very important to study in detail. The LSA would permit unobscured study of this object and its environment. R. Lucas explained how the LSA will be particularly suitable for the study of diffuse molecular clouds in absorption against extragalactic sources; thousands of sources will be accessible to the LSA, and as they will sample random (unperturbed) clouds, they will be ideal for unbiased statistical studies. T. Wilson and M. Walmsley discussed the potential contributions of the LSA to our knowledge of molecular clouds and astrochemistry. The large interferometer would contribute most from studies of molecular clouds near star-formation regions – the conditions at the start of cloud collapse, and the interaction of newly-born stars with nearby molecular clouds. Spectral scans with high resolution and sensitivity, and molecular maps with the same high angular resolution as the continuum maps, will provide new information on the chemistry, dynamics, and evolution.

Observing and understanding the formation of stars and planets is another of the main science drivers for the LSA, and was covered in talks by M. Felli, S. Beckwith, A. Dutrey, R. Bachiller, and several poster papers. The elusive protostars may best be found by virtue of their cold dust emission at millimetre wavelengths, and a large millimetre array will be ideal. In the early collapse phase the disks will be opaque at mm wavelengths, so easy to detect in the continuum. Other clues to the presence

Science with Large Millimetre Arrays

A Summary of the ESO-IRAM-NFRA-Onsala Workshop

P. A. Shaver, ESO

The next major step in millimetre astronomy, and one of the highest-priority items in radio astronomy today, is a large millimetre array with a collecting area of up to 10,000 m^2. A project of this scale will almost certainly require international collaboration, at least within Europe, and possibly with other major partners elsewhere. In order to establish a focal point for this project within Europe, a study has been undertaken by the Institut de Radio Astronomie Millimétrique (IRAM), ESO, The Onsala Space Observatory (OSO), and The Netherlands Foundation for Research in Astronomy (NFRA). In the context of this project, a workshop attended by some 100 participants was held at ESO Garching on December 11–13, 1995 to discuss the scientific advances which such an array will make possible.

In his opening remarks, the Director General of ESO, Riccardo Giacconi, stated that ESO is committed to supporting the large millimetre array project as the possible new major prospect in European ground-based astronomy. He added that the form and extent of this support will have to be discussed in the relevant committees.

The array concept under study has been outlined in a recent document ("LSA: Large Southern Array"), which is available from IRAM or ESO. The initial concept was briefly reviewed at the workshop by D. Downes: an array of some 50 $\times$ 16 m antennas with baselines up to 10 km, operating at a site in northern Chile above 3000 m altitude to wavelengths as short as 1 mm, providing the high sensitivity of a collecting area of 10^4 m^2 and angular resolution better than 0.1″. He pointed out that this array would be a reasonable next step in terms of collecting area, at the cost of a small scientific satellite. These parameters set the scene for the following talks.

The array was placed in the context of 21st century astronomy by M. Longair*, who described it as a millimetre equivalent to the Hubble Space Telescope, one which will open up new ways to tackle many of the most important problems of astrophysics. Star-forming galaxies that would be difficult to see with HST will be detectable out to redshifts of ~ 10–20, thus providing a window into the 'dark ages' beyond z ~ 5 when much of the key activity in galaxy formation may have taken place. With its high sensitivity and angular resolution, the LSA will be particularly well suited for studying gravitational lensing of high redshift galaxies – strong lensing, weak lensing (the shear field), and cluster arcs. Millimetre astronomy is currently undergoing a revolution, with observations of the high redshift Universe and an increasing diversity of objects, and Longair concluded that the LSA will play an important part in the multi-wavelength approach to the great problems of astronomy.

The study of young galaxies in the early Universe is one of the main science drivers for the LSA, and there were presentations by S. White, G. de Zotti, P. van der Werf, M. Rowan-Robinson, and A. Blain on this subject. White pointed out that HST images of distant "protogalaxies" already show them to be complex structures suggesting that they are gas-rich and dynamically evolving; the LSA will be capable of studying them in detail, and determining their space distribution over a large redshift range for comparison with theories of large scale structure evolution. De Zotti stressed that very strong dust emission may be the dominant signature of young galaxies, in which case millimetre observations will be the principal means of finding young galaxies in the early Universe and understanding their evolution. The uniform sensitivity to such galaxies over a large redshift range may even provide an opportunity to investigate the geometry of the Universe. Rowan-Robinson placed the LSA in the context of other FIR/mm surveys for distant galaxies using IRAS, ISO, SCUBA, and FIRST. A survey with the LSA would be completely dominated by galaxies at high redshift; it would have unprecedented source density, the highest proportion of z > 2 sources, and exceptional positional accuracy and resolution. A. Blain concluded that as many as 10^4 galaxies at z > 5 may be detectable in both line and continuum with the LSA, and that gravitational lenses could be up to a thousand times more numerous in the mm waveband than in optical/radio. P. van der Werf reviewed existing mm searches for, and observations of, high-redshift galaxies, commented that our own Galaxy could be detected up to z ~ 3–5 in CO or the 158 μm [CII] line with the LSA, and discussed search strategies. At still higher redshifts, P. Encrenaz discussed the prospects of searching for primordial molecules such as LiH and LiH$^+$.

The potential of the LSA for studying high-redshift quasars and quasar absorption systems was highlighted by the presentation of new results by A. Omont and T. Wiklind. Omont showed detections of mm continuum radiation from the highest redshift quasars; observations with the Plateau de Bure interferometer indicate that the emission from the z = 4.7 quasar APM 1202-07 comes from two components, the quasar itself and another object at the same redshift 2.5″ away. The LSA will make it possible to map such emission and search for other such objects, some of which may be dust-obscured. Wiklind showed results from the exciting new field of molecular absorption-line spectroscopy of quasars. As many as 15 distinct molecular transitions have already been detected in individual absorption systems in quasar spectra out to redshifts of 0.89; the highest-redshift system was discovered purely by spectral scans in the millimetre wavebands, in a radio Einstein ring which has not yet been optically identified. Several molecular transitions have been detected in individual systems. The LSA will greatly expand this work, by virtue of its high sensitivity and discrimination of point sources against extended emission, making possible such important measurements as gravitational lens time delays, the temperature of the microwave background as a function of redshift using different molecular transitions, and isotopic ratios at cosmological distances.

The LSA will contribute to studies of the physics of active galaxy nuclei, with its high sensitivity, its discrimination of point sources, and its ability to probe deeply into galactic nuclei because of low synchrotron and dust opacity at millimetre wavelengths. T. Krichbaum described the kinds of science that will be possible if the LSA can be used as a phased array for mm VLBI. At wavelengths shorter than 3 mm, VLBI is capable of resolutions of a few tens of microarcsec, corresponding to fractions of a parsec at z = 1. Space VLBI at mm wavelengths would provide still higher resolution. Unprecedented sensitivity would also be possible: ~ 1 mJy, corresponding to brightness temperatures T_B ~ 10^2–10^4 K and T_B ~10^4–10^6 K for

* Owing to transportation difficulties, M. Longair and J. Crovisier were unable to attend the workshop, and their papers were presented by A. Blain and P. Encrenaz respectively.

(b) the provision of single-mode instruments (i.e., a beam-combining instrument which covers a field of view equal to the extent of the Airy disk of an individual telescope of the array) for both of these wavelength regimes,

(c) the implementation of a narrow-angle astrometric capability in the near infrared,

(d) the deployment of three 1.8-m ATs with low-order adaptive correction (i.e., tip and tilt),

(e) the incorporation, at the earliest time possible, of two UTs augmented with low-order adaptive correction (i.e., tip and tilt),

(f) the capability to operate with up to four array elements simultaneously so as to permit reliable phase retrieval and imaging using closure techniques.

4. That the later phases should allow:

(a) operation at shorter wavelengths,

(b) incorporation of higher levels of adaptive compensation,

(c) operation using all four UTs as well as the auxiliary array elements.

The reaction of the whole ESO community to the ideas outlined in this article is warmly encouraged, and indeed may be pivotal in better defining ESO's programme. Please feel free to contact any of the ISAC members listed here or send e-mail to isac@eso.org. We also invite everyone with an interest in the scientific potential of VLTI to attend the ESO Workshop in Garching on June 18–21 where we look forward to constructive feedback.

References

Antonucci, R., 1993, *ARA&A* **31**, 473.
Barvainis, R., 1992. In: *Testing the AGN paradigm; Proceedings of the 2nd Annual Topical Astrophysics Conference*, Univ. of Maryland, p. 129.
Bjorkman, J.E., Cassinelli, J.P., 1993, *ApJ* **409**, 429.
Buscher, D.F., Haniff, C.A., Baldwin, J.E., Warner, P.J., 1990, *MNRAS* **245**, 7P.
Camenzind, M., 1990, *Rev. Mod. Astron.* **3**, 234.
Cidale, L.S., Vazquez, A.C., 1995, *ApJ* **453**, 393.
Danchi, W.C., Bester, M., Degiacomi, C.G., Greenhill, L.J., Townes, C.H., 1994, *AJ* **107**, 1469.
Doazan, V., 1987. In: IA U Colloq. 92, *Physics of Be stars*, Cambridge: Cambridge University Press, p. 384.
Duquennoy, A., Mayor, M., 1991, *A&A* **248**, 485.
Duquennoy, A., Mariotti, J., Mayor, M., Perrier, C., 1995. In: Walsh, J., Danziger, I.J. (eds.), *Science with the VlT*, ESO, p. 150.
Eckart, A., Genzel, R., Hofmann, R., Sams, B.J., Tacconi-Garman, L.E., 1995, *ApJ* **445**, L23.
Genzel, R., Eckart, A., Drapatz, S., Krabbe, A., 1995. In: Walsh, J., Danziger, I.J. (eds.), *Science with the VLT*, ESO, p. 281.
Ghez, A.M., Neugebauer, G., Matthews, K., 1993, *AJ* **106**, 2005.
Haniff, C.A., Scholz, M., Tuthill, P.G., 1995, *MNRAS* **276**, 640.
Henry, T.J., McCarthy, Donald W., J., 1993, *AJ* **106**, 773.
Ivezic, Z., Elitzur, M., 1996, *MNRAS* **445**, 415 (in press).
Leinert, Ch., et al., 1993, *A&A* **278**, 129.
Lorenz-Martins, S., Lefsevre, J., Mekarnia, D., 1995, *A&A* **300**, 214.
Malbet, F., Bertout, C., 1995, *A&AS* **113**, 369.
Marlborough, J.M., 1987. In: IAU Colloq. 92, *Physics of Be stars*, Cambridge: Cambridge University Press, p. 316.
Marsh, K.A., Mahoney, M.J., 1993, *ApJ* **405**, L71.
Mayor, M., Queloz, D., 1995, *Nat* **378**, 355.
Mourard, D., Bosc, I., Labeyrie, A., Koechlin, L., Saha, S., 1989, *Nat* **342**, 520.
Nakajima, T., Oppenheimer, B.R., Kulkarni, S.R., et al., 1995, *Nat* **378**, 463.
Neugebauer, G., Graham, J.R., Soifer, B.T., Matthews, K., 1990, *AJ* **99**, 1456.
Quirrenbach, A., Hummel, C.A., Buscher, D.F., et al., 1993, *ApJ* **416**, L25.
Quirrenbach, A., Buscher, D.F., Mozurkewich, D., Hummel, C.A., Armstrong, J.T., 1994, *A&A* **283**, L13.
Rebolo, R., Zapatero Osorlo, M.R., Martin, E.L., 1995, *Nature* **377**,129.
Reipurth, B., Zinnecker, H., 1993, *A&A* **278**, 81.
Schwarzschild, M., 1975, *ApJ* **195**, 137.
Stee, P., De Araujo, F.X., Vakili, F., et al., 1995, *A&A* **300**, 219.
Struve, O., 1931, *ApJ* **73**, 94.
Theodore, B., Petitjean, P., Hubin, N., 1994, *The Messenger* No. **77**, 20.
Tuthill, P.G., Haniff, C.A., Baldwin, J.E., 1994. In: Robertson, J.G., Tango, W.J. (eds.), IAU Symposium 158: *Very High Angular Resolution Imaging*, Kluwer, Dordrecht, Sydney, Australia, p. 395.
Van Winckel, H., Waelkens, C., Waters, L.B.F.M., 1995, *A&A* **293**, 25.
von der Lühe, O., Solanki, S., Reinheimer, T., 1995. In: Strassmeier, K.G. (ed.), IAU Symposium 176: *Stellar Surface Structure*, Vienna, Austria (in press).
Wilson, R.W., Baldwin, J.E., Buscher, D.F., Warner, P.J., 1992, *MNRAS* **257**, 369.
Winters, J.M., Fleischer, A.J., Gauger, A., Sedlmayr, E., 1996, *A&A* **302**, 483.

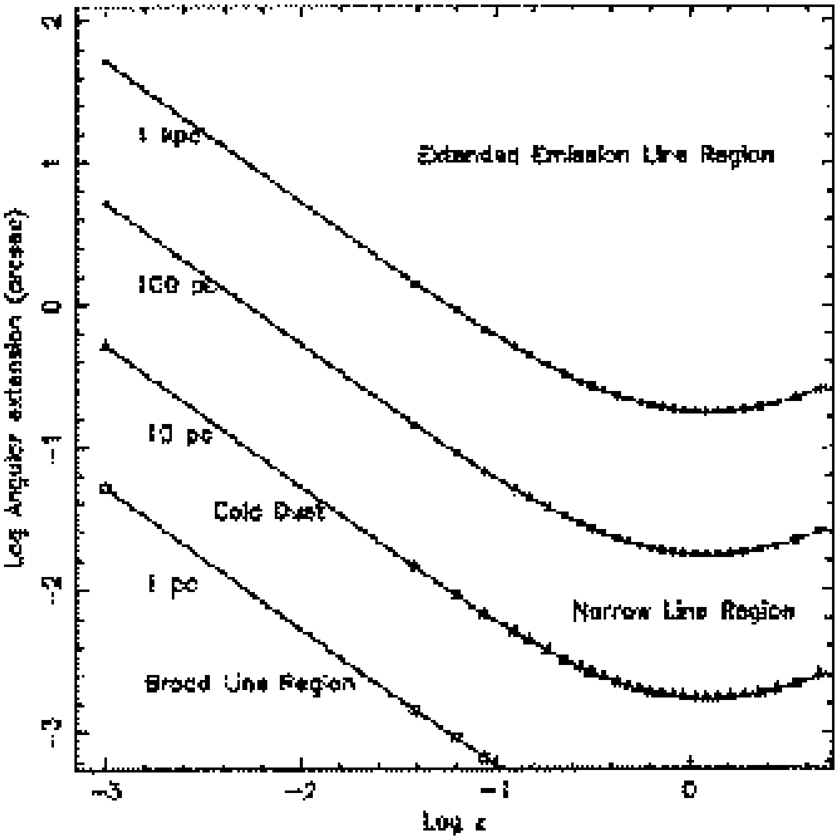

Figure 6: Angular extension as a function of redshift for regions with linear sizes of 1 pc (open squares), 10 pc (open triangles), 100 pc (filled squares) and 1 kpc (open circles). The calculations assumed H_o = 75 km/s/Mpc and q_o = 0.5. The difference in look-back time between adjacent symbols is constant and equal to about 0.5 Gyr.

mation in the vicinity of the Galactic centre, and to search for "peculiar" stars, which may be the remnants of stellar collisions. Observations at 10 µm would also reveal the distribution of warm dust associated with SgrA*.

Observing the Galactic centre is quite a challenging task for the VLTI because of the high density of sources. Hybrid configurations formed by combining the UTs with the ATs will give good coverage of the (*u*, *v*) plane, in particular when the technique of multi-frequency synthesis is employed. The focal plane instruments needed for observations of the Galactic centre are (i) an instrument for the mid-infrared with spectral resolution R ≈ 200, and (ii) a near-infrared instrument with R ≈ 2000. For the investigation of SgrA*, polarimetric capabilities would be very valuable.

2.8 Active Galactic Nuclei

AGNs are thought to be powered by accretion onto a massive black hole. For reasons that are not understood, but are probably related to the way galaxies form, there are many more AGN at high redshifts than locally. The space density of high-luminosity AGN at $z \sim 2$ is 100–1000 times greater than at the present epoch.

Although our understanding of the AGN phenomenon has increased dramatically, major fundamental issues remain unsettled. These include the precise mechanisms involved in feeding the central black hole, the relationship between AGN activity and ultraluminous starbursts, and the reason why some AGN in elliptical galaxies are radio loud (but not those in spirals). The relationship between members of the AGN zoo, ranging from the brightest quasars to barely-active Seyfert galaxies, is not understood.

There has been much debate on the relation between radio-loud quasars and radio galaxies (for a review see Antonucci, 1993). It could be that these objects are intrinsically similar but with differences that can be related either to their evolution, their environment or their orientation to our line of sight. The third possibility is currently the most favoured. In this scenario, the bright nucleus is surrounded by an obscuring torus of dust and gas, resulting in twin beams of continuum emission. If our line of sight falls along one of these beams then we see a quasar, otherwise the object appears as a radio galaxy.

A similar explanation can be applied to Seyferts, in which double cone-shaped emission has been observed directly. In Seyfert 1 galaxies, the Broad Line Region (BLR) can be seen in emission lines, but in Seyfert 2s our line of sight to the nucleus is obscured by the torus, making the BLR undetectable except in scattered light. One way to investigate the unified model directly is to image the very central part of the active nucleus.

Infrared imaging of the central regions is clearly important for our understanding of AGN. Dust near the nucleus will be heated by the UV flux from the central engine and there is good evidence that most, if not all, the infrared emission from AGN comes from heated dust (see Barvainis, 1992). The size of the emitting region is quite small. For example it is $5h_{75}^{-1}$ pc or 0.16″±0.04 (1 σ) in NGC 4151 (Neugebauer et al., 1990) at 10 µm.

About 20–30 nearby Seyfert galaxies are bright enough to be used as references for fringe tracking. For these, the central parsec will be probed in the optical and infrared. It is also useful to probe larger scales in more distant objects, to trace any cosmological evolution. Figure 5 shows simulated images of a typical AGN observed at different angular resolutions and Figure 6 shows how the angular sizes of the relevant regions scale with redshift.

If fringe tracking cannot be done on the object itself, a nearby reference star can be used. It is thus important to search for new objects (radio selected or by-products of planned surveys) located near bright stars. The overall impact of VLTI in extragalactic astronomy will depend on the sky coverage. Calculations for the adaptive optics system on a unit telescope in the visible predict a sky coverage of about 1% (Théodore et al., 1994). This increases by a factor of 4–5 if the correction is done in the near infrared and becomes even greater in the mid-infrared. A catalogue of bright stars in the near infrared is needed to search efficiently for observable objects.

3. Conclusion

On the basis of the above science goals, ISAC reached a clear consensus as to the appropriate phasing of capabilities that would minimise costs and maximise possible scientific benefits both in the short and long term. The recommendations are:

1. That the VLTI should be brought into operation as soon as possible.

2. That the development of VLTI should proceed in sequenced phases of increasing complexity, leading to the full implementation of the VLTI as endorsed by previous committees.

3. That the earliest phases should focus on:

(a) the near- and mid-infrared regimes (1–5 µm and 10–20 µm),

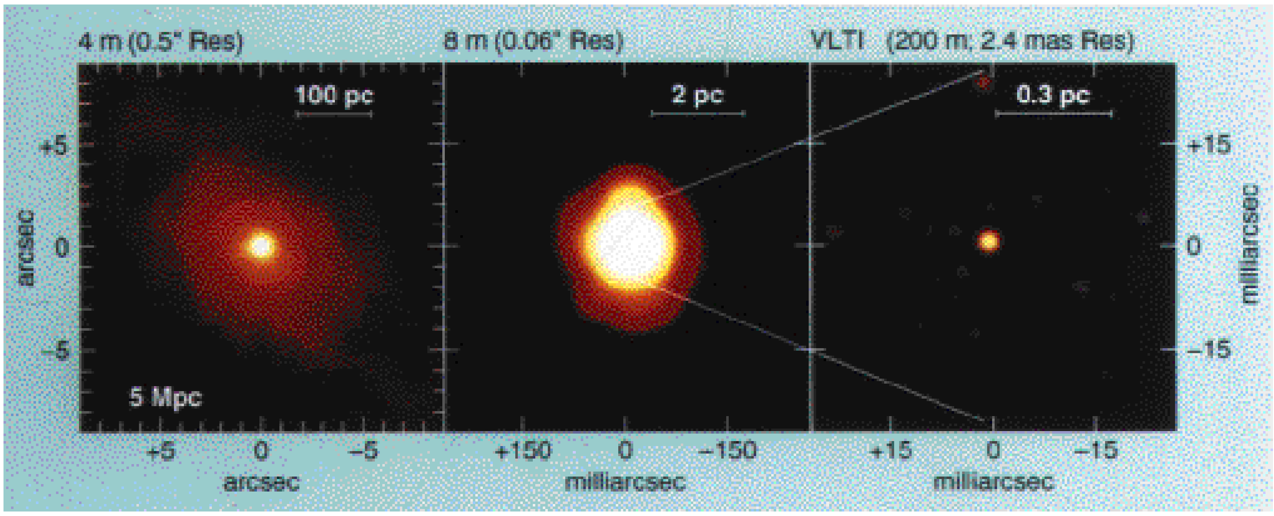

Figure 5: Simulated 2.2 µm imager of an active galaxy at a distance of 5 Mpc, when observed at three different spatial resolutions. Left: 0.5 arcsec resolution (adapted from a SHARP/NTT image of NGC 1068). Middle: 0.06 arcsec resolution (adaptive optics on a UT). Right: 0.003 arcsec resolution (VLTI). The galaxy is assumed to contain a point-like AGN surrounded by a star cluster. From Genzel et al. (1995).

large apertures of the VLTI will be vital to achieve high spectral resolution maps in a few nights.

2.6 AGB stars

All stars with initial masses $\lesssim 8M_\odot$ end their lives on the Asymptotic Giant Branch. An AGB star consists of a degenerate C/O core surrounded by a very extended convective atmosphere from which mass is lost via a dense and dusty outflow at rates of 10^{-8} to 10^{-4} $M_\odot$/yr and expansion velocities of 5–30 km/s. The mass-loss mechanism in AGB stars is poorly understood. It is believed to be related to the slow pulsations and the formation of dust, which is subsequently pushed out by radiation pressure. Improving our understanding of the physical mechanisms that drive this process is important because mass loss dominates AGB evolution and also because AGB stars play an important role in the chemical evolution of galaxies by returning gas and dust to the ISM.

Questions that may be addressed are: (i) Where does the dust form in the extended atmosphere? If it forms too far away from the photosphere the mass-loss rate resulting from radiation pressure on the dust grains is insufficient to explain the observations. (ii) What is the role of the pulsations in the mass loss process? Is the star distorted due to the large convective motions in the envelope? (iii) What molecules are depleted in the dust formation region? (iv) How does dust formation depend on the phase of the pulsation and on the chemical composition of the star?

Several theoretical studies have highlighted the potential of mid-infrared interferometry for studying AGB envelopes and addressing some of these issues (Lorenz-Martins et al., 1995; Winters et al., 1995; Ivezic & Elitzur, 1996). The mid-infrared region is ideal for studying dust formation near AGB stars and the accompanying depletion of atoms and molecules. A start has been made by Danchi et al. (1994) using the Infrared Spatial Interferometer, which has two 1.65-metre apertures (see Table 1). Their measurements, made at 10 µm using baselines up to 13 m, allowed a detailed study of the inner radii for 13 of the brightest late-type stars. The VLTI, with its 8-m apertures and 10–20 µm capability, is uniquely suited to extending this work to fainter and more distant objects and with higher spectral resolution. For example, the location and properties of the silicate dust can be studied by measuring the change in size of the object as a function of wavelength through the silicate features at 9.7 and 18 microns (Lorenz-Martins et al., 1995). The layers above the photosphere in which dust forms may extend to about 10 stellar radii, which is several tens of milliarcsec at distances of 500–1000 pc and easily accessible to VLTI. Direct imaging of the stellar disk will also be possible, so limb darkening and distortions from sphericity can be measured. If an AGB star is imaged throughout a pulsation cycle and if simultaneous radial velocity data are taken, the distance can be measured.

The mid-infrared also is the obvious wavelength region for studying post-AGB stars. Many post-AGB candidates were discovered in the IRAS point source catalogue to show warm dust (500 K) and turn out to be binaries. The most famous example of such an object is the Red Rectangle (see Van Winckel et al., 1995). It appears that mass loss on the AGB can be affected by the presence of an unseen companion, with mass being stored in a circum-binary disk. It is currently unclear whether these disks are stable and how they affect the further evolution of the object and the formation of a planetary nebula. The disks should be a few to several tens of AU in size, which means they can be resolved by VLTI at a distance of 500 pc.

2.7 The Galactic centre

The central 0.1 pc of our Galaxy will be an important target for VLTI at wavelengths from 2 to 10 µm The resolution of the VLTI at 2 µm is about 2 mas, which at the Galactic centre corresponds to 15 AU or about 1500 times the Schwarzschild radius of a 10^6 $M_\odot$, black hole. The first and most important goal will be to test for the presence of a central massive black hole by measuring the three-dimensional velocity field of the star cluster centred on IRS 16. The current astrometric programme at the NTT (Eckart et al., 1995) could be continued with higher precision and radial velocities could be determined at very small distances from the centre of the star cluster, where observations with single telescopes are limited by crowding.

Another very important goal for the VLTI will be detailed observations of the infrared sources close to the position of SgrA*. It is presently unclear whether any of the objects found at 2.2 µm is the true counterpart of the compact radio source. The study of a potential IR counterpart of SgrA* would give completely new insights into the vicinity of the central object of our Galaxy, and could perhaps give us a direct view of the putative accretion disk. In addition, the high angular resolution of the VLTI will enable us to obtain infrared spectra of individual stars in the very crowded Galactic centre region. It will thus be possible to make a census of the stellar population in this area, to check whether there is ongoing star for-

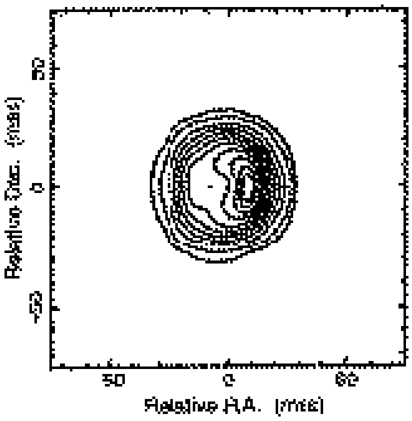

Figure 4: Image of the M2 Iab supergiant Betelgeuse at 710 nm obtained using optical interferometry with the 4.2-m WHT (adapted from Buscher et al., 1990). This maximum-entropy reconstruction shows a single bright feature that is offset from the centre of an otherwise uniform disk. It represents the first resolved image of a star apart from the sun, and shows a convective hotspot. This type of feature has recently been rediscovered by HST at ultraviolet wavelengths. The large apparent size of Betelgeuse means that it is one of the few stars than can be resolved with HST. VLTI, with its 100-m baseline, will suffer no such limitations and offers the prospect both of investigating stars such as Betelgeuse at much higher spatial resolution, and of extending surface studies to more distant populations and less extended stellar types. Contours are plotted at 5, 10, 20, 30, . . . 90, 95 % of the peak intensity. Note the scale of the axes – this is the one of the largest stars in the sky (in terms of apparent size).

shown in Figure 4 is typical of those now being regularly obtained, which show a small number of bright unresolved features containing typically 5–15 % of the stellar flux superimposed on an otherwise uniform disk. The relationship, if any, between these features and the well-documented mass loss and variability of Betelgeuse is at present unclear.

These surface features, which appear as bright “hotspots” of emission, are probably the result of large-scale convective upwellings of material from hotter regions of the stellar interior (Schwarzschild, 1975). Their number, evolution timescale and brightness are certainly all consistent with such an hypothesis, but their detection has raised a number of further questions that will likely be amenable to large interferometers like the VLTI. For this reason, cool evolved stars are among the most promising targets for pilot interferometric observations. A brief summary of the possible science goals for such observations are listed below:

Frequency of occurrence. Although now imaged on a handful of massive M supergiants, there is growing evidence that surface inhomogeneities are also present on Mira-type long-period variables, i.e., stars of much lower masses (Tuthill et al., 1994; Haniff et al., 1995). Limitations on the resolving power currently attainable from the ground mean that only the nearest and most luminous sources have been observed. The primary goal of an interferometric survey of the local neighbourhood will be to determine the frequency of occurrence of these hotspots as a function of type and luminosity class.

Evolutionary timescale. One of the most useful diagnostics in the study of surface inhomogeneities will be the precise determination of their evolutionary timescales. Predictions exist for convective models, (Schwarzschild, 1975) but there has been little effort to monitor these stellar surfaces using high-resolution imaging methods. A dedicated interferometer offers the possibility of such a programme.

Multiplicity. Current ground-based studies of stellar hotspots have been constrained by the limited resolutions of monolithic telescopes. In this sense, observations have only been able to place limits on the sizes and multiplicities of the hotspots seen on these targets. Once again, predictions for these properties exist for a number of models, implying that significant progress could be made if observations at much higher spatial resolution were available.

Location. Another useful diagnostic for elucidating the physical mechanism responsible for surface features will be the identification of the precise radial depth at which they occur. Because of the abundance of molecular and atomic species in cool stellar atmospheres, spectrally resolved measurements provide useful information as to the radial stratification of the stellar atmosphere, and so it should be possible, in principle, to map out the vertical locations of the surface inhomogeneities.

Mass loss. Perhaps the most exciting prospect lies in tying together the observed surface features with the prodigious mass loss and variability of cool giants and supergiants. Mass loss from cool stars remains a very poorly understood area, and interferometric observations offer the prospect of imaging circumstellar dust very close to the stellar surface, of monitoring the photospheric radius directly, and of directly relating spatially resolved images with photometric and polarimetric variability.

As well as the main areas listed above, one should not forget more mundane, but equally important, problems that could be addressed by the VLTI. These include precise angular diameter measurements, which lead to effective temperature, and studies of the atmospheric structure. All the questions raised here can be addressed by a combination of programmes: (i) detailed studies of selected sources, (ii) monitoring of selected sources every month, and (iii) a survey of the local neighbourhood. In many instances, interferometric data will provide the first direct measurements with which to confront — and perhaps overturn — existing theories.

2.5 Be stars

Be stars show Hα emission that is strongly variable and usually double-peaked. They are also known to be rapid rotators, which led Struve (1931) to suggest that the emission arises in a circumstellar disk of ejected matter. This model has not been universally accepted (Doazan, 1987), but optical interferometry has now confirmed that Be star envelopes are indeed flattened (Mourard et al., 1989; Quirrenbach et al., 1993, 1994; Stee et al., 1995).

Ad hoc models which assume a disk geometry have been successful in describing the winds of Be stars (e.g., Marlborough, 1987), but a theoretical mechanism for disk formation only came through the work of Bjorkman & Cassinelli (1993). They showed that Coriolis forces in the radiation-driven wind of a rapidly rotating star will force the flow of gas towards the equatorial plane and create a very thin, dense disk. Many questions remain unsolved, however. This model underestimates the amount of matter in the disk by a factor of about 100 and predicts a disk opening angle which is much smaller than that derived from the statistics of shell stars. Also, the important variable character of Be stars (short-, middle- and long-term) is not understood. Indeed different mechanisms could give the same classical measurements. Fortunately, one can show that the analysis of the interferometric data through the different variation cycles allows the determination of the correct processes.

VLTI at optical and infrared wavelengths is very well suited to resolving the disk structure of Be stars and monitoring time variability. There are more than 100 Be stars brighter than 6th magnitude and they have already been well studied by classical techniques (spectroscopy, photometry, polarimetry). Interferometry brings new constraints on the size and morphology of the disk (including velocity and density fields), on the central star itself (radius, ellipticity, surface activity and limb-darkening – see Cidale & Vázquez, 1995) and on the effects of a binary companion.

Be stars make good targets for long-baseline interferometers, thanks to the simultaneous presence of a point-like continuum source (the central star) and a resolved structure (the emitting envelope). The programme demands a good spectral resolution (R=10,000 in the visible and R=100–1000 in the near-IR). Moderate (u, v) coverage is sufficient because the geometry is simple – even without images, and strong constraints can be placed on the physical processes involved in the Be phenomenon. The

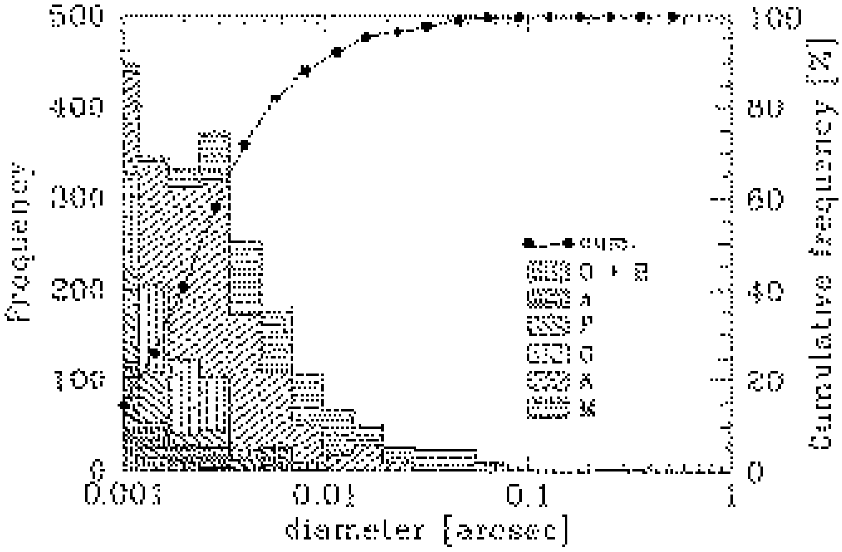

Figure 2: Histogram of CADARS (Catalogue of Apparent Diameters and Absolute Radii of Stars; Fracassini et al., 1988) stars with apparent diameters above 1 mas and declinations south of +40°. The solid line represents the cumulative frequency.

naries within a reasonable time: an orbit of 100 AU takes about 1000 years, but one of 4 AU will be completed in 8 years. Fortunately, the incidence of binaries among young stars is high (Reipurth & Zinnecker, 1993) and is probably close to 100% in some molecular clouds (Ghez et al., 1993; Leinert et al., 1993). Masses from binary orbits will finally provide urgently needed empirical checks on the evolutionary tracks used in interpreting the observations of young stars.

The key capabilities of VLTI in this field are its resolution, sensitivity and infrared response. There are many bright YSOs (V = 11–15, K = 6–9) which will make ideal targets. Once the first two ATs become available, a good first-light project would be to determine stellar masses from orbital motion and to search for new companions. Measuring visibilities at different wavelengths in the near- and mid-infrared bands will allow us to investigate the temperature and density distributions of the circumstellar material and search for gaps which might indicate the formation of planets. Finally, closure-phase imaging will be used to provide the detailed geometrical information needed to understand the fascinating phenomena mentioned above.

2.4 Stellar surface structure

A survey by von der Lühe et al. (1995) indicates that about 2000 stars with declinations less than 40° north have apparent diameters of one milli-arcsec and more and therefore are resolved to VLTI baselines in the NIR. Most of these stars are late-type giants. Some 50% have apparent diameters of 2.5 mas or more and will permit detailed studies of their surfaces. Figure 2 shows the histogram for the distribution of apparent diameters and spectral class.

The superior imaging capability of VLTI will make possible the study of physical characteristics of surface phenomena and their variation with time. Important surface phenomena are due to hydrodynamic and magnetohydrodynamic effects and result in large-scale convection cells in the outer convection zones and concentrations of magnetic fields. The study of convection through surface temperature and line-of-sight velocity variations provides clues to the fundamental properties of the convection zone. The temporal variation of active regions provides insight in the underlying dynamo processes which generate magnetic fields in stars.

Figure 3 shows the interferometric signal (visibility magnitude) which can be expected for a relatively quiet (solar-type) and an active star. It is important to notice that the signatures in the visibility functions occur at high angular frequencies and have small magnitudes. Only structures on active giants will probably be well resolved by VLTI. Although the target sources are bright (most stars have visual magnitudes between 2 and 8), the low visibility signal and the high spectral resolution required to perform measurements of velocities and Zeeman profiles will make necessary the use of the UTs.

The detection of surface features on cool giants and supergiants using large single telescopes has been one of the most important successes of interferometric imaging (Buscher et al., 1990; Wilson et al., 1992). The best-studied example is Betelgeuse. The image

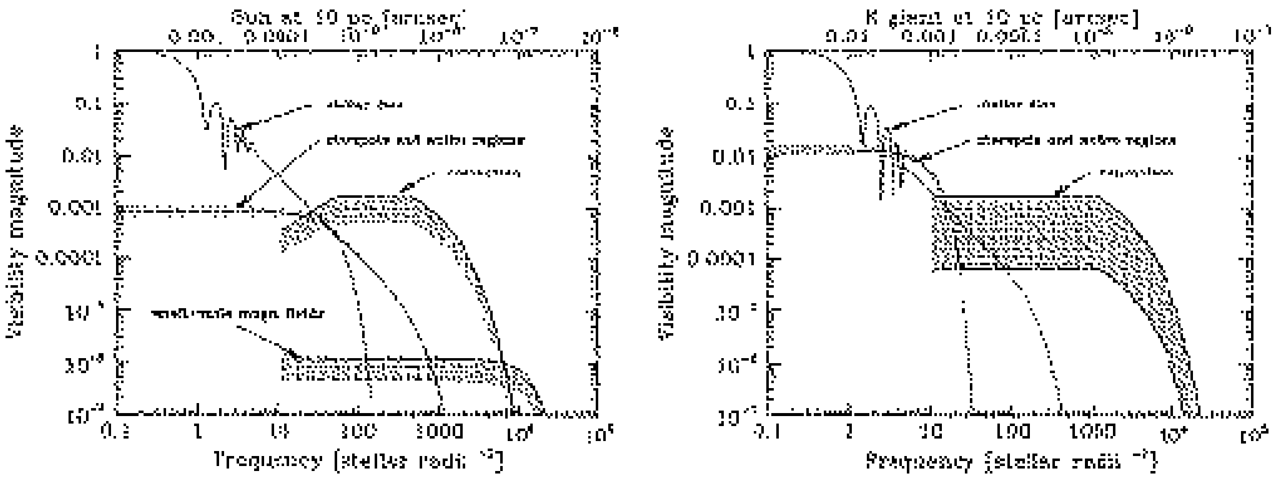

Figure 3: Distribution of visibility magnitude for a quiet (solar-type) star (left) and for an active giant (right). The phenomena shown are convection, active regions (starspots and plages) and small-scale magnetic fields. The large contribution at low frequencies is due to the sharp edge of the stellar disk. Angular frequencies are given in units of "inverse stellar radii." The corresponding scale in arcsec is shown on the top for the Sun at 10 pc (left) and for a K giant with 24 $R_\odot$ (right) .

called classical T Tauri stars, means that progress in understanding the physics of star formation may have important implications for extragalactic astronomy.

A major programme for the VLTI is to study systematically the rich circumstellar environments of YSOs at a resolution of about 2 mas, which corresponds to 20–30 stellar radii (0.3 AU) for the nearest star-forming regions (d = 150 pc). The factor of twenty increase in resolution over HST provides access to the phenomena which occur in the inner regions around young stars and should provide important input to the theoretical models. However, even VLTI will not be able to resolve the innermost parts of the accretion disk, where material is presumably funnelled via magnetic fields onto the stellar surface and where other parts of the rotating magnetosphere accelerate and collimate the outflowing matter. Nevertheless, observing just outside these regions should allow meaningful extrapolations.

Very few direct studies of circumstellar disks have been performed so far, because this requires high resolution in the near- and mid-infrared domains. Important parameters yet to be determined include the morphology of circumstellar disks, the temperature distribution, the relative contributions from scattered stellar light and thermal disk emission, the disk chemical composition and the properties of dust grains.

In a few objects, minima in the broadband spectrum have been tentatively attributed to zones cleared by a planet or faint companion (Marsh & Mahoney, 1993), although different interpretations based on material properties are also possible. These gaps lie around 1 AU and would be detectable with the VLTI (Malbet & Bertout, 1995). The determination of visibility curves at 2 and 10 microns should indicate the interesting candidates; imaging will be required to study the phenomenon with its asymmetries due to the presence of the orbiting object. Generally, distribution of dust and gas, and of the spatial distribution of temperature can be measured and will clarify the initial conditions for possible subsequent planet formation.

The question of how YSO jets are accelerated and collimated should also be addressed with the VLTI. Although the innermost region will not be resolved, important constraints on models can be derived from observations beyond about 30 stellar radii. A start has been made with HST and ground-based telescopes, and studies of jet width as a function of radius show that at least some YSO jets have full opening angles of greater than 50° for small distances from the star. This behaviour, which is observed for of at least a few YSO jets, is illustrated in Figure 1 on the basis of a recent HST/WFC image of the bipolar jets from the HH 30-star in the [SII] 6716, 6731 lines (Ray and Mundt, 1996). The figure shows how drastically larger the opening angle of this YSO jet must be on small scales (i.e. within < 0.3″ or for < 50 AU from the star). A similar behaviour has been predicted by the theoretical models of Camenzind (1990) in which the jets are accelerated and collimated by rotating magnetospheres and in which one expects large jet opening angles for jet radii much smaller than the light cylinder, which is expected to have a radius of about 30 to 100 AU for typical rotation periods for T Tauri stars of a few days.

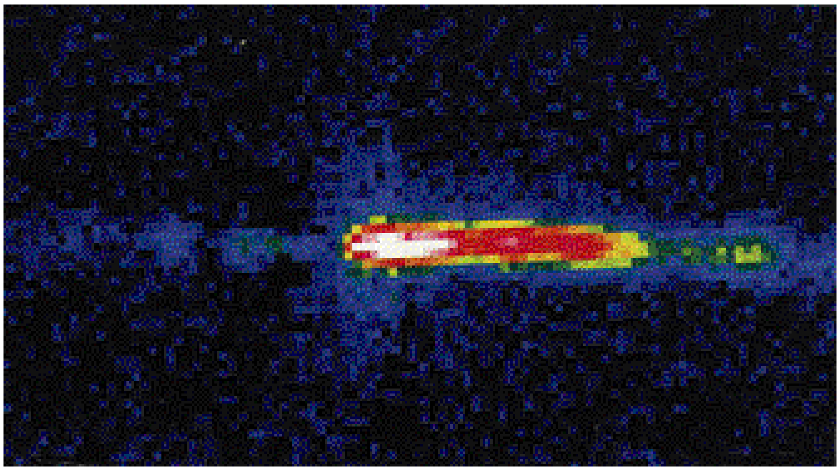

Figure 1: The top part shows a HST/WFC image of the bipolar jets from the HH 30 star in the [SII] 6716, 6731 lines (with the continuum contribution subtracted). The HH 30 star is not visible due to strong extinction in the circumstellar disk. The star is assumed to be located in the centre of the gap between the two jets (i.e. 0.3″ to the left of the very end of the brighter jet). In the lower part, the measured FWHM of the bipolar jets as a function of distance is shown. For the visible parts of the jet, average full opening angles of about 6 degrees (left part) and 2 degrees (right part) have been derived. However, for the invisible part of the jet, i.e. between the source and the first point of measurement the jet opening angle must be considerably larger (at least 50°) as indicated by the dashed line.

The VLTI can also investigate possible connections between variations of the central star and the formation of new knots in the jet. For a jet speed of 300 km/s, a new knot resulting from an outburst would move outwards and be detectable after a few days, allowing its proper motion to be accurately measured. This is similar to VLBI observations of QSO jets. The need to pursue these observations with high spectral resolution (R > 1000) and within 1–2 days because of the high proper motion of the knots (up to 1 mas/day) probably will require the inclusion of the UTs on the basis of current brightness estimates.

Measuring orbits of very close binaries would be another valuable science programme. High angular resolution is needed to produce accurate masses for lunar-occultation and spectroscopic biprecision of ~ 10 μas, albeit over much wider angles, planets would be revealed by conspicuous residuals in the astrometric fit, but the mission lifetime and temporal sampling would generally not be adequate to determine planetary orbits.

While observations of candidate exoplanets would make the VLTI programme quite efficient, the target list should also include a survey of other "interesting" objects. Examples are the closest stars, for which the VLTI can detect planets with lower masses than can radial velocity searches, IR-excess stars like β Pic, and pre-main-sequence objects in low-mass star forming regions and in Orion. The astrometric mode of the VLTI would thus open new vistas in the study of the formation and evolution of planetary systems. It could also provide an input list for even more ambitious space interferometry projects aimed at spectroscopic investigations of extrasolar giant and Earth-like planets. One such project, DARWIN, is also under study as a cornerstone mission within Horizon 2000+.

While these indirect methods will certainly yield a wealth of data about extrasolar planetary systems, the direct detection of photons originating from the planet itself would enable more detailed astrophysical studies. Examples include determining the chemical composition and temperature of the planets through spectroscopy, and studying surface structure and rotation by analysing the lightcurve. However, in the visible and near-IR regimes it is prohibitively difficult to detect planets against the glare of the parent star. The only chance lies in the mid-infrared, where the contrast is reduced by several orders of magnitude. In the 10 and 20 μm atmospheric windows, the thermal emission of a planet depends strongly on its temperature (for example, at 10 μm the Earth is brighter than Jupiter). Simple sensitivity calculations show that Jupiter at a distance of 10 pc would not be detectable against the thermal background in a reasonable time with an Earth-based (and therefore uncooled) 8-m telescope. It should be kept in mind, however, that other planetary systems may be very different from ours. In particular, other giant planets may be warmed by internal heating, which is stronger in planets that are younger or more massive. Planets may also be warmed by strong irradiation, either because the parent star has an early spectral type or because the orbit is small (as in the case of 51 Peg). There may be a realistic chance of detecting such warm giant planets in the solar neighbourhood with the VLTI at 10 or 20 μm, provided their temperature is at least 400 K. Suitable candidate objects for such an ambitious project, which would require several hours of integration time with the full array of four 8-m telescopes, could be drawn from the astrometric survey list.

2.2 Low mass stars and brown dwarfs

Ninety percent of stars in our Galaxy are less massive than the Sun. Despite this fact, the properties of stars with low or very low masses are far less certain than those of their more massive counterparts. For instance, establishing an observational mass-luminosity relationship for stars with masses smaller than 0.3 $M_\odot$, is still an active field of research (Henry & McCarthy 1993). Similarly, observations are still unable to significantly constrain the lower end of the mass spectrum that is produced by the star formation process.

Even less well understood are substellar objects: the elusive brown dwarfs. It seems that, after a long and eventful search, the question of their existence has recently been settled by clear detections (Rebolo et al., 1995; Nakajima et al., 1995). Of course, this result opens a new field of study for this latest class of cosmic objects which will finally allow theory to be related to observations. Unfortunately, this relation is rather indirect because the classical observables of a brown dwarf (broad-band photometry and spectrum) are determined by its very thin atmosphere, while its physical status depends mostly on the age and mass.

Progress in understanding low-mass stars and brown dwarfs clearly requires a method for determining masses. The first step is to perform radial velocity surveys of large samples of low-mass stars in search of spectroscopic binaries. However, while these surveys provide fundamental statistical results (Duquennoy & Mayor, 1991), they can only yield masses for each component if combined with direct imaging measurements. Duquennoy et al. (1995) have recently discussed the impact of the VLT and VLTI on such a programme. In particular, they show that the combination of high-precision (~ 15 m/s) radial velocity data with parallaxes provided by Hipparcos and angular separations from VISA would allow the determination of masses of very low mass stars with a precision at the percent level. Even the mass of a suspected 0.03 $M_\odot$ brown dwarf companion could be estimated with ~ 5% accuracy, firmly establishing its sub-stellar nature and allowing one to test evolution scenarios for these still mysterious objects.

2.3 Star formation and early stellar evolution

Young stellar objects (YSOs) exhibit a large variety of different phenomena, such as infrared excesses, luminosity variations and highly collimated jets with velocities of several hundred km/s. These phenomena suggest the presence of a circumstellar accretion disk and strong magnetic fields. Understanding the inner regions of YSOs, including their accretion disks and jets, is an important area of current research and is related to the question of how our own solar system formed. The similarity of some YSOs to AGNs, particularly the so-

TABLE 1. Current Ground-based Optical Long Baseline Interferometer (OLBI) Projects

Programme (Nation)	Number of simult. Baselines (ultimate)	Maximum Baseline [m]	Element diameter [m]	Year of operation
I2T (F)	1	140	0.27	operational
GI2T (F)	1	65	1.52	operational
ISI (USA)[3]	1	35	1.65	operational
COAST (GB)	3 (6)	100	0.40	operational
SUSI (AUS)	1	640	0.14	operational
IOTA (USA)	1 (3)	45	0.45	operational
NPOI (USA)	3 (6, 15)	250	0.35	operational
ASEPS-0 ITT (USA)	1	100	0.45	operational
CHARA (USA)	10	350	1.00	1997
KIIA (USA)	1 / 6 / 15[1]	75 / 180[2]	10 / 1.5	1998
LBT (USA/I)[4]	1	20	8	1999
VLTI (EUR)	6 / 3 / 6[1]	128 / 200[2]	8 / 1.8	2000

[1]Beam combination main / auxiliary / hybrid — [2]between main / auxiliary telescopes — [3]heterodyne, to be changed into a homodyne interferometer — [4]monolithic array. — (Last update: 02/01/96).

A New Start for the VLTI

*ISAC – Interferometry Science Advisory Committee**

1. Introduction

It has always been ESO's aim to operate the VLT in an interferometric mode (VLTI) which allows the coherent combination of stellar light beams collected by the four 8-m telescopes (UTs) and by several smaller auxiliary telescopes (ATs). In December 1993, in response to financial difficulties, the ESO Council decided to postpone implementation of the VLTI, Coudé trains and associated adaptive optics for all the UTs but included provisions for continuing technological and development programmes devoted to the aim of reintroducing these capabilities at the earliest possible date (see *The Messenger* No. 74, December 1993). In July 1994, the ESO Council approved a revised VLTI implementation plan to provide at least the VLT interferometric sub-array (VISA) consisting of three ATs by the year 2003 and, provided additional funds could be obtained, integration of the UTs by 2006.

The desirability of carrying out the full VLTI programme as originally envisaged at the earliest possible moment has not, however, diminished, especially in view of VLTI's exceptional capabilities and resulting potential for new and exciting discoveries. In recent years, interferometric projects have begun to play a central role in ground-based high-resolution astronomy, and numerous instruments have been completed or are in the process of construction (see Table 1 for a summary of the present situation in this regard). Several large-aperture interferometers will probably come on-line near the turn of the century. The impending presence of these new instruments represents an important incentive both for clarifying the scientific cases for various VLTI implementation plans and for ensuring VLTI's competitiveness in the international context over the next 10–20 years.

The complexity and ambitious scope of VLTI mean that its astrophysical repercussions are difficult to define fully, even for many of its most vocal supporters. However, the primary scientific issues that it seeks to address are well defined, although there remains a need to present these coherently to the wider community in order to justify the significant resources which the project requires. Another pressing need is to develop an implementation plan that will optimally exploit the various technological stages of the project and ensure their compatibility with a vigorous, yet realistic and timely, astrophysical programme.

In order to study these issues and to establish a clear set of guiding principles for the development of VLTI, a new Interferometry Science Advisory Committee (ISAC) was established in April 1995. This committee has met twice to review the present technical status of VLTI, its scientific rationale as elaborated by past advisory panels (ESO VLT Reports 59 and 65), and the present recovery plans. The committee has now begun to define and prioritise the key science drivers for the programme and the technical specifications that flow from them. This article briefly presents these science goals as they currently stand. The list is not meant to be frozen or complete, but rather is intended to stimulate community reflection and comment. The preliminary recommendations of the committee are discussed in the last section of this article.

To provide a forum for the discussion of the ideas presented here, ESO has decided to host a workshop on "Science with the VLTI", in Garching on June 18–21 of this year (see *The Messenger* No. 82 and the announcement in this issue). It is hoped that this will allow the whole of the ESO community to further refine the concepts outlined in this article and to make a case for any capability or role omitted here.

2. Science Goals

2.1 Extrasolar planets

Searches for extrasolar planets have started to assume centre stage both in the professional arena and in the public perception of astronomy. The recent detection of a planet orbiting 51 Peg (Mayor & Queloz, 1995) has generated much interest, and it is widely believed that more giant gaseous planets around solar-type stars can be found by precise radial-velocity and astrometric surveys. Both these methods are indirect, in that they measure the motion of the star around the barycentre of the star-planet system. While radial velocity searches could soon become a very efficient method to detect exoplanets, they have a serious drawback: they cannot determine separately the planetary mass and its orbital inclination; only M sin i is measurable. In contrast, astrometric observations give M directly. Of course, in planetary systems which are viewed "pole-on", astrometry provides the only way to detect reflex motion.

The VLTI has the potential to be an extremely powerful instrument for precise narrow-angle astrometry. For instance, the atmospheric limit for determining the separation vector between two stars which are 10″ apart is about 10 µas for a half-hour integration. Realising this potential is a challenging but solvable task. It requires monitoring the baseline vector inside the interferometer with ~ 50 µm precision and measuring the differential delay between the two stars with ~ 0.005 µm precision. Implementing an astrometric mode in VLTI with these capabilities would enable us to detect Sun-Jupiter systems out to a distance of 1 kpc and small planets (10 Earth masses) around the closest stars.

The following observing strategy could be adopted for the VLTI astrometry programme: a list of ~ 200 target stars would be observed in the near infrared with VISA. These stars must be bright enough for fringe tracking ($K \lesssim 12$), which will allow the astrometric reference sources to be relatively faint ($K \lesssim 17$) and ensure that references for phasing can be found for almost any object of interest. The integration time would be half an hour per star per night. With thirty observations of each target star over ten years, this would require a total commitment of 300 nights on VISA spread over a decade. The data for each star would be used to solve for relative parallax and proper motion, with any residuals indicating the presence of planets. In practice, one would use two or three different astrometric reference stars for each target to remove ambiguities from the motions of the reference stars themselves.

The target list would include candidate planetary systems found from radial velocity searches, for which VLTI could determine the inclination and thus the planetary mass. The list could also include candidates from a large-scale astrometric survey such as the GAIA project, a mission proposed within the Horizon 2000+ programme of ESA. In the GAIA data, which should also have a

*Francesco Paresce (ESO; co-chairman), Denis Mourard (Nice; co-chairman), Tim Bedding (Sydney), Jim Beletic (ESO), Chris Haniff (Cambridge), Christoph Leinert (Heidelberg), Fabien Malbet (Grenoble), Jean-Marie Mariotti (Meudon), David Mozurkewich (Washington), Reinhard Mundt (Heidelberg), Patrick Petitjean (Paris), Andreas Quirrenbach (MPE Garching), Thorsten Reinheimer (MPIfR Bonn), Andrea Richichi (Arcetri), Huub Röttgering (Leiden), Oskar von der Lühe (ESO), Rens Waters (Groningen).

the observations span from September 11, 1991 to October 14, 1995. For all data, standard reduction procedures were applied (BIAS subtraction, and FF correction, with preference to sky FFs when available). When available, the extinction coefficients for the night (as found in the ESO-La Silla WWW pages) were used.

The equation ($M - m = S_m \times (B - V) + K_m$) was then fitted for each filter (m = B, V, R_C, I_C) and for each night. Averaged over all the nights the corresponding equations for EFOSC1 are the following:

$B - b = +0.190 \pm 0.013 \times (B - V) + 24.06 \pm 0.09$ (*)
$V - v = +0.050 \pm 0.011 \times (B - V) + 24.75 \pm 0.08$
$R_C - r = +0.011 \pm 0.012 \times (B - V) + 24.80 \pm 0.07$
$I_C - i = -0.035 \pm 0.002 \times (B - V) + 23.62 \pm 0.05$

The instrumental magnitudes were calculated with the counts expressed in ADUs (the conversion factor for CCD #26 is $4e^-$/ADU).

The inverted A in the Figure shows the re-aluminisation date of the 3.6-m primary mirror (during October 18, 1994; the previous one was done during August, 1990). A significant increase in the efficiency is measured (especially in the V and R_C bands, see figure). If we compute the zero points for the observations before this date only, we get:

$K_B = 24.05 \pm 0.09$
$K_V = 24.73 \pm 0.08$
$K_R = 24.77 \pm 0.05$
$K_I = 23.58 \pm 0.01$

The zero points for the first point after the re-aluminisation (January 7, 1995) are 0.08 mag higher in B, 0.14 mag higher in V, and 0.16 mag higher in R_C.

From an inspection of the figure, it is clear that there is an overall fair photometric stability for EFOSC1 and that the fluctuations in the zero points are smaller than 0.1 mag for all filters. Furthermore, no obvious systematic trends are seen before October 1994.

(*) calculated without one anomalous point. This point is circled by parentheses in the Figure that shows the trend in the zero points, K_m, with time (Julian days).

Unusual View of VLT Site

Hanging from a crane, ESO photographer H.H. Heyer took this view over the VLT platform in the late-evening sunlight at the end of February 1996. Apart from the VLT Unit 1, with almost fully assembled steel structure, Unit 2 is behind at left and the interferometric tunnel stretches across at right.

the site and dome seeing. Comparison between these values and those measured by the outside seeing monitor (dimm2) will give us the dome seeing. These measurements need to be done over a one-year period so that seasonal effects can eventually be detected.

Using the experience gained at other observatories, a mirror cooling system is being studied. The heat produced inside the cage will be removed with a cooling system.

(c) Image quality measurements

We measured with a direct CCD (0.19″ per pixel) the FWHM of a star near the zenith. The measurements were done during the third night test. Antares was mounted during the beginning of the night to check the optical quality; it was still 0.65″. We stayed near zenith to avoid the non elastic movement of the telescope mechanics and optics.

The site seeing was good all night, an average of 0.73″ with 48 measurements. At the 3.6-m, the average image quality was 0.92″ (48 measurements). This is by far the best result achieved during all the test nights. The best result was around 0.73″, near the actual optical quality of the telescope (0.65″). The worst value was 1.05″. These results are compared to the results obtained during previous test nights which are shown in Table 1.

TABLE 1.

	2 Sept. 1995	3 Sept. 1995	4 Sept. 1995
Average dimm2	0.70″	0.66″	1.27″
Average 3.6-m	1.21″	1.30″	1.46″
Best value 3.6-m	1.02″	0.96″	1.21″
Worse value 3.6-m	1.40″	1.70″	1.70″
Number of measurements	13	16	6
	4 Oct. 1995	5 Oct. 1995	30 Nov. 1995
Average dimm2	1.13″	1.04″	1.11″
Average 3.6-m	1.26″	1.15″	1.18″
Best value 3.6-m	1.00″	0.93″	0.99″
Worse value 3.6-m	1.51″	1.41″	1.36″
Number of measurements	25	24	22
	1 Dec. 1995	2 Dec. 1995	9 Feb. 1996
Average dimm2	0.90″	1.00″	0.73″
Average 3.6-m	1.16″	1.26″	0.92″
Best value 3.6-m	1.01″	1.09″	0.73″
Worse value 3.6-m	1.36″	1.53″	1.05″
Number of measurements	30	48	48

The average value during the last night test is better than any single measurement made during the other test nights. Although the outside seeing values are not comparable for all the nights, the nights of September 2 and 3, 1995 showed outside seeing values very near to the night of February 9, 1996.

The good results of the last night run can be explained by:

– the temperature differences throughout the dome were smaller than normal,

– the optical alignment was good and was checked before the observations,

– the telescope stayed near the zenith,

– outside seeing was good.

So, can the astronomer expect similar results? Unfortunately, the answer is no. Even if a detector with the appropriate sampling would be available, the following conditions for good seeing at the 3.6-m have to be satisfied:

– good external seeing;

– observation only near zenith (because of the flexure in the telescope mechanics and movement of the optics);

– good optical alignment of the primary and secondary mirrors. (Even at the zenith, it is not certain that the primary and secondary mirrors will remain aligned from the previous night. This is due to the non-elastic movements produced in the M2 unit. The only way of verifying the alignment would be to do an image analysis with a wavefront sensor before observations start);

– the air temperature within the dome is homogeneous.

Conclusion

The results obtained during the last test period are very promising. We have shown that images with 0.7″ to 0.9″ FWHM are possible during a whole night. However, we also have found what is required to get these results. To progress further at the 3.6-m we need to:

– continue the effort of eliminating the hot sources in the dome and to eventually insulate the concrete walls;

– change the M2 unit to a NTT-like M2 unit that would enable us to compensate for tube flexure when observing away from zenith. It would also eliminate the non elastic phenomena present in the actual M2 unit design;

– a Wavefront analyser can easily be installed inside the rotator, it would be very easy to activate (or semi-activate) M2.

In fact, the recommendations I made above, which are a conclusion of the night tests, are not far from the following: “The potentially excellent optical quality of the 3.6-m can only be exploited if improvements in dome and telescope seeing are effected and a high precision of centring maintained” (Ray Wilson, ESO Technical Report No. 8, October 1977).

About the Photometric Stability of EFOSC1

S. BENETTI, ESO-La Silla

This brief report deals with the long-term photometric stability of EFOSC1. EFOSC1 is a focal reducer attached to the Cassegrain focus of the ESO 3.6-m telescope. EFOSC1 is equipped with CCD #26.

In this study, photometric standards, all from Landolt [*AJ* 104, 340 (1992)], were imaged during 16 photometric nights with the B, V and R_C filters. During five of these nights, standards were also observed with the I_C filter. The date of

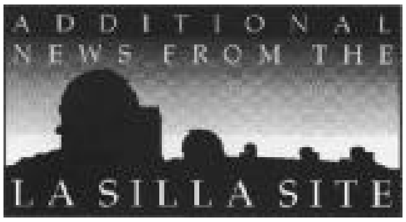

The La Silla News Page

The editors of the La Silla News Page would like to welcome readers of the third edition of a page devoted to reporting on technical updates and observational achievements at La Silla. We would like this page to inform the astronomical community to changes made to telescopes, instruments, operations, and of instrumental performances that cannot be reported conveniently elsewhere. Contributions and inquiries to this page from the community are most welcome. (P. Bouchet, R. Gredel, C. Lidman)

Image Quality of the 3.6-m Telescope

S. GUISARD, ESO-La Silla

Another 3 test nights were used during the beginning of February for testing the optical performance of the 3.6-m telescope. The first two nights were dedicated to the realignment of the secondary mirror and to the study of the relative movement of the primary and secondary mirrors with telescope position. Antares, a wavefront analyser, was used for this purpose. The third night was used for image quality measurements. Very promising results were obtained.

Image Quality

The term image quality is defined here as the full width at half maximum (FWHM), usually expressed in arc seconds, of a stellar image as measured at the detector in real observing conditions. Within the astronomical community, it is termed, somewhat improperly, "the seeing".

The image quality depends on several parameters:

(a) The optical quality (telescope and instrument)

For this study we measured the image quality at the Cassegrain focus with a direct CCD. Therefore, we do not include any image degradation from instruments.

The optical quality depends on :

– the diffraction limit;

– residual aberrations from theoretical optical design;

– intrinsic optical quality (due to the figuring of the optics);

– positioning of the primary and secondary mirrors with respect to each other (this includes spacing, tilt and decentring, and the variation of these parameters both with zenith distance and movement of the telescope);

– support of the mirrors (quality of the support at zenith and variation with zenith distance).

(b) The seeing

The seeing is the degradation of the wavefront by the entire atmosphere, from the high atmosphere down to the air layers near the detector. It is usually decomposed in several components: outside seeing (site seeing), dome seeing, mirror seeing, instrument seeing, although the phenomenon for each component is the same. The cause of seeing is temperature inhomogeneities in the air which induce phase differences in the optical path. The effect is to smear the light of a star. Usually the atmosphere is the worse part of the telescope. In the case of the 3.6-m we shall see that this is not completely true.

(c) Other parameters

– focusing the telescope
– sampling of the detector
– guiding accuracy
– vibrations of the telescope

The image quality study aims at analysing and reducing all the above-mentioned effects at the 3.6-m.

Results of the Study at the 3.6-m, February Test Nights

(a) The optical quality of the telescope

After realigning M2 with respect to M1 during the two first nights (this removes the decentring coma) the following aberrations remained. The telescope was pointing at the zenith. All the values represent the diameter of the circle containing 80% of the light. The unit is in arc seconds.

Decentring coma:	0.11″
Astigmatism:	0.40″
Triangular astigmatism:	0.45″
Quadratic astigmatism:	0.20″

The combination of all these aberrations would produce an image of 0.65″ diameter (80% light) in the absence of atmosphere and seeing effects. It is not the optimal value as the intrinsic optical quality of the telescope (mirror perfectly aligned, perfectly supported, no atmosphere) is less than 0.4″.

The remaining astigmatism and triangular astigmatism are too high. These aberrations are due to the M1 support. In fact, they appeared after the last aluminisation (October 1994). Before this, the values used to be lower than 0.20″. Several problems concerning the lateral pads of M1 were found and partly solved. It is foreseen during the next aluminisation period (June 1996) to check all the forces applied at the back of the mirror, and to also check the lateral pads.

It is important to note that these values are for the telescope pointing at the zenith. We have known for a long time that telescope flexure associated with observing away from the zenith causes the optical quality to deteriorate rapidly.

During the third night the stability in the image quality with telescope movement was measured. The telescope was first moved to the south to a zenith distance of 60 degrees and then returned to the zenith. The optical quality at the zenith was measured to be 1.0″, significantly larger than the 0.65″ measured at the zenith before the telescope was moved and after alignment of the primary and secondary mirrors. It nearly comes back to its original value if you go north and come back to zenith. Further tests will be performed to measure the movements of M1 and M2 for different positions of the telescope.

(b) Seeing at the telescope

A seeing monitor (dimm4) was installed recently on the tube of the telescope to measure the combination of the software position control module, Gianluca Chiozzi for the preset module and everything related to object oriented design and C++, and the rest of the staff in VLT/ELE department for VLT common software and VLT electronic standards. We also thank Rolando Medina for installing the antenna and fibres for the VLT timing system in advance of the test.

E-mail address: awalland@eso.org
(Anders Wallander)

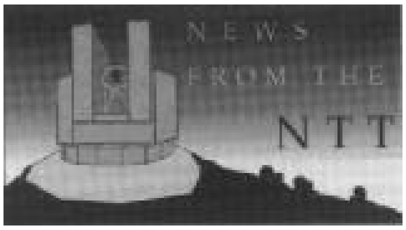

The NTT upgrade project has the following goals:

1. *Establish a robust operating procedure for the telescope to minimise down time and maximise the scientific output.*
2. *Test the VLT control system in real operations prior to installation on UT1.*
3. *Test the VLT operations scheme and the data flow from proposal preparation to final product.*

J. SPYROMILIO, ESO

This issue of *The Messenger* is the last before the NTT upgrade project goes into phase II (the Big Bang) of the upgrade. In July this year the NTT will go off-line to install the VLT control system on the telescope. Many people ask me why the NTT is going off-line for a whole year for a change in the control system. This appears to a number of people as a disproportionate length of time. The modifications to the NTT are not limited to the telescope itself. Every subsystem of the NTT is upgraded to VLT standards from the building and hydraulics to the target acquisition systems. The slow read-out electronics for the CCDs are also being upgraded to the ACE system which should cut down the read-out times dramatically. In addition the supporting systems such as scheduling, phase 2 proposal preparation tools, automatic data reduction are being upgraded as well. Alignment procedures and tools for the VLT are also being tried out during this period.

The NTT team fully appreciates that removing a resource as valuable as the NTT from the community for any length of time is painful. The astronomers within the team are also active users of the telescope and will also suffer the withdrawal symptoms. However we firmly believe that for every month that is expended on the NTT now, we shall gain a month on the VLT UT1. This does not only apply to the software and hardware installations but also to the operation of the VLT as a scientifically useful telescope. The transition from a facility that works to one that produces science is often long. The NTT project as a test bed for VLT operations aims to cut this transition time down to a minimum for UT1.

Operational News

The statistics for 1995 are in. The NTT had a total down time of less than 48 hours in 1995. This is 2.1% of the time available for observing and puts us at the bottom of the published results for 4-m-class telescopes. In this case being at the bottom is the best position to be in. This number has been achieved by a number of ways. First and foremost the dedication of the operational staff. Preventive maintenance also plays a big role. The NTT has a maintenance plan which details the activities of the team every day of the year. Operations have been moved from the minds of individuals to documents and check lists. The NTT runs according to a plan and this transparency of operations minimises the time lost due to mistakes.

Unfortunately, some bad news have also to be reported. The sensitivity of EMMI has dropped significantly. Preliminary investigations indicate that some of the very sophisticated coatings of the EMMI optics which had reflectivities as high as 98% have aged more rapidly than expected. The problems are being further investigated as this article is written and the latest EMMI sensitivities will be published on the Web. The recoating of the elements is not an operation that can be undertaken on very short timescales. However, every effort to recover the nominal sensitivity is being made.

Progress with Big Bang Preparations

On page 7 of this issue of *The Messenger,* a detailed description of the first test of the VLT Telescope Control System can be found. However it is appropriate here to say a few words about the significance of this field test. In the past the NTT team has tested a number of subsystems of the control system to be installed during the big bang. However, the TCS test can fairly be described as the biggest challenge for the VLT software to date. Problems were found during the test but no show stoppers. In the article describing the details of the test, an image where the NTT was made to write "VLT" on the sky is shown. Although this image showed a problem with the tracking in the new system, I am confident that this problem will be solved. It should be noted that this image was created by using a very large number of functions of both the new TCS and the VLT control system. The image was generated by using the differential tracking and offsetting modes of the new TCS and was run in a completely hands free mode. A script for the higher level operation software (also known as the sequencer) was written in a few minutes in the scripting language for the VLT. The script was executed at the workstation level, and the actual movement of the telescope was performed by two independent local control units synchronised by the VLT standard absolute time reference system.

The importance of the sequencer in the VLT style operations cannot be overstated. The sequencer is the primary communications tool between the outside world and the VLT control software. It makes possible the co-ordination of the telescope, instrument and detector control software.

As the article is being written, the author is on La Silla watching the EMMI instrument being controlled by VLT standard instrumentation software and electronics. These results give great confidence that baring unforeseen problems we expect to be ready for the big bang in time.

E-mail address: jspyromi@eso.org
(Jason Spyromilio)

Figure 2: VLT/NTT TCS "First Light "December 1995.

problems were discovered, which prevented the use of all four encoder heads, and in order to proceed with the test it was necessary to operate in a degraded mode using only one of the four encoder heads. These problems shall now be resolved together with the supplier.

At the early stages of the test engineering tools delivered with VLT Common Software were extensively used. The tools inducer and lcudrvTk, which allows the engineer to access and exercise the VME boards directly, made it possible to identify and solve many problems related to the hardware. The sampling tool, which allows sampling and real-time trending of signals at 20 Hz, was absolutely essential when tuning the position control loops.

On the 7th of December the first attempt was made to track on the sky. The telescope operator Jorge Miranda pointed to a bright star, and the guide probe video monitor was switched on. After some pointing model parameters were adjusted the star appeared on the screen and stayed in the same position. Figure 2 shows the reaction of the testing crew at this moment.

In order to verify as much performance and functionality as possible, a script was written using the VLT sequencer, to write star trail characters on the sky using offsets and differential tracking. It should be noted that this test also demonstrated the power and simplicity of the sequencer scripting language. The resulting CCD image is shown in Figure 3. This exercise showed a serious problem, clearly visible on the image, of tracking stability. There appears to be a low frequency (< 0.2 Hz), approximately 1.5 arcseconds peak to peak, tracking error. The same behaviour was confirmed during normal tracking. Unfortunately, the remaining test time did not allow an extensive investigation of the problem. Data for off-line analysis were obtained, but it is believed it will be very difficult to find a solution without having access to the telescope. On the other hand, we are confident that the cause and a solution can be found quickly at the beginning of the NTT Big Bang. Note that the old control system does not exhibit this behaviour and was tested extensively during the handover back to normal operation.

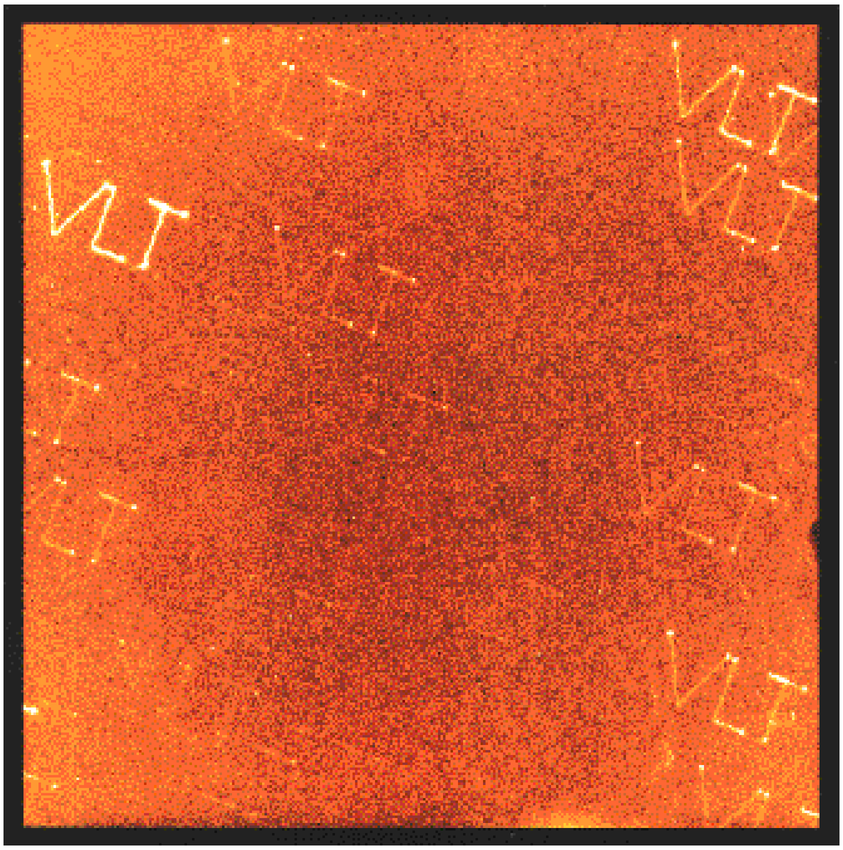

Figure 3.

Conclusion

Considering the limited amount of telescope time and the complexity of the test, we consider it to be a major step towards the NTT Big Bang and VLT commissioning.

The experience obtained will be very valuable for the ESO test period of the VLT main structure in Milan. Later, it will become a tremendous advantage during commissioning of the VLT at Paranal, when a large part of the control system has already been in operation at the NTT for more than one year.

At the same time we still have to solve some of the problems encountered, mainly encoder handling and tracking stability, as well as implement missing functionality and fine tune the system. It should also be remembered that the step from operating a system with experts present to routine operation can be rather large.

Acknowledgements

We like to acknowledge the major contributions to the system described of the following VLT staff. Martin Ravensbergen for the timing system and position control, Bruno Gilli and Norbert Fiebig for

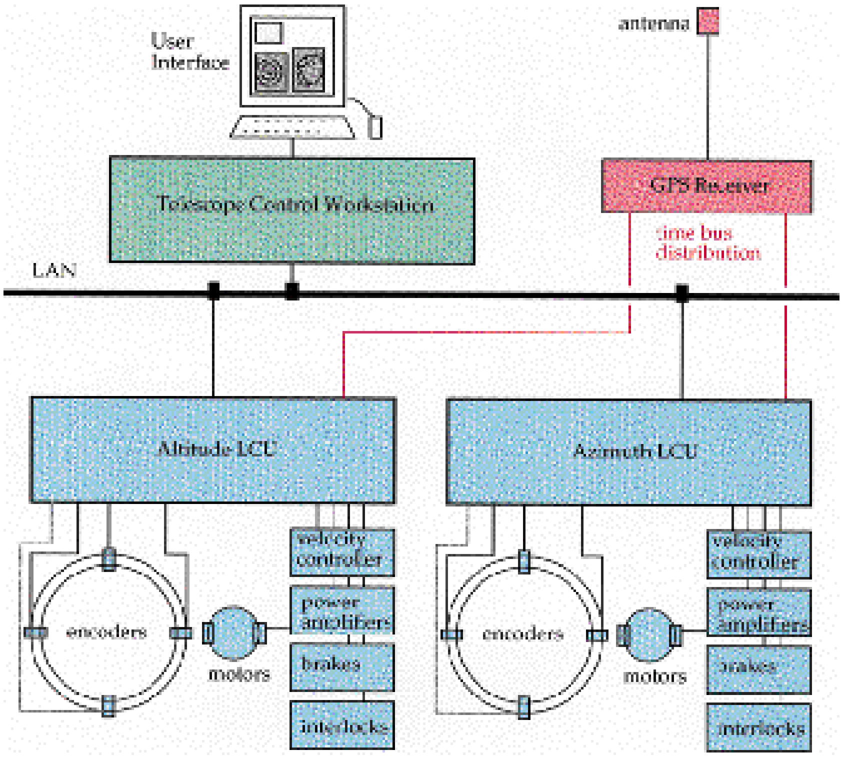

Figure 1: System Block Diagram.

applications on top of this common base and field test them on the telescope subsystem by subsystem, thereby providing feedback to the VLT development and preparing for the NTT Big Bang.

Lately, with the advancement of VLT applications as well as moving to more complex and higher level NTT applications, the common base of NTT and VLT has been found on an even higher level. The heart of TCS, pointing and tracking of the telescope, is an example of this. The design, development and test of this subsystem has been performed in close collaboration between VLT TCS group and NTT Team, with the aim of having nearly identical systems for NTT and VLT. Such an approach does not only make optimal usage of available resources, but even more important, allows a thorough testing of the control system before first usage at Paranal. The resulting application code, sitting on top of the VLT Common Software, comprises of about 75,000 lines of C and C++ code of which 50 % are comments.

Differences between the two telescopes, mainly interfaces to hardware and other subsystems, have been isolated in the code. With techniques of compilation flags, subclasses and a dedicated module per telescope defining installation procedures and configuration parameters (e.g. site location), the target telescope is specified at installation time. Thus an installation consists of checking out the standard modules from the software archive and executing an installation script unique per telescope.

The pointing and tracking of the telescope was subject of a NTT field test the first ten days (nights) of December 1995. As for all previous field tests the strategy was to replace workstations, hardware and software, execute the test, and then restore the original system. In addition to the change of VME boards and I/O wiring two major hardware changes were required. The VLT GPS based timing system replaced the old Cerme clock required for tracking, and all electronics processing the data from the encoder heads were replaced. To use the limited available test time as efficient as possible, a large number of staff working in shift participated, and a detailed test plan and formal reporting kept the activities under control.

System Architecture

Three application modules, written in C++ and based on the event handler delivered with the JUL95 release of VLT Common Software, are running on the workstation. These modules mainly have administrative responsibilities in performing system start-up and shutdown, providing hooks for user interfaces, providing interfaces to other subsystems, and forwarding requests to tracking axes. Examples of the latter are preset and offset requests and pointing modelling and meteorological data (temperatures, pressure and humidity) required by tracking. Data for status displays and alarms are generated using the CCS scan system, mirroring part of the LCU databases on the workstation database. In addition to standard VLT engineering user interfaces, prototypes of TCS GUI's, developed using the panel editor, provides the interface to the user. We believe it is important to involve the final users, in this case the telescope operators, as early as possible in this area.

A telescope preset request from the GUI results in commands sent to all configured tracking LCU's. During this test only altitude and azimuth were included, but in a final system the rotator in the active focus station will also be included. From here on the LCU's can operate autonomously by having the reference co-ordinates, expressed in right ascension, declination and epoch, and the sidereal time obtained from the time bus.

The GPs receives time information via an antenna mounted on the roof of the building and distributes absolute universal time to the tracking LCU's via the fiber optic time bus.

The two main tracking axes, altitude and azimuth, comprise encoders, velocity controllers, power amplifiers, brakes, and interlock sensors. This hardware is controlled and monitored from a VME based LCU with standard VLT I/O boards and drivers. The application software in the LCU, written in C and based on LCC delivered with the JUL95 release of VLT Common Software, is responsible for interfacing the hardware and performing position control. Having received the reference co-ordinates and the time bus signal, the tracking application calculates every 50 ms the required absolute position of the axis using *slalib* (a widely used library, developed by Pat Wallace, for astronomic position, time, and co-ordinate conversion calculations). This value is forwarded to the position controller which uses linear interpolation to produce new reference values for the velocity controller, implemented in hardware, every 2 ms.

The altitude and azimuth encoder systems are completely different for VLT and NTT. Nevertheless, it was decided to replace the existing NTT encoder interpolation electronics with a newer generation from the same supplier used also by Telescopio Nazionale Galileo. Identical systems will be used for the VLT rotators. The new generation interpolation electronics increases the theoretical resolution by a factor 4 (smallest detectable change of angle is less that 0.01″), allows a faster read-out (position control loop speed can be increased from 5 to 2 ms), is more compact, and provides a cleaner interface to the software.

Results

As was expected beforehand, most problems were encountered with the encoder handling. This part could not be tested in the lab due to lack of similar hardware. During the test, firmware

1997 June VLT Test Cam #1
FIERA with thinned chip (2k × 2k + tracker chips). We may need to deliver this system earlier.
1997 July UVES
FIERA blue arm (2k × 2k eng. grade device).
1997 September SUSI-2
FIERA with UV-sensitive 4k × 4k (two 2k × 4k devices).
1997 September NAOS
FIERA with AO chip (128 × 128), plus spare system (thermo-electrically cooled dewar).

1998 January UVES
Upgrade blue arm to science grade, deliver red arm 2k × 4k (single chip or mosaic of 2k × 2k), plus spare parts. If possible, we will deliver the red arm with the long-term goal of a 4k × 4k mosaic. In addition, the blue arm may be outfitted with a new generation 2k × 4k device.
1998 March FORS 2
FIERA with Tek/SITe 2k × 2k.
1998 March FUEGOS
FIERA with eng. grade 4k × 4k (two 2k × 4k chips).
1998 December VLT Test Cam #2
FIERA with thinned chip.

1999 March FUEGOS
Put science grade devices into system.

The ESO community should note that we are taking the position that all new CCD controllers on the VLT and new ones on La Silla (under ESO maintenance) will be FIERA systems. We take this stance because we have the responsibility to maintain all optical detector systems. In addition, ESO instruments should get the benefit of the advanced capabilities provided by FIERA. (This statement does not include the new system at the Danish telescope or FEROS, since FIERA will not be available until 1997.)

9. One Observatory – La Silla and Garching

The ODT has made great strides in improving communication between Garching and La Silla. One aspect is weekly video conferences on every Thursday. In addition, we plan for more personnel exchanges – at least one visit per year of each member to the other site for functional work. Also, all large development projects are now a shared concern, both for design and for maintenance – no more dichotomy of developing in Garching and giving to La Silla for maintenance.

FIERA is a first big step in this area. The second step we have taken is a "universal" temperature/vacuum sensing & temperature control box that will be used with VME, ACE and FIERA systems. This system is being developed in La Silla with interaction by Garching staff.

The third design area where we are combining efforts is a new CCD detector testbench. All members of the ODT will contribute to design and critique the development as it progresses in 1996.

10. Communication with the ESO Community – World Wide Web

We have taken the approach that the World Wide Web is the best avenue for communicating information to the ESO user community. A new, clearer and more concise presentation of data about ESO's CCD devices went on-line in the beginning of September 1995. Besides providing standard data, we use this medium for user requests. This information will continue to evolve as we receive comments and constructive criticism about the content and format. Please assist us with continual improvement.

11. Facilities

A new facility upgrade planned for 1996 is the design and construction of a new CCD testbench. With an increased number of new detectors and the old testbench dependent on the VME controller, Garching (and perhaps Chile) needs a new testbench. To be operated by the FIERA controller, the testbench will utilise the knowledge gained from the many years of experience with the present CCD testbench.

We are also developing an optical set-up to scan a 2 micron wide (minimal wings) spot of variable wavelength across the pixels of CCD devices. We will use this apparatus to measure the diffusion of photoelectrons that causes degradation of PSF in CCD devices. PSF degradation was an unwelcome surprise during the CES upgrade and we must become expert at measuring this behaviour for all of our CCD chips. High quality PSF is important for nearly every application, but especially so for adaptive optics and high-resolution spectroscopy.

12. Optical Detector Workshop – October 8-10, 1996

The ESO CCD workshops held in 1991 and 1993 were valuable venues of information exchange about astronomical CCD detectors. After a brief respite, ESO will continue the series with an Optical Detector Workshop to be held during October 8–10, 1996 in Garching. The attendance of the workshop is being limited due to space constraints and our desire to create an intimate setting for information exchange. We have received confirmations of attendance from most of the leading manufacturers and major observatories. (If you wish to attend, please submit a request to jbeletic@eso.org)

13. Closing Comments

The optical detector team has established a coherent plan of activities for improving ESO's technology in this critical area. Our mission is to develop, implement and maintain optical detector systems that are the best that science and technology can provide. We encourage feedback on the direction and plans that we present in this report.

(Please send comments to: jbeletic@eso.org or odteam@eso.org)

Pointing and Tracking the NTT with the "VLT Control System"

A. WALLANDER, F. BIANCAT MARCHET, M. CHIESA, P. GLAVES, D. GOJAK, M. NASTVOGEL-WÖRZ, R. PARRA, T. PHAN DUC, R. ROJAS, J. SANTANA, J. SPYROMILIO, K. WIRENSTRAND, ESO

Introduction

One of the three main goals of the NTT Upgrade Project is to test the VLT control system in real operation before installation on Paranal. Although NTT and VLT have large differences in optics, mechanics and electronics, the VLT Common Software and the standardisation of VLT control electronics provide a common base. The strategy of the NTT Team has been to develop NTT unique process follows an accelerated schedule. We are being assisted in the development by two ESO member institutions: (i) Roma Osservatorio has provided a staff member to work part-time in Garching, (ii) University Copenhagen has provided a "tiger team" for design review.

The first FIERA prototype will be running in May 1996 and we plan to take the remainder of 1996 to iterate on the hardware design and to write the control software. Production and deployment will commence in January, 1997. Since the FIERA development schedule has become a tangible reality, all instruments with detector deliveries starting in 1997 have given their approval to using FIERA for their detector systems.

The ACE system, which was successfully tested at the NTT in January 1995, is now completing final design changes and it will be used as the controller for the FORS 1 instrument delivery in March 1996. We will also use ACE for the Big-Bang upgrade in the second half of 1996.

5. CCD Procurement

In parallel with controller development, ESO is procuring the best of the new generation of CCD devices. In Table 1 we indicate the specifications of the kind of devices that we are looking for.

We are seeking two different CCD sizes with the qualities indicated in the Table:

• 2k × 4k, 15-micron pixel, 3-side buttable device with 2 readout ports along the 2k side. For use in scientific instruments as single devices or in mosaics. In many cases (e.g. SUSI-2, FUEGOS), there will be two devices in a 4k × 4k mosaic.

• 128 × 128, 25-micron pixel, split frame transfer device with a total of 16 readout ports (8 top, 8 bottom). For use in the NAOS adaptive optics system, but also may be useful for VLTI.

At present, we are involved in a preliminary enquiry to gather information from prospective manufacturers and we aim to have a procurement in place around the end of first quarter 1996.

We are pursuing a second source for 2k × 4k detectors via a consortium to obtain CCD chips from MIT Lincoln Laboratory (MIT/LL). MIT/LL produces some of the best CCDs in the world. Their devices have consistently established the lowest readout noise at rates from 50 kHz to 5 MHz and MIT/LL has much experience with thick devices with high q.e. in the near infrared. The contract with MIT/LL will produce a limited number of devices, but we expect to get high-quality thinned devices on both standard silicon and thick, high-resistivity silicon. These devices are the first choice for the red arm of UVES.

We have also initiated a contract with Mike Lesser of the University of Arizona to produce three thinned VLT test camera chips and four more thinned 2k × 2k, 3-side buttable, 15-micron Loral devices. With a number of thinned Loral 2k × 2k devices already in stock at ESO, we have CCDs that are presently first choice for UVES blue, backup for UVES red and are appropriate for upgrades at La Silla. The VLT test camera CCD, which was designed exclusively for ESO, has a 2k × 2k, 24-micron, 4-port array with four small "tracker" chips at the corners. The compatibility of the VLT test camera device with the Tek/SITe 2k × 2k devices gives the advantage that each kind of CCD serves as a backup option for the other.

We have a small contract to obtain two Philips 7k × 9k, 12.5-micron arrays from the first lot of CCDs ever made by filling the width of a 6-inch fabrication wafer with pixels. The first devices will not be suitable for scientific application since these are front-side devices with a vertical anti-blooming drain that limits sensitivity to 400–900 nm and a peak q.e. of 28%.

6. Cryostat Developments

ESO has been developing two kinds of cryostats for use with the CCD systems: (i) a bath cryostat, which has a tank of liquid nitrogen with hold times of over 2 days, and (ii) a continuous-flow cryostat that, via feed from a 100 litre liquid nitrogen tank, can keep a CCD chip cool for over two weeks. Both types of cryostats have been designed to work with the same detector head, which is removable from the cryostat body.

The new bath cryostat design was tested in January 1995 at the NTT, and during 1995, a total of 10 detector heads and 5 bath cryostat tanks were produced. One complete system has been fully tested for integration with the FORS 1 CCD. During 1996, the bath cryostat for the VLT test camera will be integrated and tested. The continuous-flow cryostat prototype has been given a thorough test at the CES facility and during 1996, the two continuous flow systems for UVES will be fabricated.

During 1996, we will begin work on thermoelectric cooling of the NAOS wavefront sensor CCD devices.

7. La Silla Upgrades

Test time has been granted February 29 – March 8, 1996 to upgrade the B&C spectrograph on the ESO 1.5-m telescope. We will install a Loral / U. Arizona 2k × 2k, 15 micron CCD chip that has high quantum efficiency (q.e.) in visible and UV, as demonstrated by the new CES chip.

Upgrade of the B&C will leave one last low q.e. device on La Silla, in EFOSC2 at the 2.2-m telescope. We plan to use another Loral / U. Arizona 2k × 2k to upgrade EFOSC2. At present, a definitive date has not been established for this upgrade, as this upgrade must be co-ordinated with the potential move of EFOSC2 to the 3.6-m telescope.

As part of the NTT Big Bang, we will upgrade the electronics of the SUSI and EMMI detectors to the ACE/LCU systems in November 1996. These systems will provide readout rates to 90 kHz out of 2 ports for the CCD devices on SUSI and EMMI. Depending on the noise vs. speed performance of the CCD devices, this will enable a sixfold decrease in readout time. The days of 5-minute readout of the EMMI Red 2048^2 CCD are numbered.

8. Schedule of Deliveries of Detector Systems to Instruments

In addition to the La Silla detector upgrades (B&C, EFOSC2), the ODT has taken the following commitments for optical detector system delivery:

1996 March FORS 1
ACE/LCU plus eng. grade Tek/SITe 2k × 2k

1996 July NTT
3 ACE/LCU systems (no new cryostats or CCDs). Telescope integration November 1996.

1996 December FORS 1
Put science grade device and final version of all electronics into the system.

TABLE 1. Specifications of the new CCD devices required by ESO

Very low noise at "slow" readout rates (50–100 kHz) – goal is 2 e^- or less
Moderate noise at 500 kHz – goal is 3–4 e^-
Fairly good noise at 1 MHz – goal is 4–6 e^-
High q.e. from 300 nm through 1000 nm, specifically

Wavelength	320	350	375	400	450	500	600	700	750	800	900	1000
q.e. (%)	70	70	70	80	80	85	85	80	75	70	50	15

Very good cosmetic quality and high charge transfer efficiency

(The term kHz refers to kpixels/sec/port, and MHz means Mpixels/sec/port; a CCD chip or a mosaic may have many ports operating in parallel.)

noise and fast readout. While fast readout is only mandatory for a few applications, such as adaptive optics and rapidly varying phenomena, high speed will make nearly every instrument more efficient. Acquisition, focusing, direct imaging and calibration data collection will greatly benefit from high-speed readout. Also, the ability to read and display images quickly will be a significant advantage during instrument integration and testing.

3. The Present Status of ESO's Optical Detector Systems

CCD detector systems are made of three basic components: CCD chips, cryostats and the CCD control electronics. At La Silla, there are backside-illuminated, high quantum efficiency (q.e.) CCDs at all instruments, with the exception of the B&C and EFOSC2. B&C is being upgraded in March 1996 and we are working with the astronomy department in Chile to define the proper time to upgrade EFOSC2.

We will always strive to obtain better CCDs, but at present the major weakness of our systems is the control electronics. The CCD controllers that are presently in use on La Silla, named the "VME controllers", are among the poorest functioning controllers of any major observatory. The standard readout rate is 15 kpixels/sec, the electronics suffer from a myriad of noise problems, and the system has internal crosstalk that prohibits use of more than one readout port. Consequently, the VME systems read slowly with relatively poor noise and occasionally suffer more dramatic problems. The La Silla detector engineers should be given credit for maintaining and optimising these systems as well as possible.

In order to remedy this situation for the VLT instruments, a new-generation CCD controller has been under development at ESO for several years. The ACE (Array Control Electronics) system provides a significant enhancement over the VME: better noise performance and reading of multiple ports to rates of 90 kpixels/sec/port. Fundamentally, there is nothing wrong with ACE, except that its specification will be outdated for future applications. ACE is not capable of operating the new generation of high-speed, low-noise CCD devices to the fullest of their capabilities.

4. Primary Development Effort Through 1996 – Advanced CCD Controller

ESO must produce many CCD systems in the next few years in order to provide for the VLT instruments and to upgrade La Silla. The most sensible approach is to produce a single "universal" controller that can operate all of ESO's CCD devices. This saves money and time in production, maintenance and training. Since the ACE controller can not satisfy the readout requirements of the new generation CCD devices, the optical detector team has started a parallel development effort for an advanced CCD controller.

We are pleased to report that the advanced CCD controller development has proceeded very well since we began this effort in the second quarter of 1995. We have established a system architecture that should be able to run any CCD chip or mosaic that is foreseen through the year 2005. The advanced controller will be able to operate up to 32 readout ports at multi-MHz pixel rates (per port), and all major parameters will be fully programmable. The system design goal is to have performance limited only by the CCD device and the imagination of the user. Thus, the system can be run slowly to get the very lowest noise (< 2 electrons) for long-exposure faint spectra or run fast (expect 4–6 electrons noise at 1 Mpixel/sec/port) for acquisition, focus, calibration or direct imaging. The advanced controller has been given a name: FIERA (Fast Imager Electronic Readout Assembly). Proposed by our Chilean staff and voted in by the ODT, FIERA has the meaning "wild animal", such as a lion, in both Spanish and Italian. The specifications for the FIERA controller are listed in the box below.

We are applying most of our research and development energies to FIERA through 1996 so that the development

Specifications of the FIERA CCD Controller

The fundamental goal for FIERA is to make a controller that can optimally operate any CCD chip or mosaic that ESO acquires for the next 10 years. The limitation of the entire detector system should be due solely to the CCD and the imagination of the user. The electronics (hardware and software) of FIERA should be transparent to the user. Later this year we will publish an article on FIERA after we complete the prototype testing. We list here some of the specifications of the FIERA design:

- *50 MHz fundamental clock*
- *Up to 32 readout ports*
- *Up to 50 Mpixel/sec total*
- *Up to 21 bits/pixel*
- *Up to 5.5 Mpixel/sec/port*
- *Initially 1 MHz pixel rate limitation at 16 bits per pixel (set by A/D limitation)*
- *Readout noise must be dominated by the CCD device for both slow and fast readout; the electronic noise must be negligible*
- *Fully programmable high-current clock drivers (25.5 V swing, 0.1 V resolution at 50 MHz, 2 amps instantaneous per driver)*
- *Nearly unlimited number of control bits (at 50 MHz)*
- *Analogue biases fully programmable with hardware limits on potentially damaging biases*
- *4 gain settings*
- *64k offset levels*
- *4 low pass filter settings (can optimise clamp & sample at 4 speeds)*
- *Gbit/sec fiber optic data link from detector head to embedded computer*
- *Embedded telemetry and test signals*
- *No software in the detector head / minimalistic design*
- *Fully modular and expandable.*

The FIERA controller consists of three modules:

• A set of detector head electronics that will be mounted as close to the CCD as possible, preferably on the CCD cryostat itself. (If there is too much distance between these electronics and the CCD, we will use pre-amplifiers to boost the video signal for low noise performance.)

• A DC power supply module that generates a set of clean voltages for the detector head electronics. This power supply should be within 3 metres of the detector head electronics.

• The detector computer with a custom-made computer interface board. The interface board contains a Gbit/sec duplex fiber link and two C40 DSP chips for system control and interface to external computers/processors. The distance of the fibre-optic data link between the detector computer and detector head electronics can be up to 500 metres with standard parts, up to 20 km with pin compatible upgrade to more expensive transmitter/receivers.

For the system we only need to custom design six printed circuit boards; the computer interface board and five boards in the detector head:

- *communications board (fiber link and bus interface)*
- *clock drivers*
- *analogue biases*
- *video processing (amplification, gain, offset, correlated double sampling, digitisation)*
- *custom backplane*

A good feature of the system is that there is no software or processors in the detector head. The detector head runs via an "extended bus" structure provided by the Gbit/sec data link. All system "smarts" reside in the C40 sequencer chip and the SPARC computer that is used as the dedicated computer for the system.

Figure 3.

tion of the assembly of the enclosures as well as of the telescopes. Near the soccer field in the foreground of the picture we will soon start the construction of the building that will be used for the aluminisation of the primary mirror and for the construction of the other technical complexes necessary to operate the new ESO Observatory. One of these technical buildings will accommodate the power generators that will produce the necessary electrical power. A contract with the company CEGELEC is about to be signed for this important and vital unit.

The Plan for Optical Detectors at ESO

J. BELETIC, ESO-Garching

1. Introduction

In January 1995, ESO gave increased emphasis to optical detectors by establishing the optical detector group within the Instrumentation Division. This restructuring was intended to provide the resources necessary to significantly improve ESO's technology in optical detectors. In addition to this group in Garching, there are several other persons, including a group of engineers at La Silla, that work on optical detectors. In order to co-ordinate our efforts, we have organised into the Optical Detector Team (ODT) and we have defined a strategy for our work. These plans have been reported to the Scientific Technical Committee (STC) and the User Committee (UC) and we have received their support. The intent of this article is to present our plans to the whole of the ESO community.

2. Our Vision

Our plans are guided by the following technological developments:

CCD devices are becoming nearly perfect detectors of optical radiation; high quantum efficiency devices can be made for wavelengths from the atmospheric cut-off at 300 nm to ~1000 nm.

Readout amplifiers for CCD devices have improved so that it is now possible to attain less than 2 electrons noise at “slow” readout rates (100 kpixel/sec/port) and 4–6 electrons noise at 1 Mpixel/sec/port.

It is possible to build electronics today that can run any CCD detector or mosaic of detectors that we can envision for the next 10 years.

Our vision is for ESO to have detector systems of high quantum efficiency, low

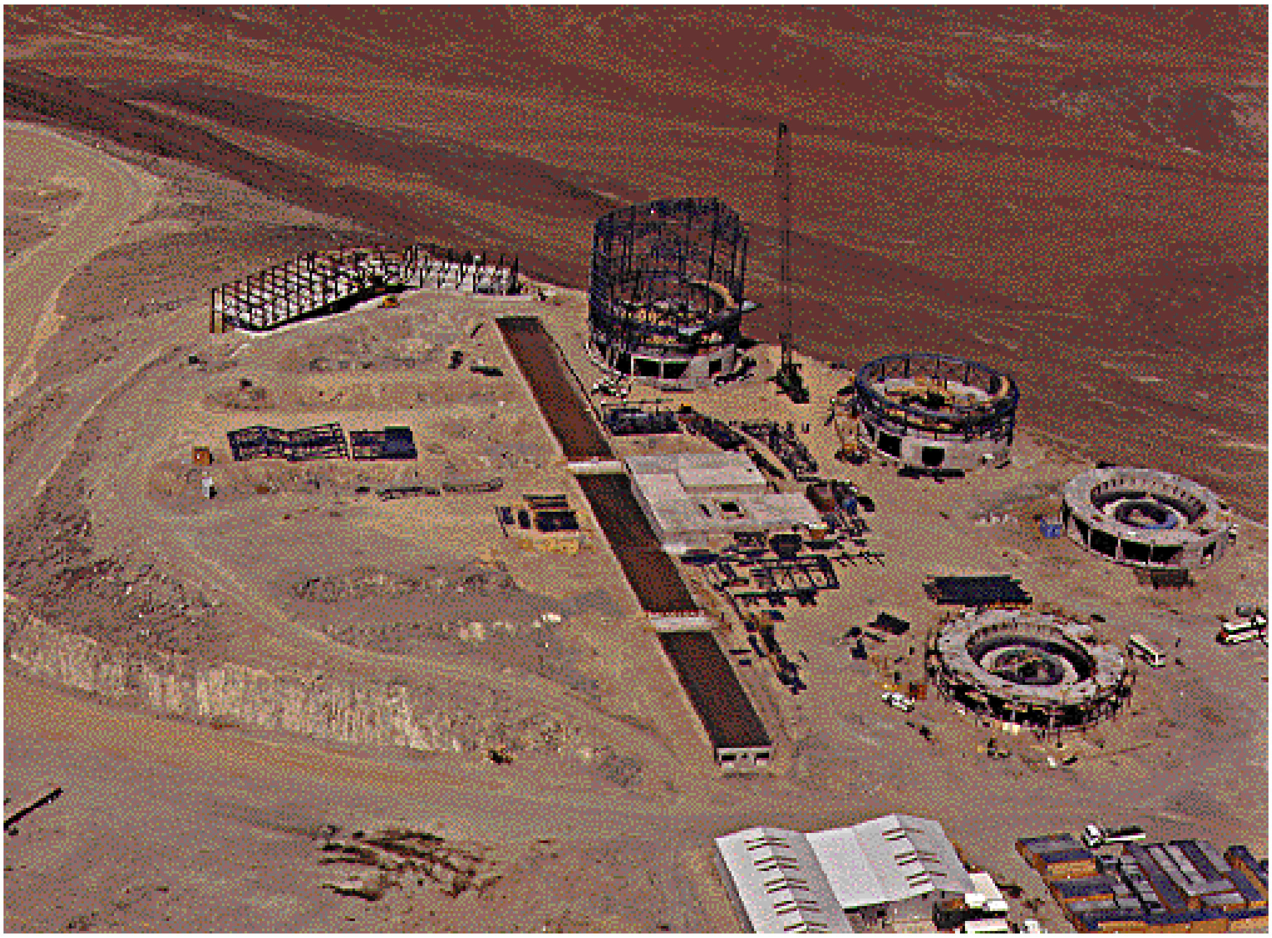

Figure1.

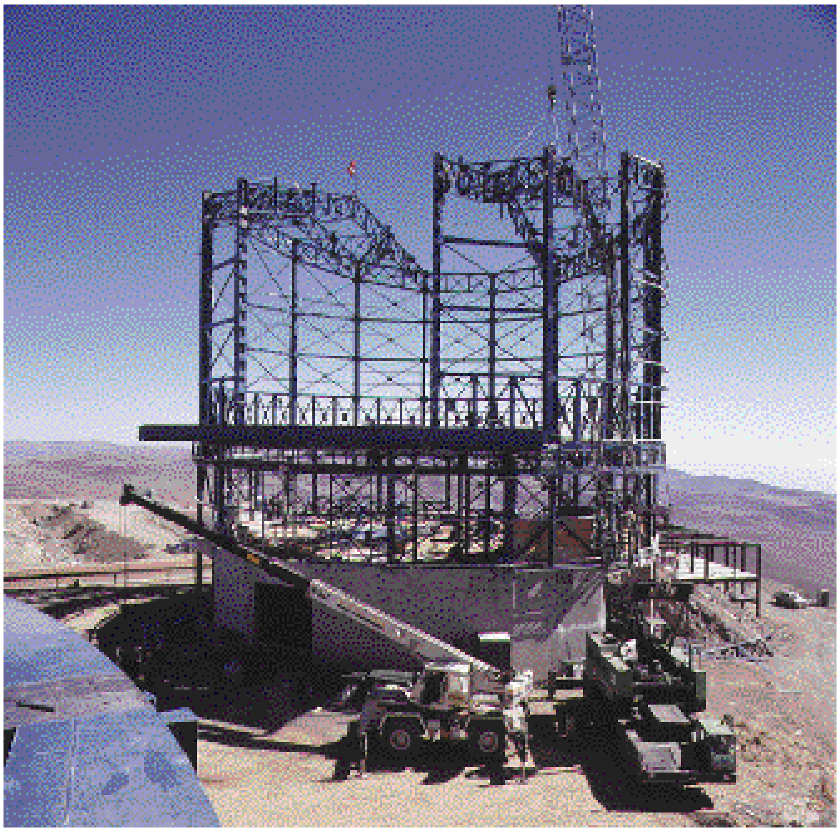

of the construction. The structure has a low-weight construction, specially designed to protect the telescopes from the strong desert wind.

Seen from the Technical and Hotel Areas, see Figure 3, the summit of Paranal is starting to take its final shape. Extensive work has been done in the course of the last months to prepare the road connecting the Hotel Area with the summit in order to be able to have a safe transport of large and delicate pieces like the 8.2-metre primary mirror. The same activity of widening the road up to 12 km and minimising the slope was performed on the 25 km separating the old Panamericana from the Hotel Area.

In the foreground of the picture one can see the present accommodation complex that is sufficient to accommodate about 300 people. On the extreme left is the old ESO camp. In the middle there is the Skanska-Belfi camp that now has been taken over by ESO and will be used in the course of the next year as a temporary hotel until the final accommodation complex has been built. On the right side of the picture above the other camps is the SEBIS camp utilised for the Italian team in charge of the erec-

Figure 2.

Relations with Chile and other States

Another important decision by the ESO Council was essential to assure the operation of the VLT on Paranal in Chile.

As part of the settlement of the claims by the La Torre family against the Government of Chile regarding the ownership of Paranal at the time of the donation, the Chilean Government will disburse approximately 10 MDM to the claimant.

While willing to make this effort in reaching this agreement, the Government of Chile required from the ESO Council some assurance that, after the settlement, ESO would not seek further damages to repay for the losses suffered.

The direct losses to ESO linked to scientific contractors had been reduced to a sum of about 8 MDM.

The Council resolved to forego these claims, with appropriate assurance to be given to the Government of Chile, at the time of exchange of the instruments of ratification of the new "Accuerdo".

As mentioned above, the Council also decided that no increase in the run out costs of VLT to compensate for the losses should be granted to the Executive, resulting therefore in additional savings required in the VLT programme.

As a result of this action, the legal proceedings regarding Paranal could be concluded on January 12, 1996 and the "Accuerdo" has been submitted for its ratification in Parliament by Chile on January 16, 1996.

It is important to point out that even without the ratification of "Accuerdo" the legal basis of ESO ownership of Paranal is now settled. Our relations with the Chilean Government are excellent, with strong assurances at the highest level of the Government of the desire of Chile to have ESO develop VLT on Paranal.

Significant steps were also taken by the Council with regard to the discussions related to new memberships. A general resolution about new members was accompanied by the appointment of an ESO Negotiating Team to initiate discussions with Australia and Spain.

Since then the Government of Australia has also formally named a negotiating team and preliminary discussions have started (February 5, 1996). The Government of Spain has expressed interest in starting the process (January 19, 1996).

Concluding Remarks

Many other significant issues were discussed and acted upon during this Council Meeting.

I would like to recall the discussion of the "Chile Operating Plan in the VLT era", the endorsement of the Chile reorganisation plan effective since December 1, 1995, the appointment of Daniel Hofstadt, Jorge Melnick and Massimo Tarenghi to head respectively the Santiago, the La Silla and the Paranal operations.

Also, I would like to mention the important report by the STC on "La Silla 2000" and the discussions regarding the forthcoming visit of the ESO Visiting Committee.

These matters have been and will be taken up in greater detail during the course of the year in future issues of *The Messenger*.

Finally, I should note actions of Council in the re-appointment of Dr. Peter Creola as President of Council, Dr. Jean-Pierre Swings as Vice President of Council, Dr. J. Gustavsson as Chairman of the Finance Committee, Dr. Steve Beckwith as Chairman of the STC, Professor Krautter as Chair of the OPC and Dr. Lequeux as Vice Chairman of the OPC.

TELESCOPES AND INSTRUMENTATION

VLT News

M. TARENGHI, ESO

During the past 3 months a great deal of work has been carried out on the Chilean site where the VLT is being assembled. Skanska-Belfi, the Swedish-Chilean consortium in charge of the construction of the foundations for all the buildings on the Paranal peak are in the process of terminating their activities and the Italian consortium SEBIS has completed the erection of the steel frame of the first enclosure unit. Figure 1 depicts in an impressive way the transition of the typical work associated with civil engineering activities to the work related to mechanical erection. Enclosure no. 1 in the middle of the picture is going through the last moments of the erection of the roof and a number of workers are operating in the proximity of the upper part of the structure.

The remaining pieces of the enclosure structure of no. 1 (the shutter of the enclosure) are lined up ready in pre-assembled form on the summit of Cerro Paranal on the left side of Figure no. 1. During the last week of February 1996 the external panels of enclosure no. 1 were installed and in the course of April 1996 the structure will be closed. The fixed part of enclosure no. 2 is being erected and is already visible in Figure 1.

The foundations of the third telescope have been completed and are ready for the integration of the enclosure. In telescope no. 4 (Figure no. 1) one can see the scaffolding around the foundations which was used to align the interface boxes of the enclosure structure. These units proved to be very effective with their special anti-seismic device during the course of the strong earthquake that occurred in July 1995. The steel structures for enclosures 3 and 4 left Italy by sea transport at the beginning of March. In the background of Figure 1 the steel frame structure of the control building is visible. This will be used in the lower floor for integration, laboratory and technical areas, and the upper floor will be used for the control rooms from which astronomers and technical people will perform their observations.

All the underground tunnels allowing access to the different telescopes as well as the interferometric tunnel and the interferometric laboratories, are embedded in the ground and are already being utilised for access to the lower part of the foundations.

The impressive delay line tunnel is a remarkable feature in the centre of the figure, also the two bridges crossing the tunnel that allow the mobile 1.8-m telescopes to go from the northern to the southern side are clearly visible.

In the interior part of the foundations of telescopes 3 and 4 one can see two rings covered by blue plastic sheets protecting the two embedded beams on which the azimuth tracks of the unit telescopes will be assembled.

In March the company SPIE Batignolles will intervene on the summit of the mountain to complete all the electrical and mechanical installations in the telescope buildings, control building and interferometeric complex, and in the summer the company AES will start assembly of the first telescope structure.

Figure 2 gives more detail of the delicate phase of the lifting of the roof. The human presence inside the enclosure gives an idea of the global dimensions

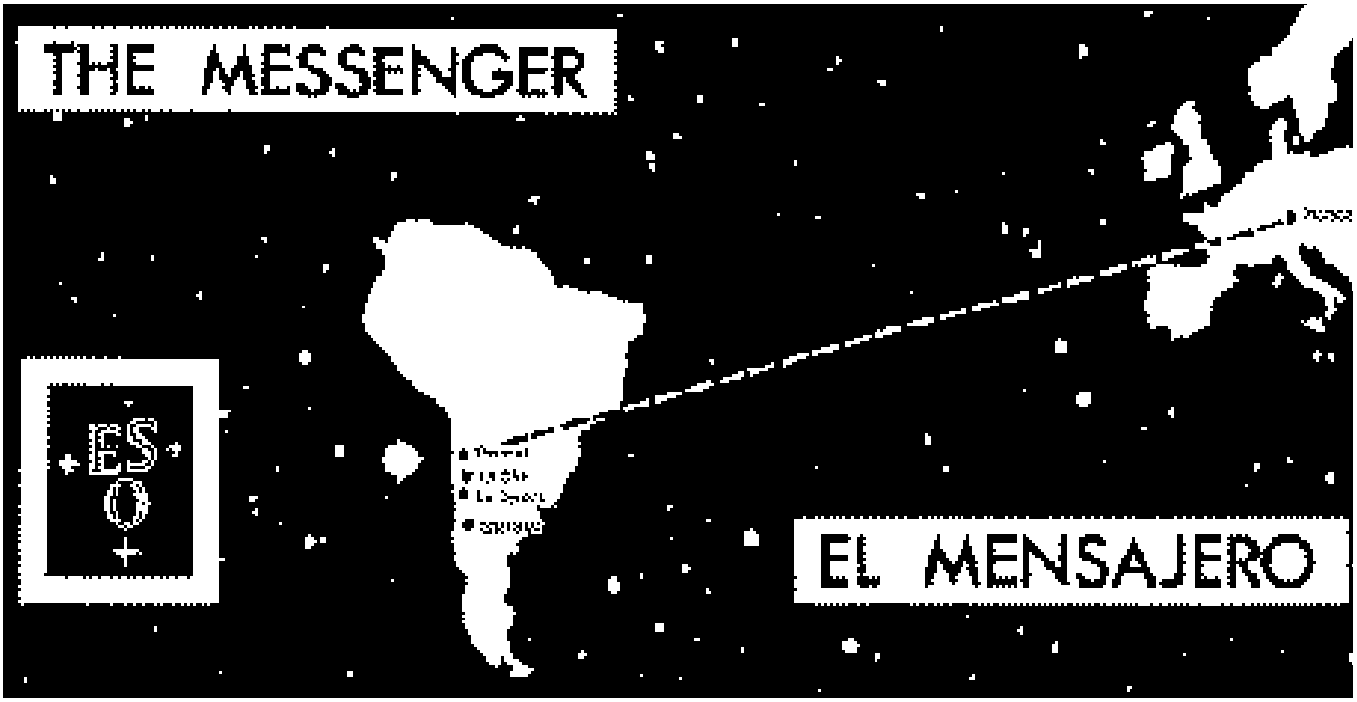

No. 83 – March 1996

Report from the Council Meeting

R. GIACCONI, Director General of ESO

The ESO Council meeting that took place in Milano on November 28–29, 1995, was of great importance to the organisation for the number and complexity of the issues that were discussed and the decisions that were reached.

I thought I would comment on some of the highlights as a means of informing the European Astronomical Community of significant developments.

Programmatic and Financial Matters

The Council was brought up to date on the very considerable progress which had occurred in all aspects of the VLT project. The Council members were able to see with their own eyes and touch the 430-ton mechanical structure of one of the VLT unit telescopes just assembled in the Ansaldo factory in Milano.

They also received reports on the successful delivery of the first 8.2-m mirror at REOSC in Paris, a few weeks before, and the satisfactory progress of all other aspects of the technical developments of the VLT telescopes.

The successful development of significant portions of software was, for instance, vividly demonstrated through its application at the NTT (see article by Jason Spyromilio in this issue of The Messenger). Programmatic reports on the development of the most important sub-units were normally accompanied by photographic or videotape reports.

Particularly important in this respect was the visual demonstration on the completion of the civil engineering works on Paranal and the degree of progress on the erection of the telescope enclosures.

From the point of view of schedule and cost, the Executive could report that notwithstanding the delay imposed on the construction by the legal issues in Chile, the official first light could still occur in the first half of 1998, although internal contingency had been severely eroded. The projected costs of VLT at completion were also reported to remain within the agreed budget, although internal contingencies had been substantially reduced due to losses associated to the programmatic delays in Chile.

This financial and schedule status report was embodied in the written VLT semi-annual report which is currently based on the Work Break Down Structure (WBS) and Management Information System (MIS) tools.

I believe it is fair to say that the Council received these reports with great satisfaction because they portray a healthy, stable and resilient programme which was able to absorb technical and political mishaps and respond positively and effectively.

The reports on all other aspects of ESO also showed an organisation which is successfully reengineering itself while carrying out its tasks and achieving the Council mandated savings in operations with good margins.

As a result, the Council was in a position to approve the 1996 budget proposed by the Finance Committee, as well as the use of the 1997–1999 financial projections as a base for planning. Furthermore, Council tackled and resolved the knotty problem of cash flow created by the demand for large payments to contractors upon delivery of the main components of VLT.

In an important resolution the Council authorised the Director General to open a line of credit in the banking sector to be used for the VLT programme, only as required, with a fixed amount of no more than 40% of one yearly contribution. This credit is to be completely refunded by the year 2003 and in any case to be kept to a minimum by several means. Member states willing to make an advanced contribution could completely avoid the loan alternative and reduce the required amount. The Executive is pledged to a total saving of 20 MDM in operating expenses over the period 1995–1998 and is required to absorb the losses due to delays in Chile within the VLT programme. The Member States committed themselves to a minimum constant contribution (inflation adjusted) for the period 1996–2002.

By these decisions the Council has created the necessary conditions for the successful completion of the technical part of the VLT programme.